Long-term changes in small size-class contribution to total phytoplankton biomass in the northern Chukchi to northern Bering Seas

（北部チュクチ海から北部ベーリング海における小型植物プランクトンの寄与の長期変化）

Division of Marine Bioresource and Environmental Science

Graduate School of Fisheries Sciences

Hokkaido university

北海道大学大学院水産科学院

海洋生物資源科学専攻

Jung-woo Park

朴 正祐

2024年

Table of contents

Chapter 1

General introduction

1.1. General description of Arctic Ocean environments

The Arctic Ocean is the northernmost, the smallest (14,060,000km^2), the shallowest with average depth (1,038 m) ocean among the five major oceans (Pidwirny, 2006). The temperature and salinity of the Arctic Ocean exhibit significant seasonal variations due to the freezing and melting of sea ice. Some oceanographers even refer to it as the "Arctic Mediterranean Sea" because it is surrounded by the Eurasian and the North American continents (Aagaard *et al.*, 1985; Coachman and Aagaard, 1974).

The Arctic Ocean has several passages connect to the Atlantic Ocean and the Pacific Ocean. The exchange of seawater through these passages significantly influences the temperature, salinity, and nutrient content of the Arctic Ocean. Among several passages, the Bering Strait, located between the United States' Alaska and Russia's Siberia, with a width of approximately 85 km and a depth of less than 50 m, serves as the gateway connecting the Pacific Ocean and the Atlantic Ocean. Although it is narrow, the Bering Strait is the only passage in the Northern Hemisphere that connects Arctic Ocean to the Pacific Ocean. The inflow of Pacific seawater (0.8Sv; Woodgate *et al.*, 2005a; Spall.*et al.*, 2018) into the Arctic Ocean serves as a primary source of heat, freshwater, and nutrient input, exerting a strong influence on the Arctic marine ecosystem (Spall *et al.*, 2018; Woodgate *et al.*, 2010). This inflow varies significantly seasonally, volume from 0.4Sv to 1.2Sv, temperature from -1.9°C to 2°C, salinity from 31.9 psu to 33 psu (Woodgate *et al.*, 2005). According to Woodgate and Aagaard (2005) the 40% of freshwater inflow into Arctic Ocean is transported through Bering Strait. Through this inflow, not only freshwater but also substantial amounts of nutrient and organic matter are supplied to Arctic Ocean (Cooper *et al.*, 1997; Grebmeier *et al.*, 2006; Woodgate *et al.*, 2005; Woodgate and Aagaard, 2005). The inflow from the Atlantic Ocean to Arctic Ocean enters through the Fram Strait and Barents Sea. It is characterized by high salinity (>34 psu), warm (>0°C) and characterized by high salinity (>32 psu) and warmth (>0°C), with a inflow water volume approximately ten times higher than the water volume (7Sv; Fahrbach *et al.*, 2001) from the Pacific ocean. The warm and high-salinity waters from the Atlantic Ocean contribute to the formation of the Arctic intermediate water while the cold and low-salinity waters from the Pacific Ocean dominate the surface water. The stratification created by these two distinct water masses is a significant characteristic of the Arctic Ocean (Steele *et al.*, 2004). The distinct environmental conditions in the Pacific-side Arctic Ocean have led to the existence of unique ecosystems and biodiversity (Ardyna *et al.*, 2020). The Pacific Arctic, including the Chukchi and northern Bering Seas, stands as one of the globe's most bountiful marine ecosystems (Grebmeier *et al.*, 2006). It boasts significant benthic biomass, a consequence of the continuous influx of nutrients via the Bering Strait, supporting robust primary production (Woodgate, 2018). According to Huntington *et al.* (2020), the decline of sea ice in the Pacific-Arctic Ocean and its biological consequences (e.g., salmon distribution shifting, marine mammal moving

to shore from sea ice, seabird species community changes) are highlighted. The study suggests that these changes could impact human activities, including fisheries and industries. Understanding these characteristics is crucial for comprehending the overall balance and interactions within the entire Arctic ecosystem (Ardyna *et al.*, 2020). The Pacific-Arctic Ocean has been recognized as one of the most significant regions affected by global climate change, making it a prominent area of focus in the context of global warming (Walsh *et al.*, 2011). Consequently, research focused on the Pacific-side Arctic Ocean plays a pivotal role in enhancing our understanding of the Arctic as a whole and in formulating effective conservation and climate change mitigation strategies for the marine ecosystem. The Pacific side of the Arctic Ocean, including the Chukchi Sea and northern Bering Sea, is a world productive region influenced by the flux of Pacific water (Harada, 2016; Lee *et al.*, 2007; Sambrotto *et al.*, 1984; Springer and McRoy, 1993). In the Chukchi and Bering Seas, large phytoplankton are generally dominant although the areal distribution of their contribution mostly depends on local water masses in different nutrient conditions (Lee *et al.*, 2007; 2013). The three water masses inflow through Bering strait : Alaskan Coastal Water (ACW), Anadyr Water (AW) and Bering Shelf Water (BSW). ACW exhibits high temperatures and low salinity due to freshwater input. ACW follows the western coast of Alaska and flows into the Beaufort Sea (Coachman and Aagaard, 1975). AW, on the other hand, flows along the eastern coast of Siberia, characterized by low temperatures and high salinity. AW provides significant nutrient supply to the Bering Sea and Bering Strait (Dunbar, 1976). BSW flows between AW and ACW, and its water density closely resembles that of AW. As the water masses pass through the Bering Strait, the water mases mix thoroughly (Grebmeier *et al.*, 1988). This mixed water, known as Bering Shelf–Anadyr Water (BSAW) delivers nutrient-rich water to the Southern Chukchi Sea. Whereas ice melt water and the fresh water inflowed from the Beaufort gyre have effect on the northern Chukchi Sea (Danielson *et al.*, 2017; Spall *et al.*, 2018; Yun *et al.*, 2016). Due to these differences, the Chukchi Sea is studied as two distinct regions: the Northern and Southern Chukchi Sea in this study.

1.2. Current small phytoplankton issue and environmental changes in Chukchi and Bering Seas

Phytoplankton, the bottom of food web, play a crucial role in the ecosystem by photosynthesis to convert carbon dioxide into organic matter by utilizing sunlight. Phytoplankton assume a fundamental role in the global carbon cycle and uphold the energy transfer within the oceanic food web (Basu and Mackey, 2018). Phytoplankton serves as the starting point for pelagic-benthic coupling by regulating particulate organic matter flux (Wassmann *et al.*, 1996). These phytoplankton communities occupy different ecological roles based on their respective sizes, micro-phytoplankton (<20 μm), nano-phytoplankton (20-2 μm), pico-phytoplankton (>2 μm), and their composition is attributed to environmental factors such as water temperature and nutrient availability (Arin *et al.*, 2002). Phytoplankton size classes (PSC) are intricately linked to phytoplankton's photosynthetic efficiency, the sinking rate of phytoplankton aggregates, and the structure of the marine food chain (Berelson, 2001; Siegel *et al.*, 2014; Turner, 2015). Li *et al.* (2008) reported increasing of small phytoplankton contribution to total phytoplankton could lead loss of biological productivity in higher trophic levels. Because a system dominated by small phytoplankton typically do not facilitate significant exports of biogenic carbon, either for removal (e.g., harvesting) or for storage (e.g., burial) (Li *et al.*, 2008). Recently, several environmental changes which could

alter phytoplankton community have been reported in the Chukchi Sea, such as the early retreat of sea ice (Crawford *et al.*, 2021; Frey *et al.*, 2015; Grebmeier *et al.*, 2015; Overland and Stabeno, 2004; Screen *et al.*, 2018; Stroeve and Notz, 2018), changes in biomass and productivity (Ardyna *et al.*, 2020; Arrigo and van Dijken, 2015; Lee *et al.*, 2012; Yun *et al.*, 2016), increased heat flux (Danielson *et al.*, 2020), increasing freshwater content (FWC; Coupel *et al.*, 2015; Yun *et al.*, 2016), overall decrease in the size of phytoplankton (Fujiwara *et al.*, 2016), and changes in bloom periods (Kahru *et al.*, 2011). These ongoing environmental changes could have consequences on biogeochemical processes and alter the marine ecosystem structure in the northern Bering and Chukchi Seas (Grebmeier, 2012; Lee *et al.*, 2019).

Small phytoplankton (<2μm, pico-phytoplankton) is the smallest photosynthesizing organisms. Various studies have been carried out on small phytoplankton in Arctic Ocean (Cottrell and Kirchman, 2009; Gradinger and Lenz, 1995; He *et al.*, 2012; Lee *et al.*, 2013; Li, 1998; Li *et al.*, 2009; Lovejoy *et al.*, 2006; Mosharov *et al.*, 2023; Sadanandan Bhavya *et al.*, 2018; Sherr *et al.*, 2003; Terrado *et al.*, 2013, 2008; Yun *et al.*, 2014). The ecological balance of organic carbon production in the upper ocean is directly influenced by the prevalence of picophytoplankton, highlighting the significant role played by their structure and functioning in planktonic communities (Falkowski *et al.*, 1998; Legendre and Le Fèvre, 1991). The relationship between temperature and the relative contribution of small phytoplankton to total primary production was positive. However, this relationship was not observed when considering total chlorophyll, indicating that total chlorophyll-*a* may not serve as an accurate proxy for biomass in the small plankton size class (Agawin *et al.*, 2000). Hence, the monitoring of small phytoplankton is considered crucial in the current ongoing of climate changes. The increasing of small phytoplankton due to recent environmental changes has been consistently observed and reported in the Bering and Chukchi Seas (Joo *et al.*, 2013; Lee *et al.*, 2013; Yun *et al.*, 2018). Generally, large phytoplankton is dominated in the Chukchi and Bering Seas, although the areal distribution of their contribution mostly depends on local water masses in different nutrient conditions (Lee *et al.*, 2007; 2013). The contribution of small phytoplankton to the total biomass is increasing and has become more important under warming conditions (Coupel *et al.*, 2015; Lee *et al.*, 2013; Li *et al.*, 2009; Morán *et al.*, 2010; Neeley *et al.*, 2018). According to Fu *et al.*, (2020), by 2300, the Arctic Ocean might have mostly small phytoplankton instead of diatom due to 53% decline in primary production. This change, combined with the peak export moving from July to May, could intensify threats to Arctic food webs post-2100. Our research underscores the critical role of these phytoplankton shifts and emphasizes the need for long-term climate predictions.

However, we still have an incomplete understanding of the specific environmental factors that drive changes in these small phytoplankton. To evaluate the potential impacts of increased small phytoplankton on the ecosystem, it is important to first determine the relationship between environmental factors and small phytoplankton abundance. By identifying the specific environmental drivers and quantifying their influence, we can better understand the ecological changes that may occur due to the proliferation of small phytoplankton. Small plankton cells (<2μm) thrive while larger cells decrease, with no change in chlorophyll-*a* concentration, due to strong stratification caused by increasing freshwater resulting from warming (Li *et al.*, 2009). Additionally, the phytoplankton community has steadily changed and become smaller (Coupel *et al.*, 2012; Fujiwara *et al.*, 2018).

Small phytoplankton are ubiquitous and significantly contribute to the biomass and productivity of the Arctic Ocean. In a warmer ocean, the contribution of small phytoplankton is expected to increase and become more important (Lee *et al.*, 2013; Li *et al.*, 2009; Morán *et al.*, 2010). Primary productivity in the Pacific Arctic regions is mainly influenced by freshwater contents (FWC) which have effect on primary productivity as limiting nutrient. (Coupel *et al.*, 2015; Yun *et al.*, 2016). From 1991 to 2015, the flux of Pacific-origin freshwater, with an increasing northward volume transport into the Arctic Ocean, has been observed to increase (Woodgate, 2018). While early studies have revealed how FWC affects primary productivity, they have not clarified the extent of its impact or how it compares to influences from other environmental factors. Thus, this study aims to examine how the ongoing increase in FWC may affect primary productivity and the size composition of phytoplankton. Furthermore, small phytoplankton contribution to the total phytoplankton and production of the phytoplankton community could be a useful indicator to investigate ecosystem changes (Li *et al.*, 2009; Morán *et al.*, 2010). It is important to know how much small phytoplankton contribute to overall primary production in marine ecosystems because of their potential impact on primary production under ongoing environmental changes. Although numerous studies have been conducted, there has been a lack of quantitative assessment regarding the relationship between small phytoplankton and environmental factors. While previous studies have elucidated the mechanisms behind these factors, they have not investigated the extent to which FWC or other environmental factors induce changes in phytoplankton. Thus, a quantitative approach is necessary.

1.3. Satellite-based approach for small phytoplankton

Nonetheless, the process of identifying and counting taxa through microscopy and determination of phytoplankton sizes are laborious and heavily reliant on expertise. It is impractical to execute with the necessary temporal and spatial resolution required for assessing the state of the oceans. Satellite remote sensing data offers a comprehensive perspective of the optical characteristics in the upper water column, covering basin to global scale oceans, with exceptional temporal and spatial resolution (Lucas *et al.*, 2023; Son *et al.*, 2014, 2005). Therefore, various methods using satellite imagery are continuously being developed to distinguish phytoplankton size classes (PSCs). The PSC approach divides the phytoplankton into three categories: pico-phytoplankton (<2 μm), nano-phytoplankton (2–20 μm), and micro-phytoplankton (>20 μm). The PSC research methods using satellite include abundance-based methods (Brewin *et al.*, 2010; Hirata *et al.*, 2008, 2011; Uitz *et al.*, 2006), Radiance-based methods (Li *et al.*, 2013), Absorption-based methods (Bricaud *et al.*, 2012; Ciotti and Bricaud, 2006; Devred *et al.*, 2011; Fujiwara *et al.*, 2011; Mouw and Yoder, 2010; Roy *et al.*, 2013). There are well-established connections between size and environmental factors such as nutrient availability and light, which govern photosynthesis, phytoplankton dynamics, and succession (Aiken *et al.*, 2008; Bouman *et al.*, 2005; Chisholm, 1992; Platt *et al.*, 2005). Among these methods, Hirata *et al.* (2008) established a model for detecting the dominant PSC at a satellite pixel. This technique offers valuable information that can be used to survey small phytoplankton contribution to total phytoplankton biomass. However, this model was developed for the global ocean, and its accuracy for specific regions like the Arctic has not been clearly established, necessitating validation.

In the Arctic Ocean, little studies are conducted for PSCs and small phytoplankton via satellite methods. Uitz *et al.* (2010) has been reported 11% of primary production is produced by small phytoplankton in the Arctic Ocean using abundance-base algorithm for PSC. Fujiwara *et al.* (2016, 2018) reported that the changes of sea ice retreat lead that phytoplankton size community become smaller. Moreover, there has been a notable lack of research investigating the association between the primary factors (freshwater contents, sea surface temperature, sea ice) known to trigger variations in small phytoplankton, as observed through field measurements, and their corresponding linkages derived from satellite-based data. Furthermore, due to inherent year-to-year fluctuations, it's challenging to identify a long-term trend without a more extensive observational time series (Li *et al.*, 2008). The small phytoplankton in the Pacific-Arctic Ocean is undergoing changes; however, the specific causes behind these changes remain poorly understood. There is a lack of research examining the extent of variations resulting from changes in environmental factors.

1.4. Objectives and research procedure of this dissertation

Therefore, this study aims to assess the influence of environmental factors on the changes in small phytoplankton in Arctic Ocean and evaluate the extent to which small phytoplankton changes are influenced by the environmental factors quantitatively. The objectives of this study are to:

[1] Assess the biomass and contribution to primary production of small phytoplankton and to investigate their relationship with environmental factors with *in-situ* measurement.

[2] Validate both *in-situ* data and the phytoplankton size model (PSC) using satellite data to investigate the long-term changes (1998-2020) in small phytoplankton derived from satellite datasets.

[3] Quantitatively assess the associations between these changes and the environmental factors—FWC, SST, and sea ice—that contribute to such variations.

At the outset, in chapter 2, we conducted field measurements of the phytoplankton community in the North Bering Sea and Chukchi Sea through ARA07B and OS040 Cruises. Through field observations, we investigated the biochemical characteristics of small phytoplankton and their contribution to the total biomass. Following this, in chapter 3, we validated the PSC model using collected *in-situ* data and tracked long-term trends of small phytoplankton contribution. Lastly, in Chapter 4, we conducted various statistical methods to understand how changes in small phytoplankton relate to the environment. We figured out which environmental factors—FWC, SST, and sea ice—are most important in causing these changes in each region. Based on these results, overall conclusion in terms of small phytoplankton variation in the Bering and Chukchi Seas was discussed in Chapter 5.

Table 1. Summary of abbreviations used in this dissertation

Abbreviation	Definition
ACW	Alaskan Coastal Water
AHC	Agglomerative Hierarchical Clustering
a_{ph}	Phytoplankton absorption coefficient
ARA07B	R/V Araon cruise during August, 2016
AW	Anadyr Water
BCWW	Bering Chukchi winter water
BS	Bering Strait
BSAW	Bering Shelf–Anadyr Water
BSW	Bering Shelf Water
CTD	Conductivity-Temperature-Depth
FWC	Fresh Water Contents
HLY0702	Healy cruise during May-June, 2007
HPLC	High-Performance Liquid Chromatography
IMW	Ice Melt Water
NB	Northern Bering Sea
NC	Northern Chukchi Sea
OC-CCI	Ocean Colour Climate Change Initiative
OS040	T/S Oshoro-maru cruise during July, 2017
PAR	Photosynthetically Active Radiation
PDO	Pacific Decadal Oscillation
POC	Particulate Organic Carbon
PON	Particulate Organic Nitrogen
PP	Primary Productivity
PSC	Phytoplankton Size Class
RUSALCA	Russian-American Long-term Census of the Arctic
SD	Standard Deviation
SSS	Sea Surface Salinity
SST	Sea Surface Temperature

Chapter 2

Contribution of small phytoplankton to primary production in the northern Chukchi to northern Bering Seas in 2016, 2017 through field observation

2.1. Introduction

Several studies for small phytoplankton (<2um) contribution to total primary productivity (PP) were conducted in various area of arctic ocean. Those studies have reported the factors of changing small phytoplankton community vary by region and season in Pacific Arctic Ocean. Phytoplankton production and community composition have been found to be affected and altered by the freshening of surface water (Coupel *et al.*, 2015; Li 2009). The volume of freshwater flowing through Bering Strait has increased by 40% over the past two decades (Cooper *et al.*, 2022). FWC increasing trend is strongly related to the functional phytoplankton group (Coupel *et al.*, 2015). SST is also identified as one of factors influencing the community structure of phytoplankton (Nona *et al.*, 2000; Behrenfeld *et al.*, 2006). In the Arctic, an increasing trend in SST has been observed over the past few decades, and the rate of increase has been accelerating (Comiso *et al.*, 2014). Seasonal sea ice cover has been retreating earlier and forming later in the Pacific Arctic region over the last decade (Frey *et al.*, 2015). The changes of sea ice retreat could largely influence phytoplankton community composition (Fujiwara *et al.*, 2016). These factors (FWC, SST, sea ice) are commonly mentioned as causes of changes in phytoplankton community, however, previous studies have not well illuminated the relationship between small phytoplankton and environmental factors. Yet, they have not determined the extent to which environmental changes affect these relationships over long-term variations. Therefore, observing small phytoplankton is considered important research for monitoring environmental changes because these reasons are known to cause changes in the community structure of small phytoplankton with different biochemical characteristics compared to large phytoplankton.

Moreover, the biochemical characteristics of phytoplankton such as C:N ratio are critical for understanding marine biogeochemical processes responding to environmental conditions. Frigstad *et al.* (2014) reported higher C:N ratio related with low chlorophyll-*a* concentration and lower C:N ratio to high chlorophyll-*a* concentration in the Arctic Ocean. The C:N ratio could differ in various environmental conditions related to nutrients. However, little information on the small phytoplankton contribution to the total primary production and their biochemical traits such as C:N ratio is currently available in the northern Bering and Chukchi Seas.

In this study, our objectives are to investigate the dominant phytoplankton communities and to assess the relative contribution of small phytoplankton (0.7–2.0 μm; picophytoplankton) to the total primary production and their biochemical characteristics (e.g., C:N ratio) in the northern Bering and Chukchi Seas. Furthermore, this chapter investigate the correlation between the contribution of small phytoplankton and environmental factors. This chapter is preliminary research to be used for the validation of the PSC model of satellite data in the following chapter.

2.2. Methods

2.2.1. Study Area and Water Sampling

A couple of arctic research cruises was conducted in the Chukchi Sea onboard the icebreaker R/N Araon in 2016 (ARA07B) for 16 stations and mainly in the northern Bering Sea onboard T/S Oshoro-Maru in 2017 (OS040) for 9 stations. The ARA07B cruise was conducted in the northern Bering Sea and the Chukchi Sea during 5–19 August, 2016 onboard the Icebreaker R/V Araon (Figure 1; Table 2). As a total of 16 stations during the ARA07B cruises, only one station (st.1) was located in the northern Bering Sea and 15 stations were in the Chukchi Sea. Water was sampled by Niskin bottles on conductivity-temperature-depth (CTD)/rosette sampler for the total chlorophyll-*a* and size-fractionated chlorophyll measurement. Euphotic depths were measured by a Secchi disk (Kirk 1985). The OS040 cruise was executed mostly in the northern Bering Sea (8 stations) and partly in the southern Chukchi Sea (2 stations) during 9–21 July, 2017 onboard T/S Oshoro-Maru (Figure 1; Table 2). Physical properties and water samples were collected by CTD/rosette with Niskin bottles. The euphotic depths were calculated by comparing downward irradiance and surface irradiance measured by compact optical profiling system (C-OPS; Biospherical instrument Inc., San Diego, CA, USA).

2.2.2. Chlorophyll-*a* Analysis

The water samples were obtained from 6 different light depths (100%, 50%, 30%, 12%, 5% and 1% of the surface photosynthetically active radiation, PAR) for measuring the chlorophyll-*a* concentration. For the total chlorophyll-*a* concentration, 300 mL of seawater was filtered through 25 mm diameter glass fiber filter (GF/F; Whatman, 0.7 μm pore). To obtain size-fractionated chlorophyll-*a* concentration, 500 mL seawater was filtered through 20 μm and 2 μm pore size membrane filters (Whatman Nuclepore) and then 47 mm GF/F (Whatman, 0.7 μm pore) sequentially. After the filtration was done, the filters were wrapped with aluminum foil and stored at −80◦C freezer until analysis at the home laboratory. Chlorophyll-*a* was extracted by acetone following Parsons *et al.* (1984) and the concentrations were measured with a fluorometer (Turner Designs 10AU).

2.2.3. High-Performance Liquid Chromatography Analysis for Accessory Pigment Concentration

For high-performance liquid chromatography (HPLC) analysis, the water from 3 light depths (100%, 30% and 1%) were sampled during the ARA07B and OS040 cruises. Seawater (0.8–2.5 L) was passed through 2 μm membrane filter (Whatman Nuclepore) and 47 mm diameter GF/F (Whatman, 0.7 μm pore) filters to measure pigments concentration of small size phytoplankton (<2 μm) under gentle vacuum pressure (<13 kPa). Seawater (0.5–1.5 L) was filtered onto GF/F for pigments of total phytoplankton during the ARA07B. For the OS040, samples were obtained only for total phytoplankton. For avoiding degradation, the filters for HPLC analysis were immediately frozen as storing in liquid nitrogen on research vessel and kept in freezer at −80◦C until analysis at

home laboratory. In the laboratory, the filter samples were broken into small pieces and then soaked in 3 mL of N'N-dimethylformamide (DMF) with canthaxanthin served as an internal standard. After 20 min of sonication, the filters were extracted at 4◦C in dark for 24 h and then extracts were filtered through a 0.45 μm pore membrane filter (Whatman Nuclepore) to remove the fragments of GF/F. For minimizing photo-degradation of pigments, all the procedures were conducted under a low light condition. Pigments were analyzed using HPLC (Agilent Infinite 1260 in operation by JAMSTEC, Mutsu, Japan) with a ternary linear gradient system to separate each pigment. The pigment concentrations were calculated by the function of peak area, standard response factors and peak area of the internal standard following (Suzuki *et al.*, 2005). All the standards for each pigment were purchased from DHI in Denmark. The CHEMTAX software based on a factorization program was used for estimating the relative contributions of different phytoplankton communities to the total chlorophyll-*a* concentration (Wright *et al.*, 1991). The ratios of accessory pigments to chlorophyll-*a* for each phytoplankton taxon for the CHEMTAX program were based on marker pigment concentrations of algal groups present in the Arctic Ocean (Coupel *et al.*, 2015; Vidussi *et al.*, 2004) (Table 3). Since our two research cruises were in different periods and years, the final ratio matrix was separated for phytoplankton communities (Table 3). The contributions of diatoms. Dinoflagellates, Cryptophytes, Pelagophytes, Prasinophytes (Type 2 and 3), Chlorophytes, Haptophytes and *Phaeosystis* were estimated by the CHEMTAX program. Small phytoplankton community was estimated from HPLC results by the equations described in the literature (Wright *et al.*, 1991; Vidussi *et al.*, 2004). The relative proportions of the three size classes are derived from the concentrations of phytoplankton diagnostic pigments for the Chukchi and Bering Seas using the equations described in Fujiwara *et al.* (2011) and Fujiwara *et al.* (2014).

2.2.4. Particulate Organic Carbon and Primary Productivity

The water samples for particulate organic carbon (POC) and primary productivity (PP) were obtained from 6 light depths (100, 50, 30, 12, 5 and 1% of PAR). 300 mL of seawater was filtered through 0.7 μm GF/F (pre-combusted at 450 ◦C for 4 h) for total POC and 500 mL was passed through 2 μm pore size membrane filter (Whatman Nuclepore) and then filtered onto GF/F filter for small POC (0.7–2 μm). Carbon and nitrogen uptake experiments were conducted using a ^{13}C-^{15}N dual isotope tracer technique previously reported from the Chukchi Sea (Lee *et al.*, 2007; 2009). After a 4 h incubation on deck, 300 mL water was filtered onto pre-combusted GF/F for total PP and 500 mL water was filtered through 2 μm pore size membrane filter (Whatman Nuclepore) and sequentially onto GF/F filter for small phytoplankton productivity (0.7–2 μm). The filters were immediately preserved and stored in a freezer (−20 ℃) until further mass spectrometric analysis using a Delta V+ Isotope Ratio Mass Spectrometers at Alaska Stable Isotope Facility in the University of Alaska Fairbanks, USA for ARA07B samples and using a 20–22 Isotope Ratio Mass Spectrometer (SERCON) at Japan Agency for Marine-Earth Science and Technology (JAMSTEC, Mutsu, Japan) for OS040 samples after HCl fuming overnight to remove carbonate. The carbon and nitrogen uptake rates were calculated based on Hama *et al.* (1983).

2.2.5. Freshwater contents

FWC were calculated following Carmack *et al.* (2008) with reference salinity 34.8 psu (S_{ref} = 34.8; the average salinity of the Arctic Ocean; Aagaard and Carmack, 1989; Serreze *et al.*, 2006; Holland *et al.*, 2007; Haine *et al.*, 2015). The equation of FWC calculation following Carmack *et al.* (2008) :

$$FWC = \int_{Z_{lim}}^{0} \left(1 - \frac{S(z)}{S_{ref}}\right) dz$$

, where FWC is freshwater contents at a specific depth (m), S(z) and S_{ref} are the *in-situ* salinity (psu) on specific depth (m) and reference salinity, Z_{lim} is the depth where S equals S_{ref}.

2.2.6. Statistical Analysis

Student's t-test was applied to verify correlations among factors and differences between the mean values of POC:chlorophyll-*a* ratio, PON:chlorophyll-*a* ratio, C:N ratio of each cruise and size group. The agglomerative hierarchical clustering (AHC) with Ward's method (XLSTAT software, Addinsoft, Boston, MA, USA) was performed to calculate the dissimilarity in observed 20 variables; temperature and salinity), size-fractionated PP, POC of each size, size-fractionated chlorophyll-*a* and accessory pigments, among stations.

2.3. Results and Discussion

2.3.1. Physical oceanographic condition

The temperature for the OS040 were from –1.1 to 13.3°C (mean ± SD = 6.2 ± 3.6°C) and the salinity ranged from 28.9 to 32.9 (mean ± SD = 31.7 ± 0.9). Water mass at the most stations in the northern Chukchi corresponded to melting glacier water, which called Ice melt water (IMW; temperature <2.0°C and salinity <30.0) and Bering Chukchi winter water (BCWW; −2–0°C and <30–33.5 for temperature and salinity; Danielson *et al.*, 2017) during the ARA07B cruise. Other stations during the ARA07B were influenced by Bering shelf water (BSW; 0.0–10.0°C and 31.8–33.0 for temperature and salinity). During the OS040 cruise, the relatively warm and low salinity Alaskan coastal water (ACW; 2.0–13.0°C and <31.9 for temperature and salinity) and the warm and saline Bering shelf water (BSW) were predominant (Figure 2). The Bering shelf Anadyr water (BSAW; −1.0–2.0°C and 31.8–33.0 for temperature and salinity), which is a mixed BSW with cold/saline Anadyr water (AW; Coachman *et al.*, 1975; Springer *et al.*, 1989), was observed at some stations for the OSO40.

2.3.2. Distribution of size fractionated chlorophyll-*a* concentration

The average euphotic depths were 45.6 m (SD = ± 22.2 m) for the ARA07B cruise and 23.8 m (SD = ± 9.1 m) for the OS040 cruise, respectively. In ARA07B, Chlorophyll-*a* concentrations were 0.02–1.3 mg chl-*a* m^{-3} (mean ± SD = 0.2 ± 0.3 mg chl-*a* m^{-3}) at surface, 0.02–15.0 mg chl-*a* m^{-3} (mean ± SD = 1.0 ± 2.5 mg chl-*a* m^{-3}) for euphotic layer. In OS040, Chlorophyll-*a* concentrations were 0.002–5.5 mg chl-*a* m^{-3} (mean ± SD = 0.7 ± 1.4 mg chl-*a* m^{-3}) at surface, 0.002–5.5 mg chl-*a* m^{-3} (mean ± SD = 1.6 ± 2.2 mg chl-*a* m^{-3}) for euphotic layer. Within the euphotic zone, integral chlorophyll-*a* concentrations were 3.2–172.1 mg chl-*a* m^{-2} (mean ± SD = 34.2 ± 48.0 mg chl-*a* m^{-2}) during the ARA07B and 12.3–107.8 mg chl-*a* m^{-2} (mean ± SD = 45.4 ± 34.1 mg chl-a m^{-2}) for the OS040, respectively (Figure 3). The average euphotic-depth integral chlorophyll-*a* concentrations in this study are within the range reported previously in the northern Bering Sea and the Chukchi Sea (Lee *et al.*, 2007; 2013; Yun *et al.*, 2016).

The chlorophyll-*a* contributions of each size phytoplankton (pico-, nano- and micro-phytoplankton) to the total phytoplankton were plotted in Figure 4 for the three different depths (100, 30 and 1% of light depths) at every station of the ARA07B and only surface for the OS040. The contributions of small phytoplankton to the total chlorophyll-*a* concentrations were found largely variable among the stations during both cruises.

The contributions of small phytoplankton to the total chlorophyll-*a* concentrations ranged from 2.9% to 71.1% with a depth-integrated average of 32.2% (SD = ± 23.1%) during the ARA07B. In the ARA07B, the dominant size group of phytoplankton was micro-phytoplankton (mean ± SD = 43.5 ± 29.7% of chlorophyll-*a* concentration) followed by pico-phytoplankton (32.1 ± 23.1%) and nano-phytoplankton (24.3 ± 9.1%) during the observation period. In the Chukchi Sea, large phytoplankton are generally dominant although the areal distribution of their contribution mostly depends on local water masses in different nutrient conditions (Lee *et al.*, 2007; 2013). Normally, large phytoplankton growing under nutrient-enriched conditions are predominant in AW or BSW, whereas small phytoplankton are dominant in nutrient-depleted ACW (Lee *et al.*, 2007; 2013). Our average contribution of small phytoplankton is relatively higher than that value (24.8 ± 23.0%) previously reported by Lee *et al.* (2013) in the Chukchi Sea during the middle of August to early September 2004. By contrast, our average contribution of small phytoplankton is relatively lower than that value (55.1 ± 26.8%) from the study by Yun *et al.* (2015) that was conducted in the northern Chukchi Sea during mid-July–mid-August, 2012. This difference among the studies could be caused by different regions with non-homogeneous nutrient conditions and different observation periods with a seasonal phytoplankton succession. The relative contribution of small phytoplankton could be caused by freshwater content in the Chukchi Sea since the nutrient concentrations and primary production rates of phytoplankton are largely governed by the nutrient-depleted freshwater content in the Chukchi Sea (Yun *et al.*, 2016; Yun *et al.*, 2014).

In comparison to the Chukchi Sea, the contributions of small phytoplankton were 0.7–80% (mean ± SD = 37.2 ± 31.0%) to the total chlorophyll-*a* concentration in the northern Bering Sea for the OS040 in this study. The proportions of different size chlorophyll-*a* were 40.2% (± 35.4%), 22.5% (± 10.5%) and 37.2% (± 31.3%) for micro-, nano- and pico-phytoplankton, respectively, during our observation period in 2017. In the northern Bering

Sea, the dominant size groups of phytoplankton are generally nano- and micro-phytoplankton based on PSC results derived from satellite ocean color data from 1998 to 2016 (Lee *et al.*, 2019). The overall dominant size of phytoplankton is composed of nano-phytoplankton (49.0 ± 9.6%), followed by micro-phytoplankton (34.9 ± 8.0%) and pico-phytoplankton (16.1 ± 7.3%) in the Chirikov Basin of the northern Chukchi Sea (Lee *et al.*, 2019). However, the chlorophyll-*a* contributions of small phytoplankton are largely variable among different seasons (Lee *et al.*, 2012). The average contribution of small phytoplankton was 14.8% in late May to early June during the phytoplankton bloom period and largely increased up to 50.0% in middle June after the bloom (Lee *et al.*, 2017b). Consistently, Coupel *et al.* (2015) found a seasonal increasing contribution of small phytoplankton in the northern Bering Sea (around Chirikov Basin) from May (5.2%) to July (31.8%). In addition to the seasonal variation, it was found that spatial variation of the biochemical environmental conditions in the northern Bering Sea are also generally influenced by northward advection of AW, BSW and ACW (Lee *et al.*, 2007; Grebmeir *et al.*, 2015). Over recent decades, several environmental changes have been reported in the northern Bering Sea (Bluhm and Gradinger 2008; Grebmeier *et al.*, 2015). A steady increasing trend in the annual contribution of small phytoplankton is distinct in the Chirikov Basin from 1998 to 2016, although no significantly strong relationship was observed between the annual contribution of small phytoplankton and SST (Lee *et al.*, 2019). Long-term changes in dominant phytoplankton communities should be monitored for Arctic marine ecosystems under ongoing environmental changes. Especially, the contribution of small phytoplankton could be used as one of indicators for changing marine ecosystems.

2.3.3. Major dominant phytoplankton groups predicted by pigments composition

The euphotic depth-integral concentrations of marker pigments from the two cruises are shown in Figure 5. Fucoxanthin (a marker pigment of diatoms), chlorophyll-*c*1+*c*2 and chlorophyll-*b* (a marker pigment of chlorophytes) were major accessory pigments during the ARA07B, although the pigment compositions spatially varied significantly across the stations. Among the pigments, fucoxanthin was the most dominant pigment with an average value of 12.58 ± 21.8 mg m^{-2} and the second and third predominant pigments were chlorophyll-c1+c2 (4.04 ± 4.83 mg m^{-2}) and chlorophyll-b (2.64 ± 2.53 mg m^{-2}). Previous studies reported that fucoxanthin dominating the Chukchi shelf is a typical characteristic during fall (Fujiwara *et al.*, 2011; Coupel *et al.*, 2015). For the small phytoplankton group for the ARA07B (data not shown), major predominant pigments were chlorophyll-*b* (1.59 ± 1.83 mg m^{-2}), fucoxanthin (1.46 ± 1.47 mg m^{-2}) and chlorophyll-*c*1+*c*2 (0.65 ± 0.62 mg m^{-2}). In comparison, fucoxanthin, chlorophyll-c1+c2 and peridinin (a marker pigment of dinoflagellates) were major accessory pigments for the OS040. Fucoxanthin was the most dominant pigment with an average value of 23.03 ± 19.89 mg m^{-2}, followed by chlorophyll-c1+c2 (9.35 ± 7.23 mg m^{-2}) and peridinin (7.54 ± 9.89 mg m^{-2}) for the OS040. High proportions of diatom-related pigments (fucoxanthin, chlorophyll-*c*1+*c*2) were observed in both cruise periods. Small diatoms appeared to be major phytoplankton communities for the small phytoplankton group during the ARA07B, based on the high proportions of chlorophyll-b and fucoxanthin. No pigment data were available for the small phytoplankton during the OS040 cruise.

Based on the CHEMTAX results, eight major phytoplankton communities were identified in the study area (Figure 6). Diatoms (43.1% ± 31.5%) and *Phaeocystis* (33.2% ± 14.9%) were co-dominated during the ARA07B. In comparison, diatoms were the most dominant community (46.1 ± 17.3%) and the second dominant community was Prasinophyte (Type 2) (11.8% ± 5.3%) for the OS040. Micro-phytoplankton communities were most dominant (59.7 ± 30.5%), followed by nano-phytoplankton (11.5 ± 9.7%) and pico-phytoplankton (28.9 ± 23.5%) during the ARA07B. For the OS040, micro-phytoplankton contributed 51.5% (± 18.2%) of the total chlorophyll a concentration. In comparison, nano-phytoplankton and pico-phytoplankton contributed 11.0% (± 10.5%) and 37.5% (± 15.7%), respectively. The relative proportions of the three size classes based on the diagnostic pigments from HPLC are different from those of the size-fractionated chlorophyll-*a* concentrations (Figure 4). This is probably due to a simple assumption that diatom-related pigments belong to the micro-phytoplankton although small diatoms (<2 μm) could rather contribute to the phytoplankton group.

2.3.4. Contribution of small phytoplankton to primary production

The daily primary productivities of total phytoplankton which were integrated over the euphotic zone at each station were 33.9–811.8 mg C m^{-2} d^{-1} (mean ± SD = 142.6 ± 205.7 mg C m^{-2} d^{-1}) for the ARA07B and 202.1–3100.1 mg C m^{-2} d^{-1} (mean ± SD = 942.1 ± 969.9 mg C m^{-2} d^{-1}) for the OS040 (Figure 7). In comparison, the daily primary productivities of small phytoplankton ranged from 4.9 to 227.7 (mean ± SD = 42.3 ± 53.1 mg C m^{-2} d^{-1}) and 56.1 to 322.2 mg C m^{-2} d^{-1} (mean ± SD = 152.8 ± 85.2 mg C m^{-2} d^{-1}) for the ARA07B and the OS040, respectively (Figure 8). The contribution of small phytoplankton to the total PP ranged from 8.1 to 71.7% (mean ± SD = 38.0 ± 19.9%) for the ARA07B and from 6.0 to 40.3% (mean ± SD = 25.0 ± 12.8%) for the OS040 (Figure 9). In analyzing POC and PON in this study, the C/N ratio (mean ± S.D. = 15.2 ± 5.2) and $\delta^{13}C$ (mean ± S.D. = -28.6 ± 2.7 ‰ VPDB) of filtered samples were considered. Based on these results, the C/N ratio of this study was slightly higher than the expected Redfield ratio. Despite the relatively high C/N ratios, a significantly linear relationship was found between the POC and chlorophyll-a concentration (R^2=0.66), PON and chlorophyll-a concentration (R^2=0.68). And the carbon stable isotope ratios of POC fell in the previously reported range of POC which was mainly composed of Arctic marine autotrophs.

Biochemical compositions (POC:chlorophyll-*a*, PON:chlorophyll-*a* and C:N ratios) were compared between small and large phytoplankton in Figure 11. Large phytoplankton group has relatively lower POC:chlorophyll-*a* ratios (*t*-test, $p < 0.01$) which were 78.0–3549.0 (mean ± SD = 1358.6 ± 1170.8) for the ARA07B and 41.4–340.2 (mean ± SD = 173.8 ± 110.4) for the OS040 (Figure 9a). In comparison, POC:chlorophyll-*a* ratios of small phytoplankton were 408.5–6547.4 (mean ± SD = 2590.2 ± 1523.0) for ARA07B and 274.9–2303.6 (mean ± SD = 623.4 ± 639.2) for the OS040. The PON:chlorophyll-*a* ratio of large phytoplankton was 1.9–184.2 (mean ± SD = 62.4 ± 48.7) whereas the ratio of small phytoplankton ranged from 50.0 to 328.7 (mean ± SD = 211.9 ± 88.3) for the ARA07B (no data for OS040). The C:N ratios were 7.5–251.9 (mean ± SD = 34.1 ± 58.9) for large phytoplankton and 7.0–19.9 (mean ± SD = 11.9 ± 3.8) for small phytoplankton during the ARA07B cruise. Small phytoplankton showed a comparatively higher POC:chlorophyll-*a* ratio than

large phytoplankton during both cruises (Figure 11). This result is consistent with the previous result in the Chukchi Sea, which suggests that higher carbon contents per unit of chlorophyll-*a* concentration in small phytoplankton in comparison to large phytoplankton (Lee *et al.*, 2013). In the Antarctic Ocean, Lee *et al.* (2012) observed the consistent results in non-polynya and polynya regions in the Amundsen Sea. A similar pattern was observed for the PON:chlorophyll-*a* ratio in this study. However, the C:N ratios of small phytoplankton were lower than those of large phytoplankton in this study. Similarly, the overall C:N assimilation ratio of small phytoplankton was previously reported as significantly lower than that value of large phytoplankton (Lee *et al.*, 2013). These results are consistent with the result in the Gulf of St. Lawrence, Canada (Hodal and Kristiansen, 2008). In the Antarctic Ocean, the similar result was obtained in the Amundsen Sea (Lee *et al.*, 2012). The C:N ratios were negatively correlated with chlorophyll-*a* concentrations for small and large phytoplankton in this study ($R^2 > 0.6$). However, there was no statistically significant difference in the relationship between small and large phytoplankton ($p>0.05$; Figure 11).

Overall, the primary productions of total and small phytoplankton communities during the study period were different depending on the sea area. Indeed, agglomerative hierarchical clustering (AHC) analysis based on 25 stations and phytoplankton size-related variables sorted stations into three distinct groups (Figure 10; Table 4). The clustering was based on a Euclidean distance of 1000. Cluster A include station 1 of OS040 and station 7 of OS040 that was extremely high primary productive region (2547 mg C m^{-2} d^{-1}) near Bering strait. Cluster A had the lowest contribution of small phytoplankton in PP (6.4%) and surface chlorophyll-*a* (1.8%). The physical properties of Cluster A (4.5°C and 32.7 psu). This cluster is influence by BSW (Lee *et al.*, 2007; 2013). Cluster B contains all the stations of the northern Chukchi Sea and two stations of the Bering Sea. The stations form Cluster B had a lower productivity and lower concentration of surface chlorophyll-*a*. In Cluster B, small phytoplankton contribution was the highest among the clusters. 40.5% of primary production, 39.1% of surface chlorophyll-*a* were contributed by small phytoplankton, 40.9% of POC were contributed by small POC. Dominant water mass, IMW can explain the high contribution of small phytoplankton in Cluster B because IMW has nutrient-depleted water from sea ice melting (Danielson *et al.*, 2017). Cluster C includes most of the stations in the Bering Sea and 3 stations of the southern Chukchi sea in ARA07B. Cluster C had a lower productivity (559.2 mg C m^{-2} d^{-1}) than cluster A but higher than cluster B. Cluster C seems to be affected by nutrient-depleted ACW but not too low productivity for Cluster C. This suggests that water masses that had an effect on Cluster C were not only ACW but also other source such as mixed water of AW, ACW and BSW.

The primary production contributions of small phytoplankton are rather different from their chlorophyll-*a* contributions in this study. Normally, the contributions of small phytoplankton are higher to primary production in comparison to those in chlorophyll-a concentrations in the polar oceans (Lee *et al.*, 2012;2013) and temperate oceans (Lee *et al.*, 2017a). This is probably due to the considerably higher POC contribution of small phytoplankton (and consequently higher production contributions of small phytoplankton) than the chlorophyll-*a* contribution (Lee *et al.*, 2013;2017a;2017b). We also observed the higher POC:chlorophyll-*a* ratio in small phytoplankton than large phytoplankton during both cruises (Figure 11) as discussed later. However, the case in the northern Bering Sea in this study is against the general pattern previously reported. The lower contribution of

small phytoplankton was observed in the primary production rather than chlorophyll-*a* concentration in the northern Bering Sea. This indicates higher standing stock (represented by chlorophyll-*a* concentrations) of small phytoplankton but their significantly lower contribution to the primary productions in the northern Bering Sea during this study than in other studies. Lim *et al.* (2019) argued that seasonal increasing contribution of small phytoplankton is not caused by their increasing biomass and photosynthetic rate but caused by relative declining in biomass and photosynthetic rate of large phytoplankton in the Amundsen Sea, Antarctic Ocean. Based on these results, the biomass of large phytoplankton could have had decreased faster than their photosynthetic rate in the northern Bering Sea during our observation period.

The regional contributions of small phytoplankton to the primary production are summarized at various regions in the Arctic Ocean (Table 5). The average contribution of small phytoplankton in this study is comparable to the previous results in the Chukchi Sea. However, it is considerably lower than those (average ± SD = 56.7 ± 20.0%) in the Kara, Laptev and East Siberian Seas (Bhavya *et al.*, 2018). Similarly, Lee *et al.* (2012) found a similar contribution (average ± SD = 60 ± 7.9%) of small phytoplankton in the high northern Chukchi Sea and Canada Basin. Because of no data in the northern Bering Sea, the small phytoplankton contribution to the primary production in this study could not be compared. Regionally, the primary production contribution of small phytoplankton in the northern Bering Sea (average ± SD = 25.0 ± 12.8%) is considerably lower than those in others (Table 5). At this point, we do not know whether this is a latitudinal pattern (i.e., increasing contribution of small phytoplankton in higher latitude) or simply seasonal difference among the different regions in the Pacific Arctic Ocean. Indeed, Lee *et al.* (2019) found a seasonal patterns of different phytoplankton size compositions with increasing contribution of small phytoplankton in the northern Bering Sea. Since the seasonal contribution of small phytoplankton to the primary production would be different, further seasonal observations on the small phytoplankton contribution to the primary production will be warranted for better understanding their ecological roles in the Bering and Chukchi Seas.

2.3.5. Small phytoplankton contribution and FWC

Yun *et al.* (2016) has reported that an increase in FWC is associated with a decrease in the total PP. However, the relationship between the total PP and FWC did not show any correlation (Figure 12a, R^2 <0.1). When phytoplankton were categorized by two size group, a conspicuous correlation with FWC was observed (Figure 12). The PP of small phytoplankton exhibited an increasing trend as FWC rose, and this pattern was consistent in the size-specific proportions of the PP. This study found that the contribution of small phytoplankton and FWC has strong positive relationship on the northern Chukchi Sea (Figure 12b; R^2=0.6639). In addition to the contribution ratio, the productivity of small phytoplankton also exhibited a positive correlation with FWC (Figure 12a, R^2= 0.5554). In biomass, the pattern appeared somewhat differently. While the contribution of small chlorophyll-*a* contribution (%) showed a strong proportional relationship with FWC, there was little correlation observed in Chlorophyll-*a* concentration. It was revealed that only small chlorophyll-*a* concentration exhibited a weak proportional relationship with FWC (Figure 12c,d). In summary, there is no significant relationship between the total PP or total biomass (chlorophyll-*a* concentration) and FWC. However, when phytoplankton is categorized by size groups, distinct relationships become evident. With an increase in FWC, there is an observed increase in

both PP and biomass of small phytoplankton, while the PP and biomass of large phytoplankton decrease. Yun *et al.* (2016) suggested that this relationship associated with variation in nitrate inventory, regulated by the nitracline. The high efficiency of regenerated-nitrite utilization by small phytoplankton could explain this phenomenon. From this, we could infer that small phytoplankton might be crucial primary producers in nitrate-depleted ocean. Additionally, minimal changes in the PP and total biomass of phytoplankton, despite alterations in their composition, suggest the potential for ecological shifts within the ecosystem. Changes in environmental factors such as wind stress, ice melting, and river runoff could further emphasize the role of small phytoplankton with changing FWC.

However, since the above research results are based on a limited season accessible by ship, further studies covering the entire period from May to October are necessary to understand the relationship between FWC and small phytoplankton throughout the entire season. Together with these results, we could conclude that small phytoplankton incorporate more nitrogen in relation to carbon into their bodies and thus produce nitrogen-rich organic matters which could be relatively faster regenerated than carbon-rich organic matters such as carbohydrates. This conclusion is consistent with previous studies, which highlighted that small phytoplankton utilize nitrogen efficiently (Bhavya *et al.*, 2018) and regenerate faster than carbon-rich organic matter (Kim *et al.*, 2018). Therefore, the study for small phytoplankton which could be an important basic food source in the Arctic ecosystem should be further conducted under the current warming ocean scenario.

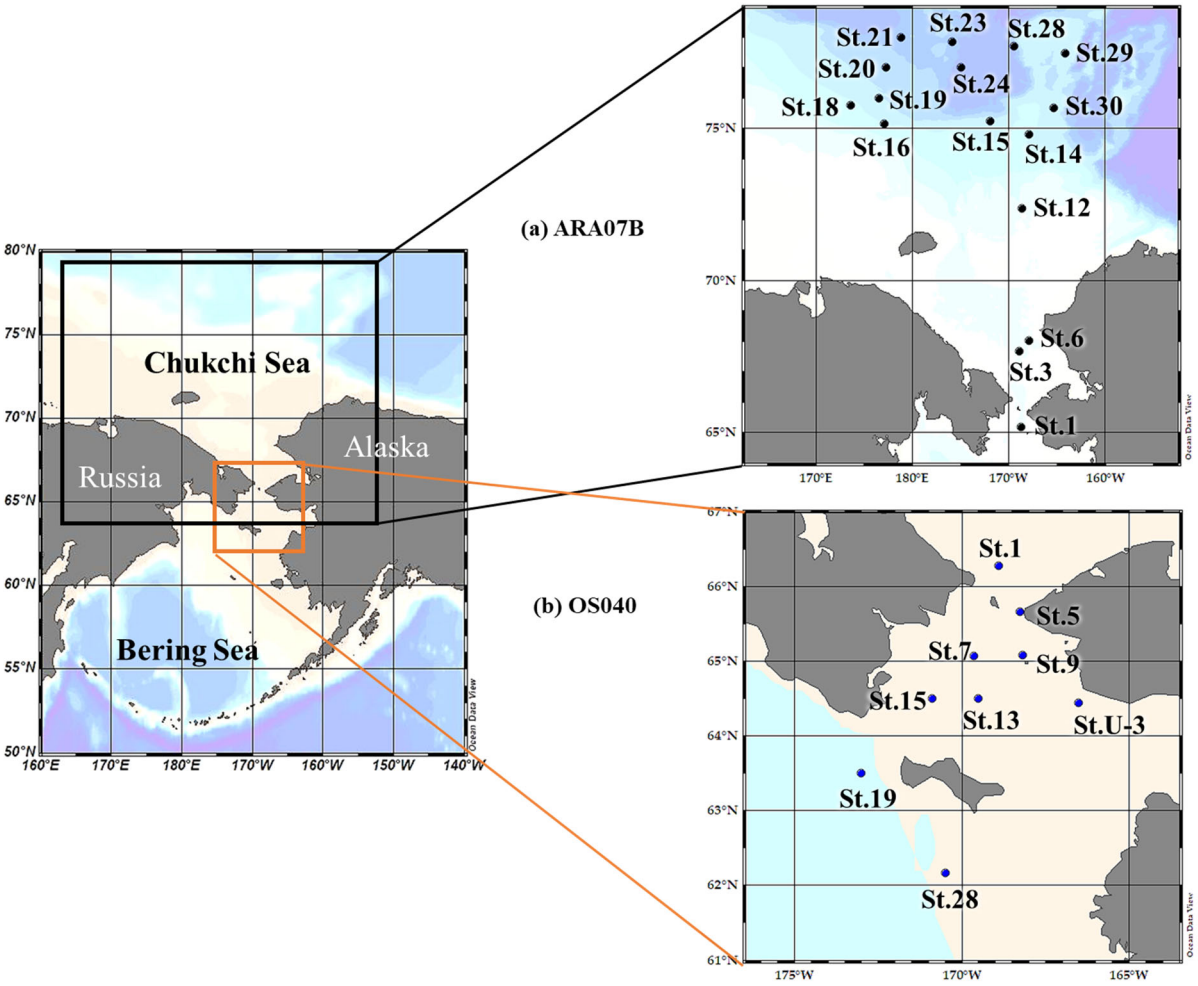

Figure 1. Study area of (a) ARA07B and (b) OS040. A couple of arctic research cruises was conducted in the Chukchi Sea onboard the icebreaker R/N Araon in 2016 (ARA07B) for 16 stations and mainly in the northern Bering Sea onboard T/S Oshoro-Maru in 2017 (OS040) for 9 stations.

Table 2. Sampling locations in the Northern Bering and Chukchi Seas. 16 stations for ARA07B, 9 stations for OS040 were sampled.

	Station	Date	Latitude (°N)	Longitude (°E)	Bottom depth (m)
ARA07B	st. 1	5 Aug 2016	65.17	−168.69	49
	st. 3	6 Aug 2016	67.67	−168.96	50
	st. 6	6 Aug 2016	68.01	−167.87	52.3
	st. 12	8 Aug 2016	72.36	−168.67	55
	st. 14	9 Aug 2016	74.80	−167.90	223
	st. 15	17 Aug 2016	75.24	−171.98	512
	st. 16	10 Aug 2016	75.15	−176.00	331.57
	st. 18	11 Aug 2016	75.77	177.07	486
	st. 19	12 Aug 2016	76.00	173.60	282
	st. 20	12 Aug 2016	77.00	176.57	1232
	st. 21	13 Aug 2016	78.00	177.28	1693
	st. 23	15 Aug 2016	77.87	−175.91	1564
	st. 24	16 Aug 2016	77.00	−175.00	2008
	st. 28	18 Aug 2016	77.70	−169.50	1756
	st. 29	18 Aug 2016	77.47	−164.12	280
	st. 30	19 Aug 2016	76.58	−165.38	987
OS040	1	9 Jul 2017	66.28	−168.90	57
	5	11 Jul 2017	65.66	−168.26	45
	7	12 Jul 2017	65.06	−169.64	51
	9	14 Jul 2017	65.07	−168.19	42
	U−3	16 Jul 2017	64.44	−166.52	27
	13	17 Jul 2017	64.50	−169.52	42
	15	18 Jul 2017	64.50	−170.89	46
	19	19 Jul 2017	63.50	−173.02	66
	23	21 Jul 2017	62.17	−170.50	46

Table 3. Pigment: chlorophyll-*a* ratio for nine algal groups referred to Ardyna *et al.* (2020). CHEMTAX initial ratio matrix and final pigment ratios obtained by CHEMTAX on the pigment data. Abbreviations: chlorophyll-*b* (chl-b), chlorophyll-*c*3 (chl-c3), fucoxanthin (fucox), peridinin (period), alloxanthin (allox), 190-butanoyloxyfucoxanthin (19butfu), 190-hexanoyloxyfucoxanthin(19hexfu), chlorophyll-*c*1+*c*2 (chl-c), neoxanthin (neox), prasinoxanthin (prasinox), lutein (lut). Chrysophytes and Pelagophytes (Cryso-pelago). Prasinophytes type 2 (Prasino-2), Prasinophytes type 3 (Prasino-3), Haptophytes (Hapto-7).

Class	chl-b	chl-c3	fucox	perid	allox	19butfu	19hexfu	chl-c	neox	prasinox	lut
Initial ratio matrix											
Diatoms	0	0	0.425	0	0	0	0	0.171	0	0	0
Dinoflagellates	0	0	0	0.6	0	0	0	0	0	0	0
Cryptophytes	0	0	0	0	0.673	0	0	0	0	0	0
Chryso-Pelago	0	0.114	0.285	0	0	0.831	0	0.285	0	0	0
Prasino-2	0.812	0	0	0	0	0	0	0	0.033	0	0.096
Prasino-3	0.764	0	0	0	0	0	0	0	0.078	0.248	0.009
Chlorophytes	0.339	0	0	0	0	0	0	0	0.036	0	0.187
Phaeocystis	0	0.208	0.35	0	0	0	0	0	0	0	0
Hapto-7	0	0.171	0.259	0	0	0.013	0.491	0.276	0	0	0
ARA07B Final ratio matrix											
Diatoms	0	0	0.785	0	0	0	0	0.395	0	0	0
Dinoflagellates	0	0	0	0.6	0	0	0	0	0	0	0
Cryptophytes	0	0	0	0	0.673	0	0	0	0	0	0
Chryso-Pelago	0	0.114	0.285	0	0	0.831	0	0.285	0	0	0
Prasino-2	0.593	0	0	0	0	0	0	0	0.007	0	0.007
Prasino-3	4.006	0	0	0	0	0	0	0	0.166	0.803	0.027
Chlorophytes	0.339	0	0	0	0	0	0	0	0.036	0	0.187
Phaeocystis	0	0.1791	0.301	0	0	0	0	0	0	0	0
Hapto-7	0	0.171	0.259	0	0	0.013	0.508	0.276	0	0	0
OS040Final ratio matrix											
Diatoms	0	0	0.722	0	0	0	0	0.328	0	0	0
Dinoflagellates	0	0	0	1.409	0	0	0	0	0	0	0
Cryptophytes	0	0	0	0	0.673	0	0	0	0	0	0
Chryso-Pelago	0	0.114	0.285	0	0	0.831	0	0.285	0	0	0
Prasino-2	0.812	0	0	0	0	0	0	0	0.033	0	0.096
Prasino-3	0.280	0	0	0	0	0	0	0	0.107	0.471	0.011
Chlorophytes	0.643	0	0	0	0	0	0	0	0.029	0	0.969
Phaeocystis	0	0.558	1.457	0	0	0	0	0	0	0	0
Hapto-7	0	0.171	0.259	0	0	0.013	0.617	0.276	0	0	0

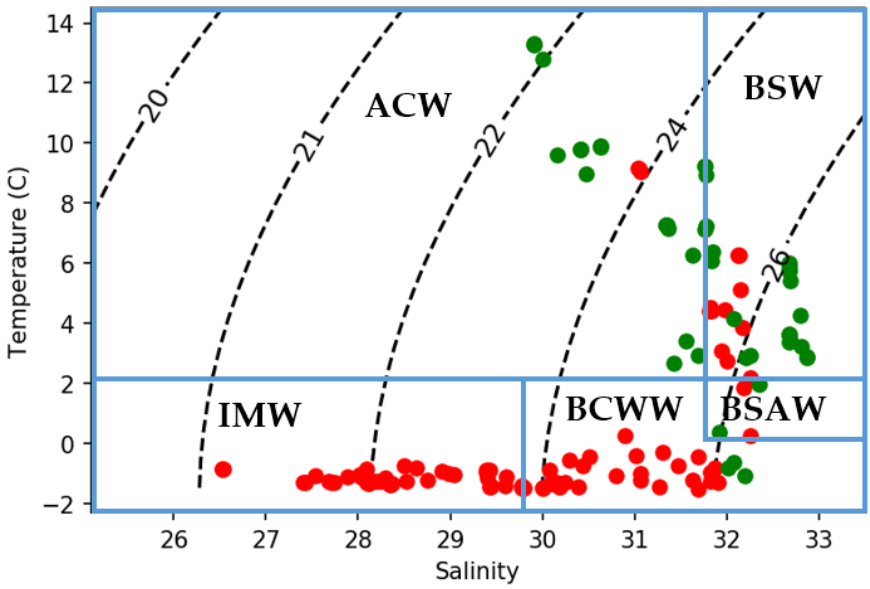

Figure 2. T–S diagram in the ARA07B (Red) and OS040 (Green) in euphotic zone. Alaskan coastal water (ACW), Bering Shelf water (BSW), ice melt water (IMW), Bering-Chukchi winter water (BCWW), Bering Sea Anadyr water (BSAW). The data were obtained from the water of light depths 100%, 50%, 30%, 12%, 5% and 1% in PAR.

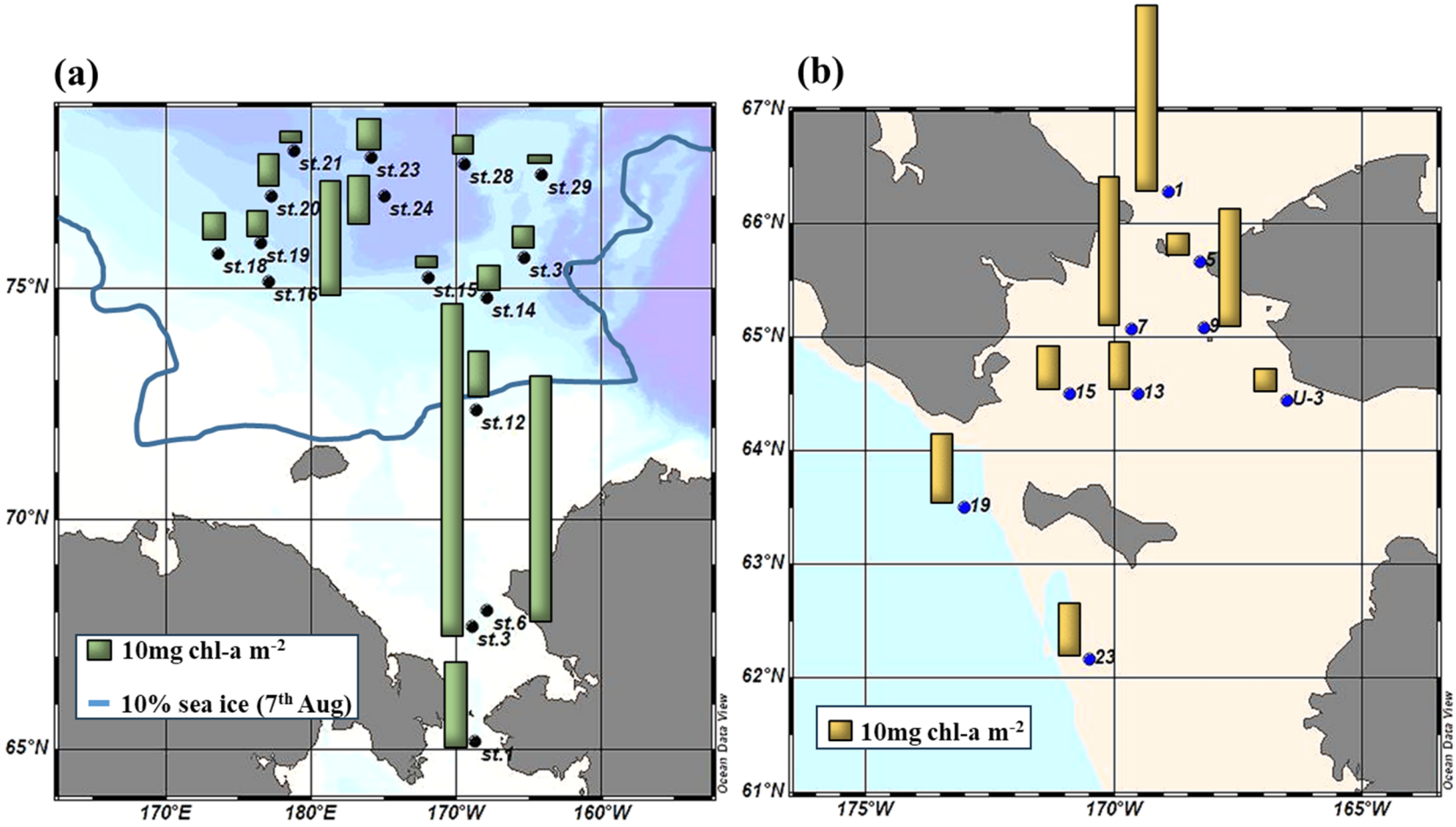

Figure 3. Spatial distributions of column-integrated chlorophyll-*a* concentration of (a) ARA07B and (b) OS040. The blue line is 10% of sea ice concentration in Aug, 7th, 2016.

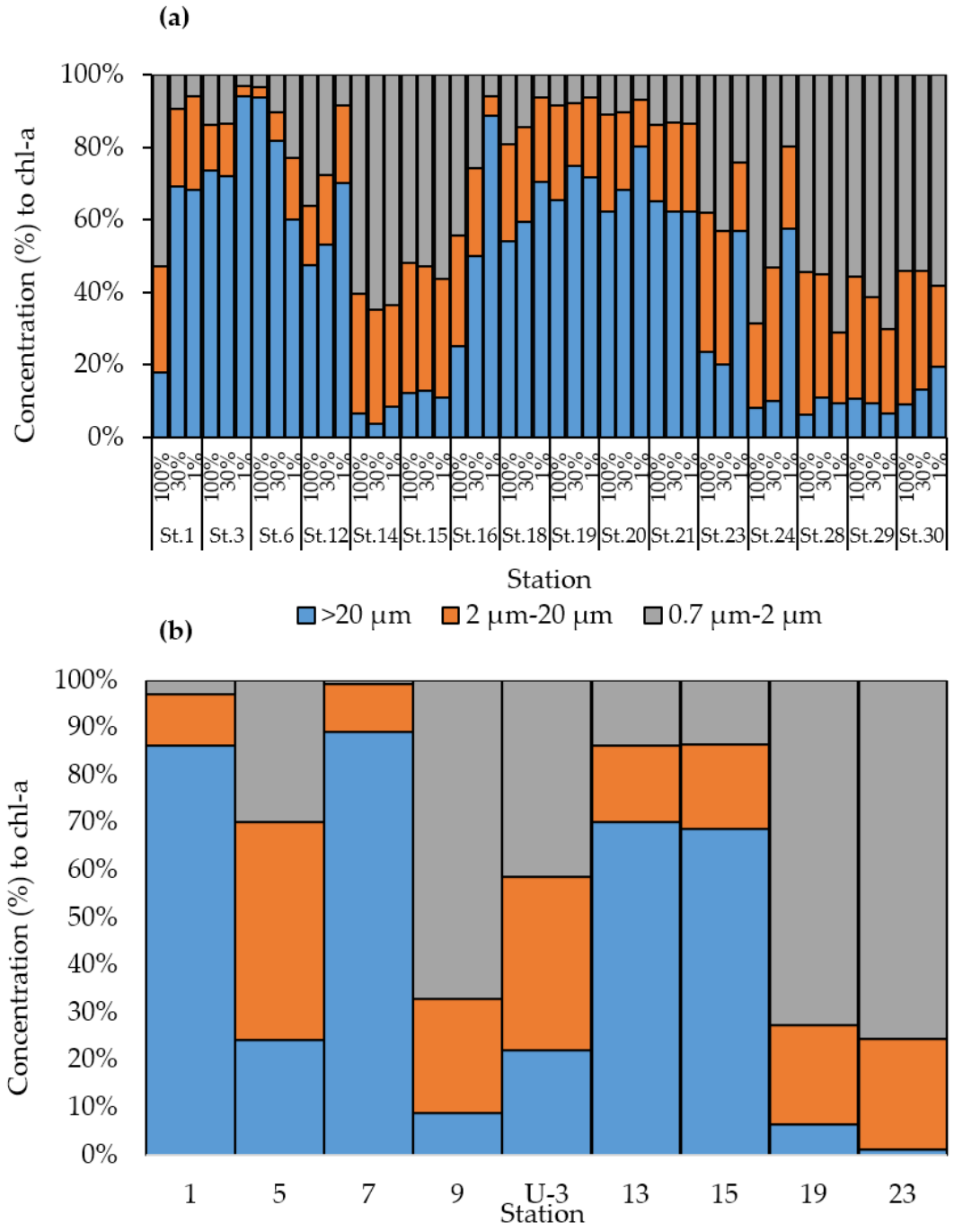

Figure 4. Composition of size fractions in chlorophyll-*a* concentration during (a) ARA07B and (b) OS040 cruises.

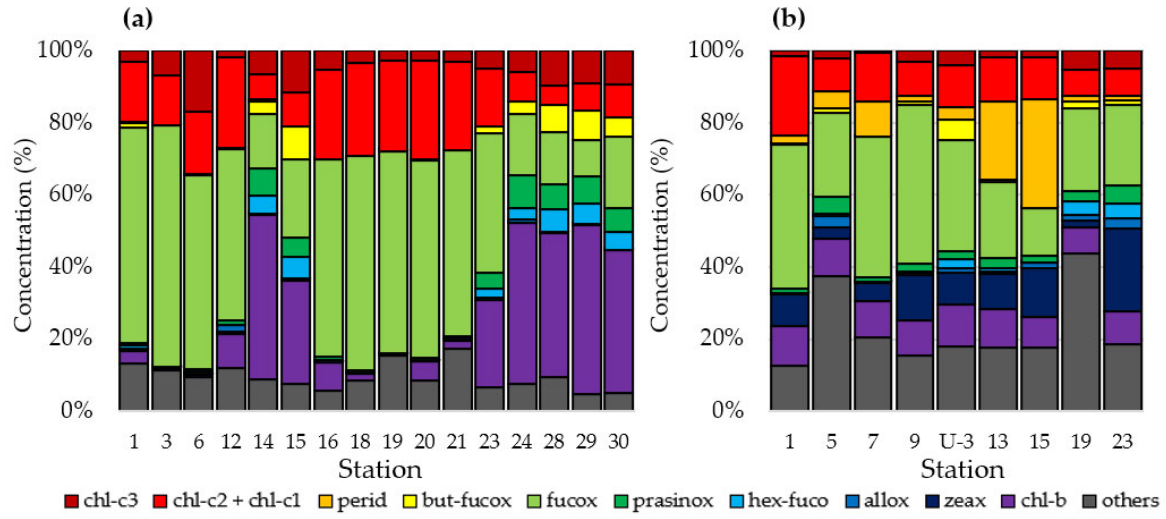

Figure 5. Pigment compositions of total phytoplankton in the (a) ARA07B (b) OSO040.

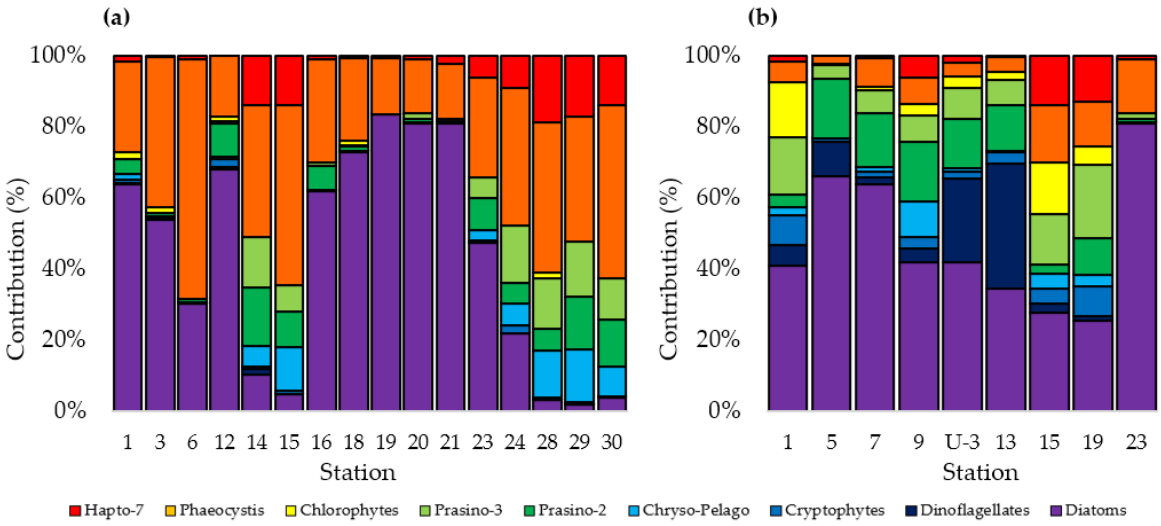

Figure 6. Phytoplankton community compositions of (a) ARA07B and (b) OS040.

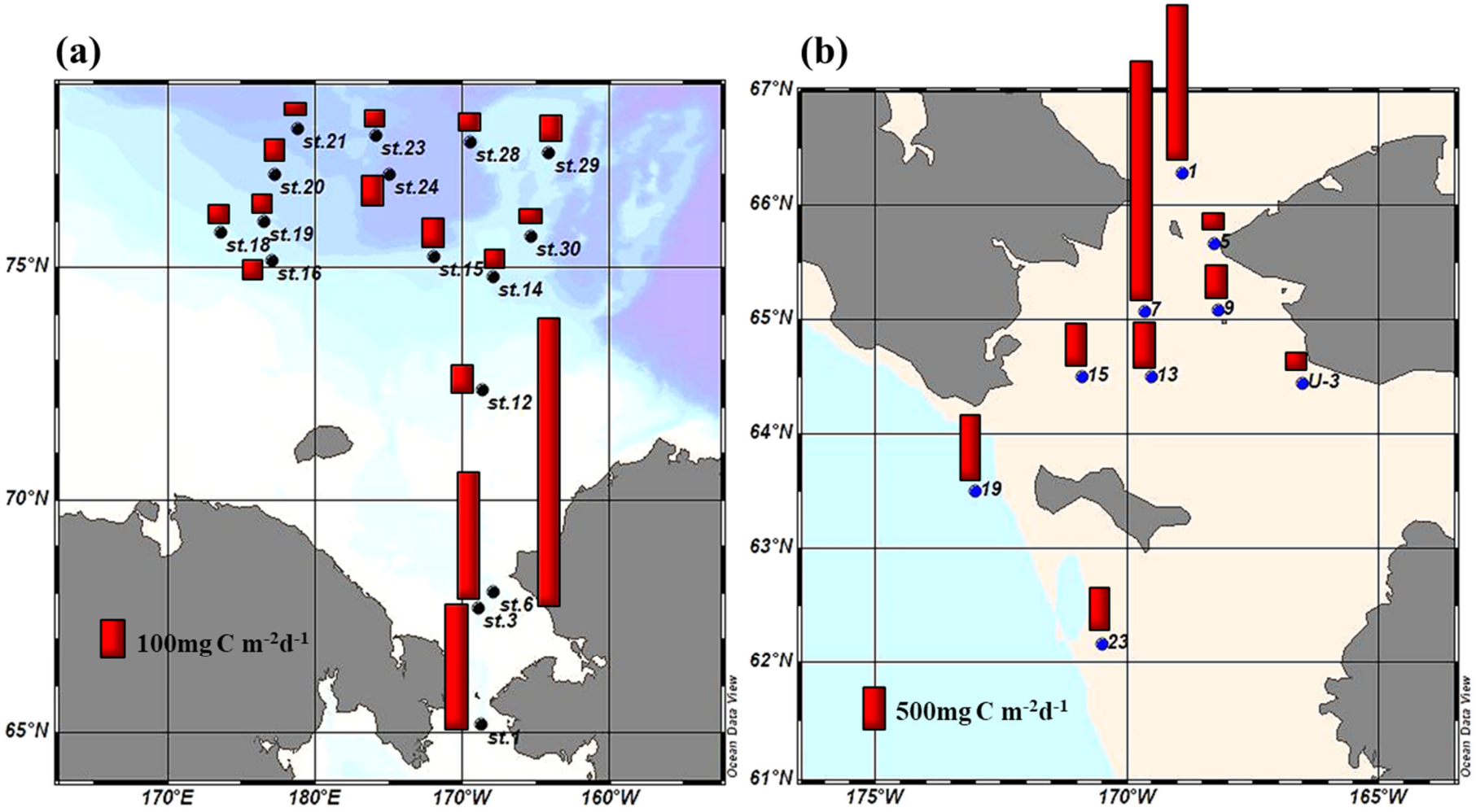

Figure 7. Primary production of total phytoplankton during the (a) ARA07B and (b) OS040.

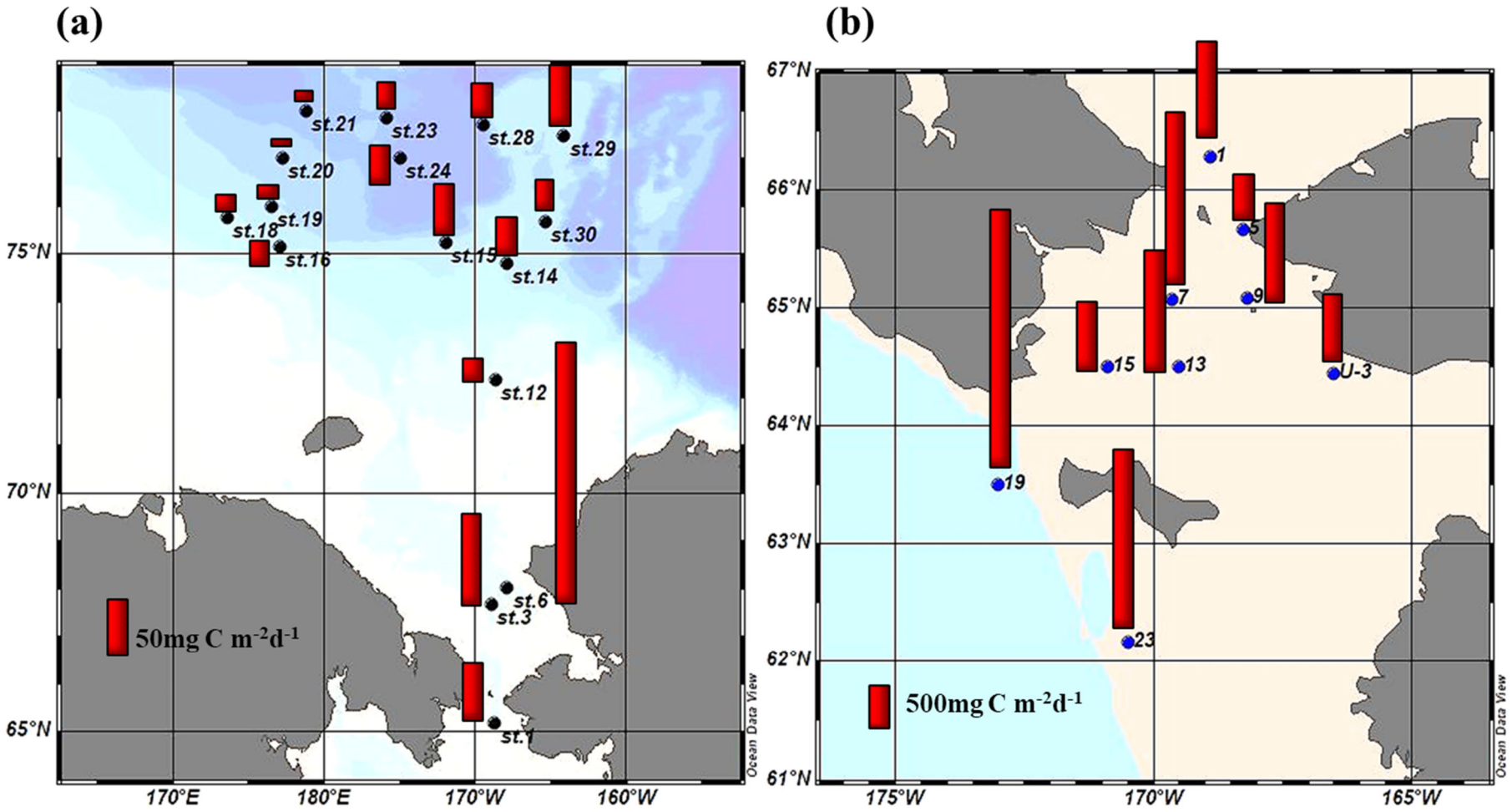

Figure 8. Primary production of small phytoplankton during the (a) ARA07B and (b) OS040

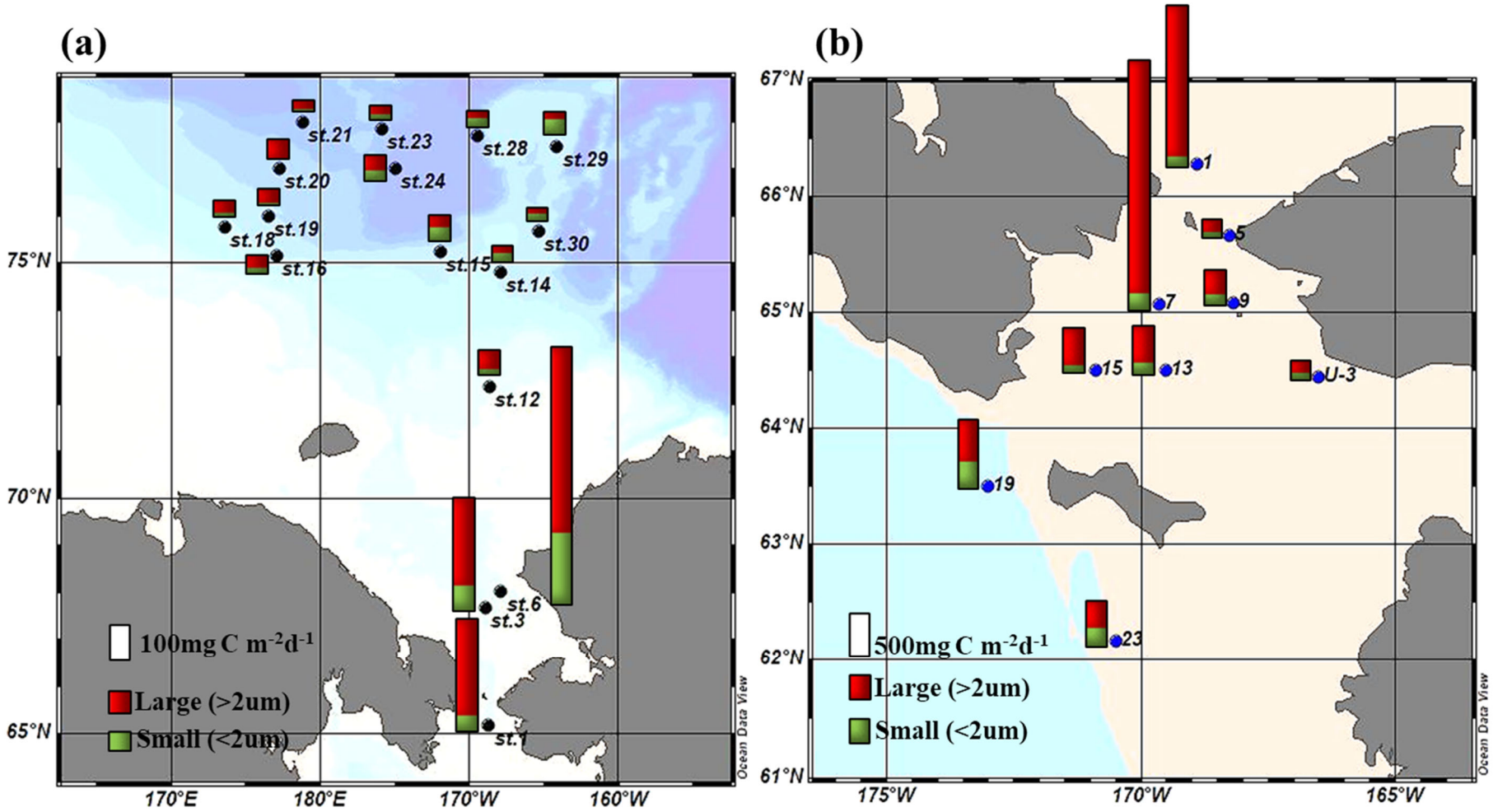

Figure 9. Primary production of small phytoplankton of (a) ARA07B and (b) OS040.

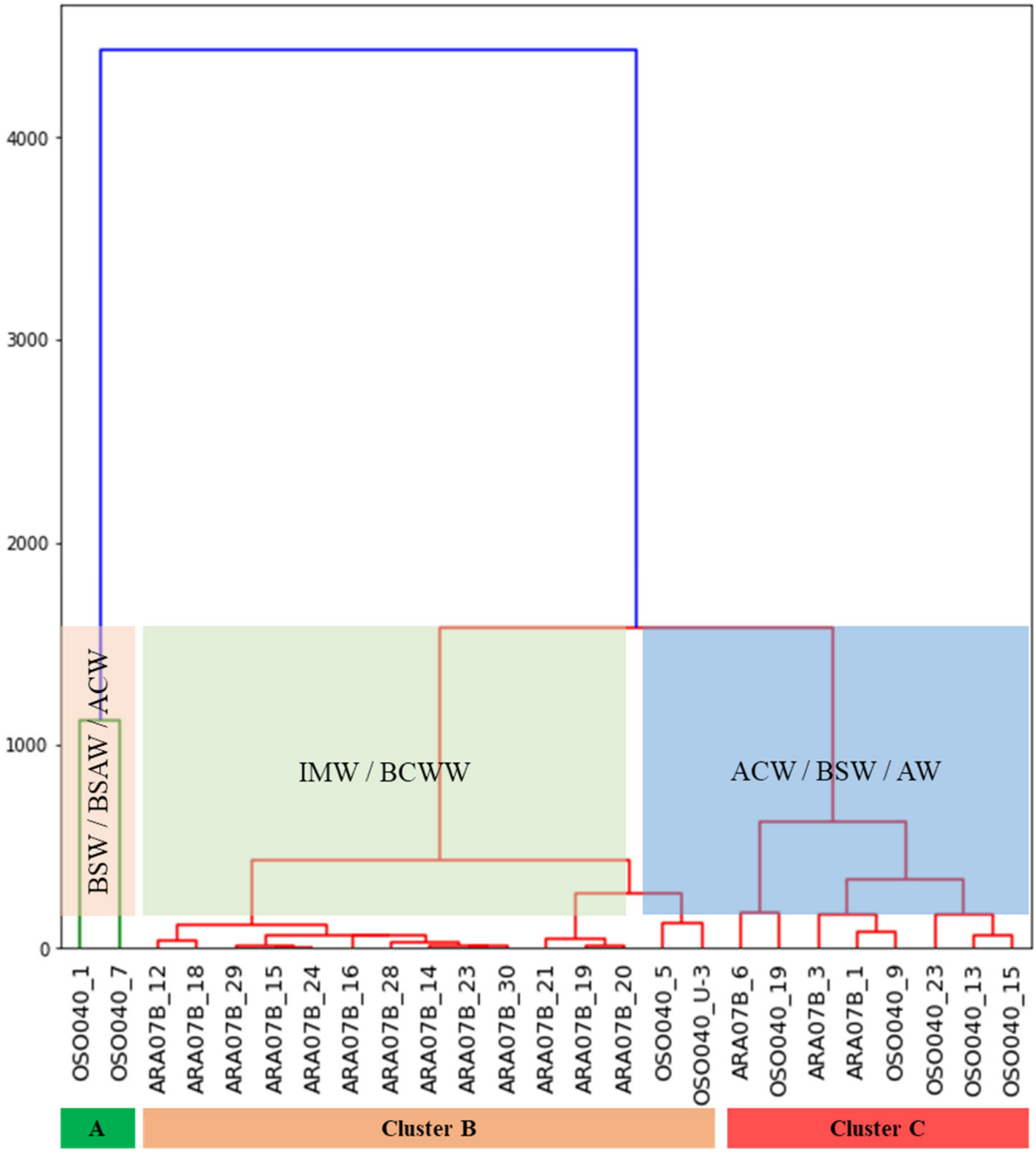

Figure 10. Dendrogram stands for sampling stations were divided into three clusters by agglomerative hierarchical clustering (AHC). Various water masses influenced to each cluster.

Table 4. Mean values of properties for the three clusters classified by the AHC.

Cluster	Temp (°C)	Salinity (psu)	Small contribution to PP	Small contribution to surface chl-*a*	Small contribution to POC	PP (mg C m^{-2} d^{-1})	Chl-*a* (mg m^{-3})	POC (mg m^{-3})
A	4.5	32.7	6.5%	1.8%	21.8%	2547	97.5	414.3
B	0.1	29.7	40.5%	39.1%	40.9%	79.6	13.9	177.7
C	5.6	31.7	26.7%	39.1%	43.9%	559.2	60.7	236.1

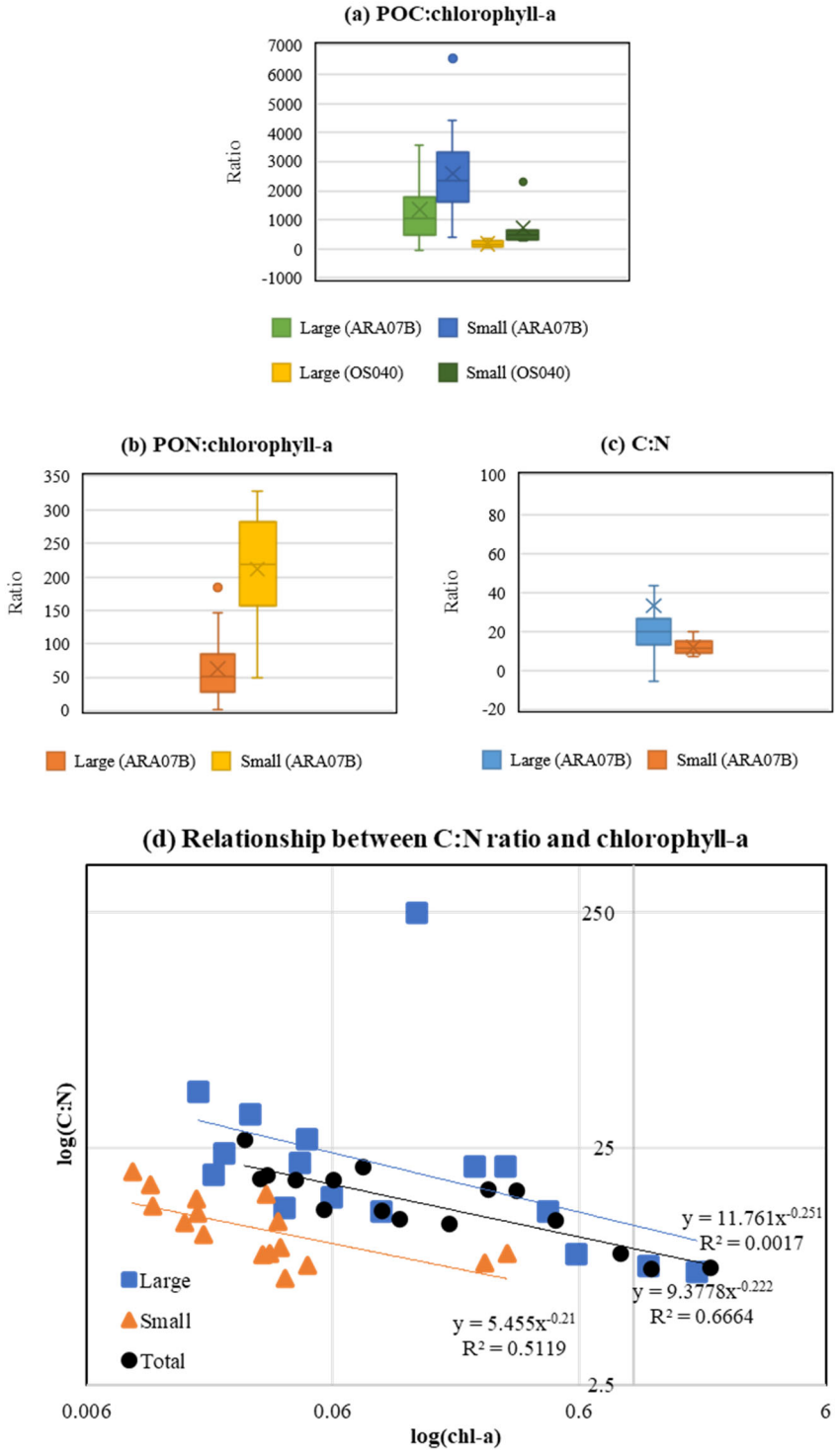

Figure 11. Comparison of (a) POC:chlorophyll-*a* ratios, (b) PON:chlorophyll-*a* ratios and (c) C:N ratios be-tween small and large phytoplankton in the northern Bering and Chukchi seas. Only POC:chlorophyll-*a* data available for the OS040. (d) C:N ratio and chlorophyll-*a* of each size group.

Table 5. Early studies of small phytoplankton contribution. According to previous study, small phytoplankton

contributed 19.8% to 87% to total phytoplankton.

Study area	Year	Season	Small contribution	Methods	Size	References
Northern Chukchi Sea and Canada Basin	2008	August-September	19.8-60.3%	*In-situ*	< 5µm	Lee *et al.* (2012)
Bering Strait and Chukchi Sea	2004	August-September	31.72± 23.59%	*In-situ*	< 5µm	Lee *et al.* (2013)
Kara, Laptev, and East Siberian Sea	2013	August-September	52.7-71.2%	*In-situ*	< 5µm	Bhavya *et al.* (2018)
Barents Sea	2003-2005	Early to late bloom period	31-87%	*In-situ*	< 10µm	Hodal and Kristiansen (2008)
North water polynya	1998	April-July	19%	*In-situ*	< 5µm	Mei *et al.* (2003)
Chukchi Sea and Bering strait	**2016**	**August**	**38.0±19.9%**	***In-situ***	**< 2µm**	**This study**
Northern Bering Sea and Bering strait	**2017**	**July**	**25.0±12.8%**	***In-situ***	**< 2µm**	

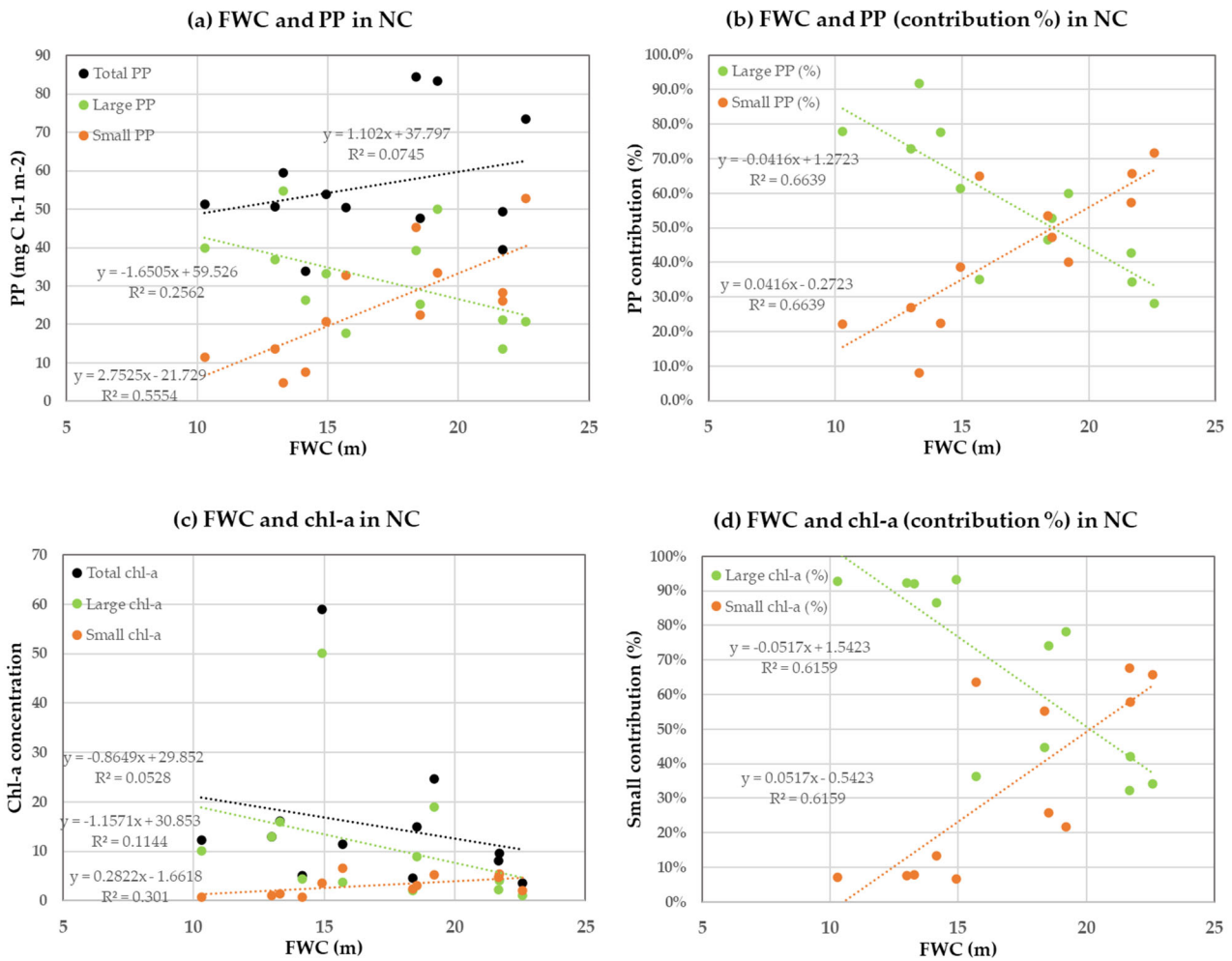

Figure 12. Correlation between small phytoplankton contribution and FWC in the northern Chukchi Sea**.** While previous studies have reported that FWC reduces PP and chl-*a*, this research reveals distinctions in composition rather than total quantities.

Chapter 3

Estimation of small phytoplankton distribution using satellite ocean color images in the northern Chukchi to northern Bering Seas

3.1. Introduction

According to reports of the International Ocean-Colour Coordinating Group, No. 15 : Phytoplankton Functional Types from Space (Sathyendranath, IOCCG, 2014), phytoplankton belonging to distinct size classes occupy specific physical and chemical properties characterized by differences in their light-harvesting efficiency, nutrient uptake capacity, biogeochemical functions, and distribution within the euphotic zone. Phytoplankton cell size has been widely recognized as a significant indicator of their functional contribution in numerous ecological and biogeochemical processes (Finkel *et al.*, 2009; Marañón, 2015; Nair *et al.*, 2008; Sieburth *et al.*, 1978).

The small phytoplankton has intrinsic physical and chemical properties, including higher metabolic rates than larger phytoplankton at a constant pigment concentration (Key *et al.*, 2010). This is attributed to the light-absorption effectiveness known as the package effect (Morel and Bricaud, 1981), which contributes less to the biological pump (Chisholm, 1992). The ecological and biogeochemical processes in the oceanic environment are intricately connected to the phytoplankton community size structure or phytoplankton size classes (PSCs) (Liu *et al.*, 2018). Due to these unique characteristics, research on small phytoplankton is being conducted. However, there are temporal constraints associated with the methods used for field measurements such as chemical anal ysis for genetic information and microscopic methods. Satellite remote sensing data offer a comprehensive and detailed view of the optical characteristics in the upper ocean waters, spanning from local to global scales, with exceptional temporal and spatial resolution (Son *et al.*, 2014, 2005). For these reasons, there is increasing interest in developing PSCs models using satellite data, which helps overcome the constraints of field measurements.

Numerous algorithms have been developed to extract PSCs using satellite ocean color remote sensing data. The PSCs methods using satellite include abundance-based methods (Brewin *et al.*, 2010; Hirata *et al.*, 2011; Uitz *et al.*, 2006), radiance-based methods (Li *et al.*, 2013), absorption-based methods (Bricaud *et al.*, 2012; Ciotti and Bricaud, 2006; Devred *et al.*, 2011; Fujiwara *et al.*, 2011; Hirata *et al.*, 2008; Kostadinov *et al.*, 2009; Mouw and Yoder, 2010; Roy *et al.*, 2013; Waga *et al.*, 2019, 2017). Waga *et al.* (2017) developed Chlorophyll-*a* size d istribution (CSD) model and following research have revealed that changes in phytoplankton size composition are most strongly correlated with SST in global scale. Hirata *et al.* (2008) established a model for detecting the dominant PSC at a satellite pixel using phytoplankton absorption. These technique offers valuable information that can be used to survey small phytoplankton contribution to total phytoplankton biomass. Lee *et al.* (2019) has reported that small phytoplankton-dominant area increased along with annual mean SST in Bering Sea and Bering strait using the algorithm of (Hirata *et al.*, 2008). Arctic ocean is undergoing warming at a rate four times faster

than other regions (Rantanen *et al.*, 2022). It is anticipated that the changes in phytoplankton size composition due to SST will be more pronounced in polar regions. In addition to SST, Fujiwara *et al.* (2018, 2016) states that timing of sea ice retreat change influences the size of phytoplankton in the Chukchi shelf region. Furthermore, freshwater was identified as another factor influencing the size of phytoplankton leading to a reduction in size (Li *et al.*, 2009; Yun *et al.*, 2016). In particular, the northern Chukchi Sea exhibits significantly different physicochemical characteristics compared to the southern counterpart of Chukchi Sea. However, there has been relatively limited research conducted in the northern region compared to the southern Chukchi Sea. Based on these previous studies, this chapter aims to examine the long-term variation of small phytoplankton from 1998 to 2020 using satellite remote sensing data and analyze their practical relationships with environmental factors to provide estimates of potential future changes.

This study concentrates on the contribution of small phytoplankton, and Hirata's PSC model can effectively illustrate how to dominate small phytoplankton in a clear and concise manner. Due to the model's simplicity, which relies on a single variable, it maintains data continuity even when adjusting gaps using data from various satellites. Although, Hirata *et al.* (2008) developed the PSC model globally, lacks comprehensive validation specifically in regions such as the Arctic and Subarctic. Similarly, its validation is notably absent in coastal areas, including shelf regions. Lee *et al.* (2019) partially validated the model in the Bering Strait and the Bering Sea. This study extends the validation to the Chukchi Shelf (the southern part of Chukchi Sea) and the northern Chukchi Sea. This research's objective is to apply the model to long-term data, correcting for satellite data discrepancies, to study prolonged variations in different regions. Specifically, this chapter focuses on examining the long-term variations of small phytoplankton from 1998 to 2020 using satellite remote sensing data. The analysis aims to identify regions dominated by small phytoplankton and investigate their long-term temporal patterns over this period.

3.2. Methods

3.2.1. Study area and *in-situ* measurement of size fractionated chlorophyll-*a*

The cluster analysis in chapter 2 resulted in the identification of three regions in the northern Bering Sea and Chukchi Sea: the northern Chukchi Sea (NC; 72-77°N, 165-177°W), Bering Strait (BS; 64-68°N, 167-171°W) and northern Bering Sea (NB; 61-63°N, 170-175°W) (Figure 13). The NC region exhibits lower productivity than the southern Chukchi Sea which is consistent with chlorophyll-*a* abundance (Lee *et al.*, 2007; Nishino *et al.*, 2016), low salinity (29.7 psu; chapter 2) nitrogen limitation (Codispoti *et al.*, 2009; Lowry *et al.*, 2015) and a correlation with sea ice retreat (Fujiwara *et al.*, 2016). Additionally, the NC region displayed the highest contribution of small phytoplankton, as discussed in chapter 2. The BS is the most productive region (3100.1 mg C m^{-2} d^{-1}; Chapter 2) among three regions by nutrient fertile water flux. The NB has properties of low chlorophyll-*a* concentration than other regions (chapter 2) and has had Saint Lawrence polynya in winter.

Water samples for size-fractionated chlorophyll-*a* (0.7 and 2 μm for small- and large-phytoplankton)

concentration were obtained from surface at 21 stations of HLY0702, 7 stations of ARA07B and 9 stations of OS040. HLY0702 (U.S. Coast Guard Cutter Healy) was conducted from May 18 to 18 June 2007 and size fractionated chlorophyll-*a* data was obtained from (Lee *et al.*, 2019), ARA07B was performed in 5-19 August, 2016 by R/N Araon mainly in the Chukchi Sea and Bering strait, OS040 was conducted during 9-28 July, 2017 onboard T/S Oshoro-Maru in the NB and BS. Water was sampled by Niskin bottles on rosette sampler. The water (500ml) filtered by size using GF/F filter (Whatman) with pore size 0.7 µm and 2 µm pore size membrane filters (Whatman Nuclepore). Chlorophyll-*a* was extracted following Parsons *et al.* (1984) and analyzed with a fluorometer (Turner Designs 10AU).

3.2.2. Satellite remote sensing data

The long-term period data of the absorption coefficient by phytoplankton at wavelength 443 nm, $a_{ph}(443)$ was obtained from Ocean Colour Climate Change Initiative (OC-CCI) products which was generated by The European Space Agency (ESA). OC-CCI products were created by combining data from five ocean color sensors on different satellites, that contains Sea-viewing Wide Field-of-view Sensor (SeaWiFS), Moderate resolution Imaging Spectroradiometer (MODIS) on Aqua, Medium Resolution Imaging Spectrometer (MERIS) on Envisat-1, and Visible Infrared Imaging Radiometer Suite (VIIRS) on the Suomi National Polar-orbiting Partnership (SNPP) (Mélin *et al.*, 2017). The main purpose of OC-CCI is to create reliable ocean color data over time for studying climate change (Brewin *et al.*, 2015). The OC-CCI version 5.0 global level-3 monthly ocean color products from 1998 to 2020 with 4 km resolution were acquired from May 1998 to October 2020 from ESA OC-CCI website (https://climate.esa.int/).

3.2.3 Optical model for phytoplankton size classes and the definition of small phytoplankton domination.

Following Hirata *et al.* (2008), small phytoplankton dominant regions were quantified. The algorithm of Hirata *et al.* (2008) is one of abundance-based models for the PSCs using single parameter (absorption coefficient by phytoplankton at wavelength 443 nm) as a threshold-based method. This model splits PSCs as follows: $a_{ph}(443) < 0.023$ m^{-1} for pico-phytoplankton domination; $0.023 \leq a_{ph}(443) < 0.069$ m^{-1} for nano-phytoplankton domination; $0.069 \leq a_{ph}(443)$ m^{-1} for micro-phytoplankton domination. To focus small phytoplankton, we reorganized phytoplankton community in two groups (> 2 µm, small phytoplankton; < 2 µm, large phytoplankton) as modifying the algorithm of Hirata *et al.* (2008). The contribution of small phytoplankton was estimated by calculating the proportion of small phytoplankton dominant regions in each area. For validation purposes, the OC-CCI derived PSCs corresponding to each *in-situ* measurement data were matched up and compared. Small phytoplankton domination was defined as the condition in which small phytoplankton constitutes more than 50% of the total phytoplankton community (Table 6) in *in-situ* measurement data.

3.3. Results and discussion

3.3.1 Validation of optical method for PSCs

The size-fractionated Chlorophyll-*a* ratios of each size groups (small and large phytoplankton) were calculated from *in-situ* chlorophyll-*a* measurement. The dominated size groups were derived from the *in-situ* chlorophyll-*a* measurements. These phytoplankton size community were compared with optical estimation derived from $a_{ph}(443)$, as shown in Table 6. The dominant phytoplankton size groups estimated by the model were in good matches with those obtained from the chlorophyll-*a* measurements, except for 6 stations of all 37. The discrepancy between the satellite data (monthly averages) and the field survey results (single-day measurements) is presumed to be due to the difference in their temporal resolutions. The poorly fitting stations had significantly different chlorophyll-*a* distribution between surface and whole euphotic zone. For instance, St.1 and St.16 stations in ARA07B, St.9 and St.U-3 stations in OS040 observed large phytoplankton was dominant in whole water column but small phytoplankton was dominant only in surface water. Small phytoplankton group was dominant at the 14 stations with *in-situ* measurement (or 10 stations with optics model-derived approach). In general, this model was well validated with an accuracy of 84% (31 of 37 stations were matched) for dominant size group of phytoplankton (Table 6).

3.3.2 Climatological properties and seasonal patterns of small phytoplankton

Climatology images of small phytoplankton contribution in the NC, BS and NB (Figure 14; 15) were derived using satellite remote sensing data. Figure 14 provided the climatologic image (May 1998 to October 2020) of the small phytoplankton domination. In the NC, small phytoplankton contributed 0 to 93.1 % (mean ± S.D. = 44.8 ± 26.2 %), 0 to 40.8 % (mean ± S.D. = 2.9 ± 6.0 %) in the BS, and 0 to 99.6 % (mean ± S.D. = 35.3 ± 35.1 %) small phytoplankton dominant ratio respectively. Based on 1998-2020 climatology, small phytoplankton contributed mostly on the NC (44.8 ± 26.2 %) among all area. The least contribution of small phytoplankton was observed in the NB region, with a maximum of only 40.8%. The small phytoplankton were dominant in the open water and deeper area (near the Chukchi plateau; around 77°N, 165°W), while large phytoplankton dominated shallow and near shore (coast, the northern Bering Sea, and the Chukchi shelf). In the NC, phytoplankton size structure was affected by sea ice melting significantly (Fujiwara *et al.*, 2016) as well as Canada Basin (Coupel *et al.*, 2012). The significant contribution of small phytoplankton in the NC suggests its association with sea ice. In typical conditions, picophytoplankton tend to thrive in oligotrophic waters due to their ability to efficiently acquire nutrients in low-nutrient environments (Agawin *et al.*, 2000). Furthermore, Li *et al.* (2009) and Yun *et al.* (2016) has reported the nitrogen deficiency inhibited phytoplankton growth in NC. For these reasons, it indicates that small phytoplankton has a competitive advantage over large phytoplankton, allowing it to thrive in the NC.

All three regions present seasonal patterns of small phytoplankton dominant ratio (Figure 15; 16, Table 7). In the NC, the smallest contribution of small phytoplankton was observed in June, and it increased until August

before decreasing again in September (Figure 16, Table 7). In June, the contribution of small phytoplankton was 26.7%, while in July it increased to 32.9%, further rising to 62.2% in August, and then decreasing to 48.6% in September. In the BS, the contribution of small phytoplankton was relatively low compared to other regions, with 1.5% in May, 5.0% in June, 6.8% in July, 3.0% in August, 0.6% in September, and 0.6% in October. In the NB, the contribution of small phytoplankton showed varying percentages throughout the months, with 5.8% in May, 52.4% in June, 76.8% in July, 53.7% in August, 17.5% in September, and 4.4% in October. Lee *et al.* (2019) which reported an increase in small phytoplankton contribution up to 45.8% in the southern Chukchi Sea during July and up to 31.8% in the area north of St. Lawrence Island, this study did not observe such high values in our data. Indeed, the differences in the definition of 'small phytoplankton dominant' between this study and Lee *et al.* (2019) could explain the contrasting results. In this study, 'small phytoplankton dominant' was defined as a contribution of 50% or more, whereas Lee *et al.* (2019) defined the dominant group as the one among pico-, nano-, and micro-phytoplankton with the highest abundance. These varying criteria for dominance could lead to different outcomes and interpretations of the data.

The peak point of small phytoplankton contribution mostly over whole period is the NB in July (76.8 % of small phytoplankton contribution). Bloom occurred usually on the NB in May, June and August usually (Frey *et al.*, 2021). Therefore, the highest values of small phytoplankton domination observed in July is likely a result of phytoplankton succession following the bloom. The BS has very low proportion of small phytoplankton contribution consistently throughout the year (> 7%, Table 7, Figure 16). The BS is productive region dominated by diatoms (46% of total phytoplankton; chapter 2) which are mainly classified as large phytoplankton. This productivity is maintained by the influx of nutrient-rich AW waters through the northern branch of the split Bering Slope Current (Lowry *et al.*, 2015). Small phytoplankton in the NC were contributing constantly all year round (at least 27.6 %). This suggests small phytoplankton contribute largely within whole primary production on the NC throughout the year.

As indicated in Figure 15, significant variations in phytoplankton size groups were also observed in the vicinity of the Hope Valley and Herald Shore (near BS) in the Chukchi Shelf. This suggests that this region is also crucial for studying fluctuations in small phytoplankton. However, due to the limited availability of *in-situ* data, this study was unable to extensively investigate this area.

In this chapter, the optical method for phytoplankton size estimation was effectively validated, showing strong agreement with *in-situ* measurements. Small phytoplankton exhibited distinct climatological and seasonal patterns depending on regions, The NC, a hotspot for small phytoplankton dominance, is likely influenced by the disappearance of sea ice, especially in areas that transition to open water. The study underscores the importance of considering methodological differences in defining dominance and emphasizes the need for further investigation in specific regions, such as the Chukchi Shelf, to better understand fluctuations in small phytoplankton.

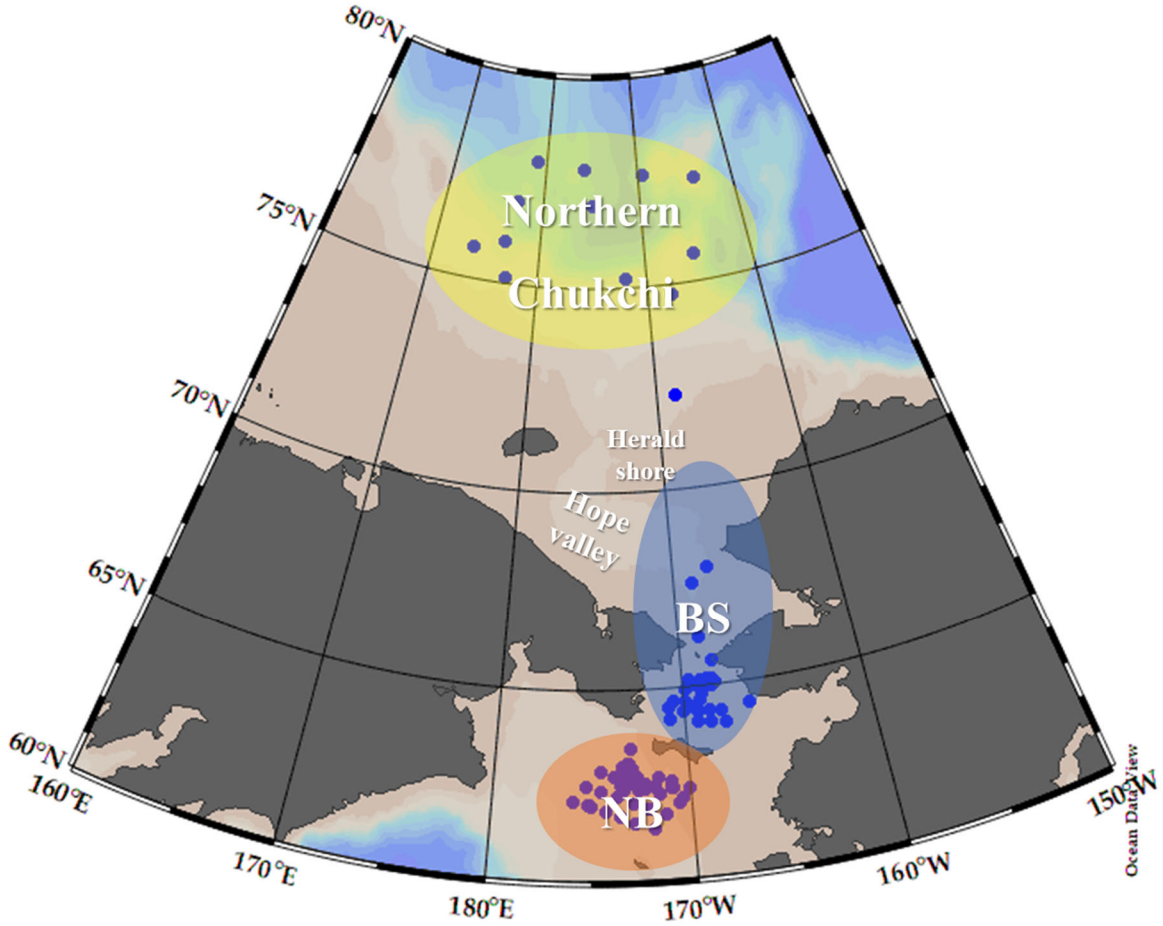

Figure 13. Study area and stations of chapter 3. The three areas include the northern Chukchi Sea (NC), Bering strait (BS) and northern Bering Sea (NB).

Table 6. Comparison between *in-situ* measured small phytoplankton proportions and satellited derived small phytoplankton domination.

	Field measurements				Satellite
	Chlorophyll-*a* ratio			*In-situ*	PSC
Cruise	**Stations**	**Large**	**Small**	**Dominant size class**	**Dominant size class**
HLY0702 2007	1	92%	8%	**Large**	**Large**
	14	94%	6%	**Large**	**Large**
	18	89%	11%	**Large**	**Large**
	22	64%	36%	**Large**	**Large**
	27	68%	32%	**Large**	**Large**
	31	92%	8%	**Large**	**Large**
	35	91%	9%	**Large**	**Large**
	41	97%	3%	**Large**	**Large**
	51	83%	17%	**Large**	**Large**
	57	72%	28%	**Large**	**Large**
	61	84%	16%	**Large**	**Large**
	65	97%	3%	**Large**	**Large**
	69	92%	8%	**Large**	**Large**
	73	98%	2%	**Large**	**Large**
	81	45%	55%	*Small*	*Large*
	103	96%	4%	**Large**	**Large**
	109	40%	6%	**Small**	**Small**
	115	60%	4%	**Small**	**Small**
	119	54%	46%	**Small**	**Small**
	137	45%	55%	**Small**	**Small**
	140	51%	49%	**Small**	**Small**
ARA07B 2016	1	47%	53%	*Small*	*Large*
	3	86%	14%	**Large**	**Large**
	6	97%	3%	**Large**	**Large**
	12	64%	36%	**Large**	**Large**
	15	48%	52%	**Small**	**Small**
	16	56%	44%	*Small*	*Large*
	30	46%	54%	**Small**	**Small**
OS040 2017	1	97%	3%	**Large**	**Large**
	5	70%	3%	**Large**	**Large**
	7	99%	1%	**Large**	**Large**
	9	33%	67%	*Small*	*Large*
	U-3	59%	41%	*Small*	*Large*
	13	86%	14%	*Large*	*Small*
	15	87%	13%	**Large**	**Large**
	19	27%	73%	**Small**	**Small**
	23	24%	76%	**Small**	**Small**

* The word marked in italics represents unmatched stations.

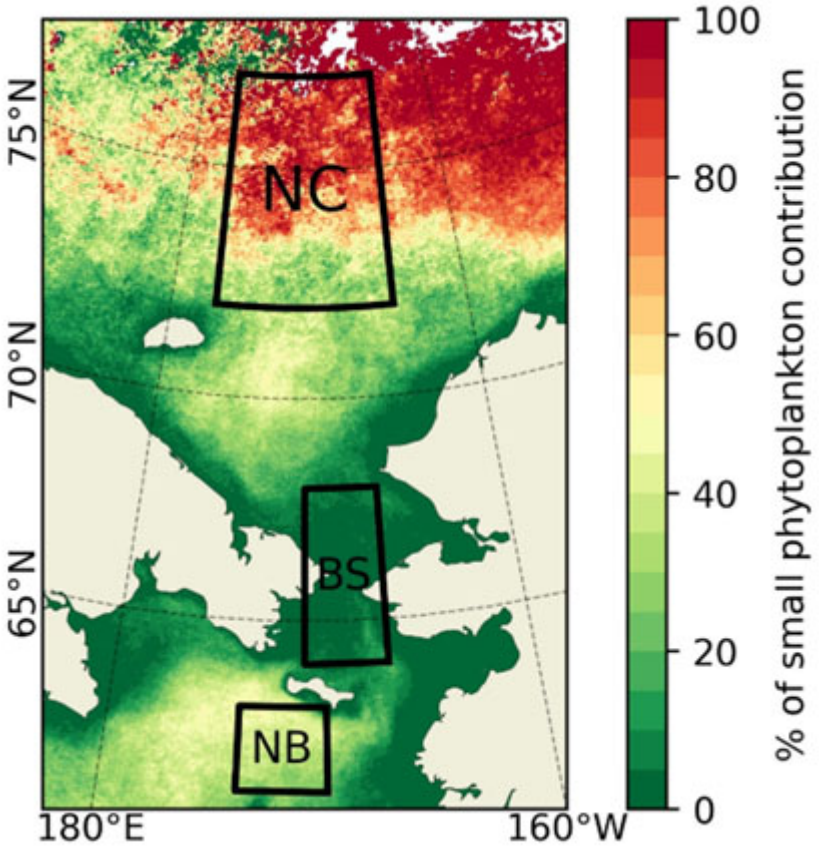

Figure 14. Climatology image of small phytoplankton contribution of each region from 1998 to 2020**.** Small phytoplankton contributed largely on NC.

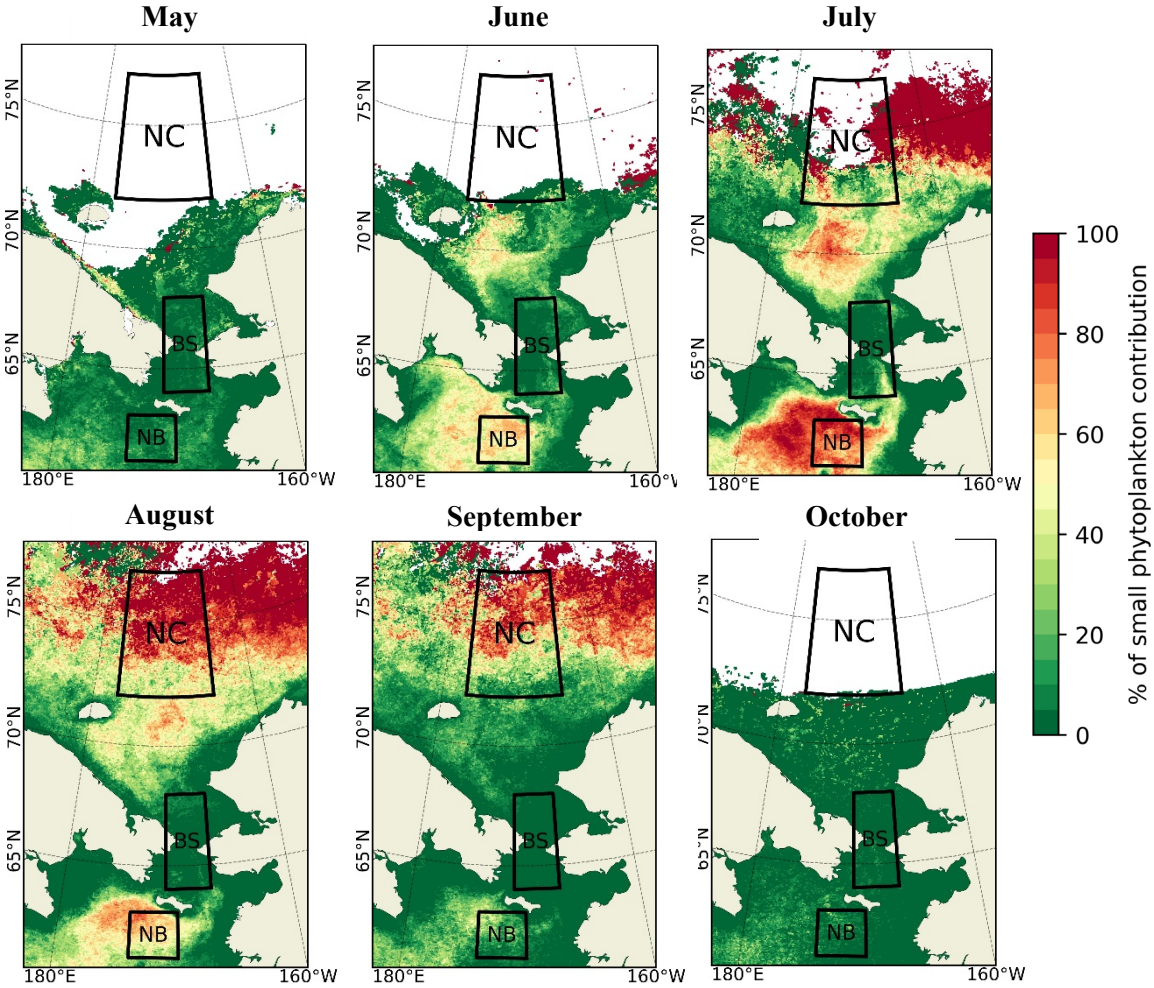

Figure 15. Seasonal climatology images of small phytoplankton contribution. All three regions present seasonal pattern. Small phytoplankton ranged from 0% to 99.6%.

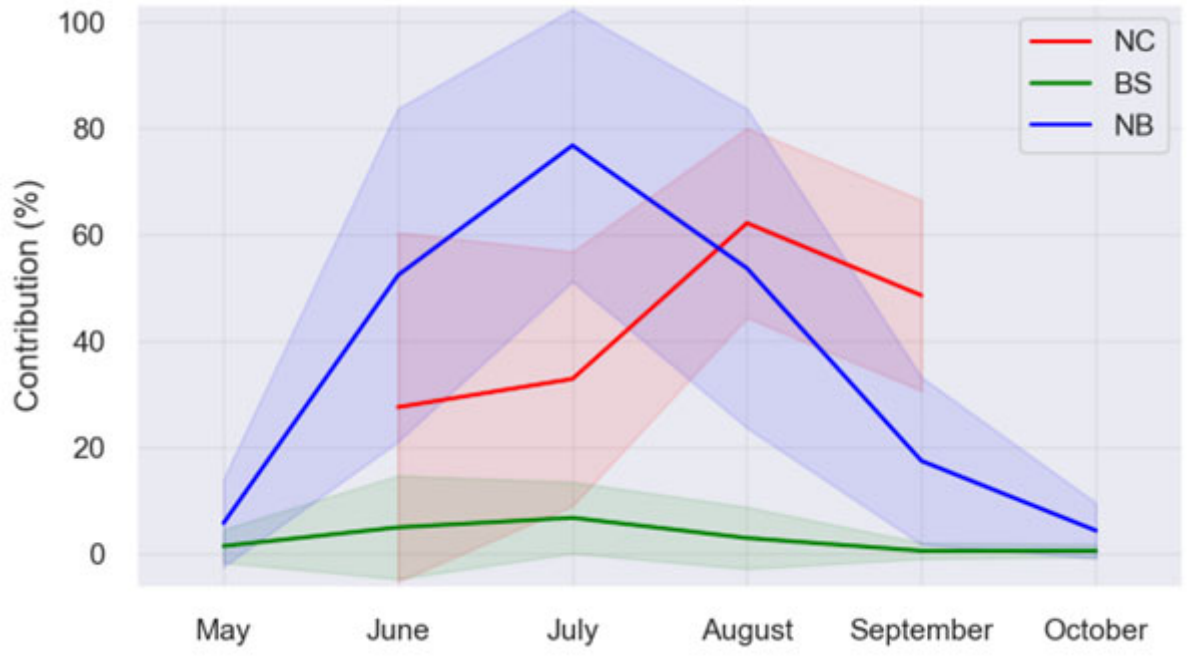

Figure 16. Small phytoplankton contribution of climatology from 1998 to 2020. The highest contribution of small phytoplankton was NB in July (76.8% of small contribution). The BS have low proportion of small phytoplankton generally (< 7%). Small phytoplankton in NC were contributing constantly all year round (27.6%-62.2%).

Table 7. The small phytoplankton contribution in climatology. High values were observed in NC, with a lower proportion of small phytoplankton in BS and significant variability in NB.

	NC	BS	NB
May		1.5(± 3.2)%	5.8(± 8.4)%
June	27.6(± 32.8)%	5.0(± 9.7)%	52.4(± 31.4)%
July	32.9(± 23.9)%	6.8(± 6.7)%	76.8(± 25.7)%
August	62.2(± 17.8)%	3.0(± 5.6)%	53.7(± 29.8)%
September	48.6(± 17.9)%	0.6(± 1.4)%	17.5(± 15.4)%
October		0.6(± 1.2)%	4.4(± 5.1)%

Chapter 4

Environmental factors that affect small phytoplankton community in the northern Chukchi to northern Bering Seas via numerical studies

4.1. Introduction

Numerous studies have been conducted on small phytoplankton in the Arctic Ocean (Bhavya *et al.*, 2020; Cottrell and Kirchman, 2009; Gradinger and Lenz, 1995; He *et al.*, 2012; Lee *et al.*, 2023, 2019, 2018; Li, 1998; Li *et al.*, 2009; Lovejoy *et al.*, 2006; Park *et al.*, 2022; Sherr *et al.*, 2003; Terrado *et al.*, 2008; Yun *et al.*, 2019, 2016). These studies have revealed that small phytoplankton are influenced by sea surface temperature (SST), sea ice, and freshwater contents (FWC) in the southern part of Pacific-Arctic Ocean. Notably, significant relationships between phytoplankton communities and SST in the Bering Sea and Chukchi shelf have been reported (Fujiwara *et al.*, 2011; Waga *et al.*, 2017). Moreover, Lee *et al.* (2019) found that the implication of SST on small-phytoplankton dominant regions varies depending on the region in the Bering Sea and Bering Strait. However, in Chapter 2 of this study, it was found that the annual contribution of small phytoplankton is not related to SST. Perhaps the limited findings of previous study to the Bering Sea and Bering Strait regions explain this discrepancy of relationship between small phytoplankton and SST.

Fujiwara *et al.* (2016)concluded that the early sea ice retreat can influence the phytoplankton size composition larger during the Marginal Ice Zone (MIZ) bloom period by more nutrient supply from subsurface following weak stratification (Yun *et al.*, 2016) stated that FWC had a significant negative effect on PP related to the nitrate inventory. Furthermore, in recent decades, there has been an increase in the freshwater content of the Arctic Ocean, encompassing river discharge, Pacific water inflow through the Bering Strait, sea ice meltwater, and net precipitation (Jones *et al.*, 2008). Consequently, there is a possibility that the contribution of small phytoplankton will increase. FWC plays a crucial role in determining the nutrient distribution, nitrate inventory and nutrient availability for phytoplankton growth in the Arctic Ocean, showing strong relationships with primary production (Coupel *et al.*, 2015; Yun *et al.*, 2016, 2014). Li *et al.* (2009) reported that strong stratification caused by freshwater can lead to smaller phytoplankton in the surface ocean. Also, in Chapter 2 of this study, a positive relationship between FWC and small phytoplankton contribution was observed. However, these studies were limited to observing specific summers or conducted over short periods (less than 5 years). In such short periods, it is challenging to discern the effects of larger-scale environmental changes spanning over five years. Moreover, due to the significant influence of major events in particular years, longer-term studies are necessary to gain a comprehensive understanding. Furthermore, previous studies were unable to sensitively quantify how much environmental factors influenced phytoplankton due to temporal and spatial limitations. Further research is needed to comprehensively understand the relationships between small phytoplankton and environmental factors on a larger temporal scale. Specifically, most research related to the Chukchi Sea is confined to the southern region of the Chukchi Shelf. Therefore, this chapter delves more deeply into the uniqueness of the northern Chukchi Sea

(NC), as identified in Chapter 2.

Therefore, this chapter of the study will quantitatively investigate the trends of small phytoplankton using satellite remote sensing data over a long-term period (1998-2020) and elucidate the correlations with environmental factors. Environmental factors such as SST, sea ice and FWC are obtained from the gridded model data provided by CMEMS. To ensure the accuracy of the data, a validation process is conducted by comparing it with *in-situ* measurements. Subsequently, a quantitative analysis will be performed to assess the relationships between these environmental factors and small phytoplankton in the northern Chukchi to the northern Bering Seas (NC to BS). This analysis will allow us to determine the extent to which each factor influences small phytoplankton in these regions.

4.2. Methods

4.2.1. Small phytoplankton contribution

Small phytoplankton dominant region data were derived using the methodology outlined in Hirata *et al.* (2008), as described in Chapter 2, method 2.3 of this study. The data was processed to extract regional monthly average values and analyzed for long-term variations. In this study, I defined the contribution of small phytoplankton by calculating the frequency of dominance by small phytoplankton in each pixel over a year. To see the anomaly, the small phytoplankton contribution of each pixel from 1998 to 2020 were averaged annually and the anomaly of small phytoplankton contribution was calculated for each PDO phase. PDO phases were determined following their moving average. PDO index were obtained from National Centers for Environmental Information, National Ocean and Atmospheric Administration (NOAA).

4.2.2 Environmental factors from 1998 to 2020

SST and FWC were provided from model-gridded data. Global Ocean-Delayed Mode gridded CORA *in-situ* observation objective analysis in Delayed Mode (Cabanes *et al.*, 2013; Szekely *et al.*, 2019) was obtained from the Copernicus Marine Service (https://marine.copernicus.eu). To validate the ocean model-gridded data, I utilized *in-situ* salinity and *in-situ* SST collected during the ARA07B (August, 2016) and OS040 (July, 2017) by CTD. Salinity in the water column and SST data from 1998 to 2020, with a horizontal resolution of 1/12 degree were used for analysis. Sea ice concentration was derived from Global Ocean Physics Reanalysis based on NEMO with 1/12°horizontal resolution. This was also acquired from Copernicus Marine Service. FWC were calculated following (Carmack *et al.*, 2008) with reference salinity 34.8 psu (S_{ref} = 34.8; the average salinity of the Arctic Ocean; Aagaard and Carmack, 1989; Serreze *et al.*, 2006; Holland *et al.*, 2007; Haine *et al.*, 2015). The equation of FWC calculation following (Carmack *et al.*, 2008) :

$$FWC = \int_{z_{lim}}^{0} \left(1 - \frac{S(z)}{S_{ref}}\right) dz$$

, where FWC is freshwater contents (m), $S(z)$ and S_{ref} are the *in-situ* salinity (psu) on specific depth (m) and reference salinity, Z_{lim} is the depth where S equals S_{ref}. SST, salinity, FWC were validated with the *in-situ* data presented in Chapter 2 (Figure 17). To establish the correlations with environmental factors, Pearson's correlation coefficients were calculated. Multiple regression method was employed to determine the contribution of each factor. 80% of data were used for modeling, 20% of data were used for testing. All factors were rescaled for normalization. In the study, a multiple regression analysis was employed encompassing four distinct factors : SST, FWC, sea ice, Sea Surface Salinity (SSS). Given that SSS contributed to the computation of FWC, the potential for multicollinearity within the model was rigorously examined. The Variance Inflation Factor was determined to be 1.53, indicating that multicollinearity was not a concern in the analysis.

4.3. Results and discussion

4.3.1. The annual variation of small phytoplankton contribution in three regions (NC, BS and NB)

Figure 18 provides a general overview of the annual changes in small phytoplankton contribution. In the NC region, there was limited data available in 1998-2001, however, starting from 2002, there has been an increase in satellite data. It has been observed that the areas dominated by small phytoplankton have expanded with sea ice uncovered area. This appears to be due to the gradual retreat of sea ice, leading to a wider expanse of open sea. Liu *et al.* (2021) reported the sea ice concentration in the NC has decreased dramatically in the past decade. And open-water duration could shift longer (Wang and Overland, 2015). Figure 18 showed most of the expanded open water areas are dominated by small phytoplankton. In Chapter 2, the influence of ice-melt water in the NC was observed in 2016. Yun *et al.* (2016) mentioned ice-melt water is a one of component of FWC. This suggests that ice-melt water as FWC could contributes to small phytoplankton in NC. FWC is strongly related to the primary production (Coupel *et al.*, 2015; Yun *et al.*, 2014). It could suggest the phytoplankton community on the NC also varies according to sea ice change. Especially, more ice-melt freshwater could influence to phytoplankton community becoming smaller in the NC. A decreasing trend of monthly small phytoplankton contribution in the NC during September was observed, showing an average annual decline of about 1.2%. On the other hand, July and August exhibited a very slight increasing trend, 0.6 % and 0.4 % annually, respectively (Figure 19a). The highest small phytoplankton contribution is generally observed in August each year (61%; 14 of 23 years) and second highest contribution occurred frequently in September (26%; 6 of 23 years) (Figure 20). Particularly, during the years 2003 to 2005, the highest contribution occurred in September rather than August (Figure 20).

In the BS region, the small phytoplankton contribution consistently remained relative low value below 22% (Figure 19b). The nutrient-rich flow from the western Bering Strait is connected to a substantial phytoplankton standing crop in the Bering Sea (Sambrotto *et al.*, 1984). Due to the disadvantageous proliferation of small phytoplankton under nutrient-rich conditions compared to large phytoplankton, the contribution of small phytoplankton is consistently lower and exhibits minimal variability. However, a recent study reported the decline of primary productivity (PP) in western Bering strait (Frey *et al.*, 2022). Small phytoplankton contribution appears

to slightly increase in July (0.4% annually), while showing a slight decrease in August (0.4% annually) and September (0.1% annually) (Figure 19b). This suggests that there may have been changes in bloom patterns in the Bering Strait region. Considering that Frey *et al.* (2022) also discuss the east-west environmental variations within the Bering Strait, it seems important to conduct further studies by dividing the changes in the Bering Strait into smaller regions for more detailed analysis.

In 2011, the lowest contribution of small phytoplankton was observed in the NB (Figure 18, Figure 19). Ardyna and Arrigo (2020) has reported 2011 is the lowest sea ice extent year over recent 40 years. However, there were no notable changes observed in the environmental factors of FWC, sea ice, and SST in 2011 of this study. It is speculated that the influence could be attributed to other environmental factors such as nutrient balance. In the NB, the significant increase trends were observed in July and August by 1.7 % and 1.3 annually, respectively.

4.3.2. Decadal variant of small phytoplankton contribution with PDO index

According to several studies, changing of PDO phase could explain variability of some environmental parameters in Pacific side arctic ocean (Kim *et al.*, 2020; Kodaira *et al.*, 2020; Simon *et al.*, 2022; Svendsen *et al.*, 2021, 2018). Similarly, in this research, changes in the contribution of small phytoplankton across different regions were identified in correlation with fluctuations in the PDO index. Small phytoplankton contribution changes along with PDO, ranged from 32.9% to 56.2% in the NC, from 0.8% to 8.7% in the BS, from 32.2% to 43.3% in the NB (Table 8, Figure 21). In 2002-2006 positive PDO (Figure 22), productive regions were expanded northward with sea ice retreat, however, most new open area dominated by small phytoplankton. This could be affected by increased amount of ice melting water (Chapter 2). Small dominant region in the NB became more frequent after 2006 (27.0% to 41.2%). PDO shifted from positive to negative in 2007-2014 but phytoplankton in NB became smaller (20.8% - 40.4% - 43.3%). The BS has changed little relatively with each PDO phase. Small phytoplankton contribution raged from 0.8 to 8.7% and mean value was 2.9% (± 6.0%). There were opposite tendencies between the NC and NB (Figure 21). When the PDO index shifts from negative to positive the contribution of small phytoplankton increases in NC while it decreases in NB. Screen and Francis (2016) suggests PDO-like SST anomalies could regulate a series of arctic environmental condition as sea ice loss. From this, it can be speculated that the influence of SST might work in opposite directions in these two regions. Although significant variations were observed in accordance with each PDO phase, the correlation with the PDO itself did not appear to be strong.

4.3.3. The relationship between small phytoplankton and environmental factors

A significant negative correlation (Pearson's r = -0.7426) was observed between SST and the rate of small phytoplankton contribution in the NC region (Figure 23). Additionally, FWC exhibited a significant positive influence on the small phytoplankton contribution in the NC region (Pearson's r = 0.7895), and a correlation consistent with *in-situ* measurements (Figure 23). However, in both the BS and the NB regions, SST did not show a significant relationship, while FWC displayed only a modest correlation (Pearson's r = 0.2338) with small

phytoplankton in the BS region. Among the various regions, sea ice concentration had the most pronounced impact on the NC. Notably, the extent of small phytoplankton dominant regions could increase with expanding sea ice cover (Pearson's r = 0.5041) (Figure 23). Based on the above results, a multiple regression analysis was conducted to determine the most significant variable in the NC region. The R-square of multiple regression was 0.700 (Adjust R-square =0.698) (Figure 24, Table 9). This suggest 69.8% of the variance in the dependent variable is explained by the model for 4 factors (SST, SSS, FWC, sea ice concentration). The equation of multiple regression results is :

$$[Small\ phytoplankton\ contribution\ (ratio)] = -0.1054[SST\ (℃)] + 0.0473[SSS\ (psu)] + 0.1632[FWC\ (m)] - 0.0229[Seaice\ (ratio)] + 0.6561$$

This result is an estimate based on the following range of values : SST (-1.40 to 1.60°C), SSS (29.16 to 30.25 psu), FWC (3.0 to 14.2 m), Sea ice concentration (0.57 to 0.79), The obtained result indicates that the p-values were less than 0.01 (SST, SSS and FWC), p-value for sea ice less than 0.05 signifying statistical significance. The factor that influenced small phytoplankton most was FWC (t = 12.439) (Table 9) in the NC. In the NC region, there are similarities in the patterns of change between FWC distribution and small phytoplankton contribution, with a Pearson's correlation coefficient of 0.7895. This relationship appears to be influenced by factors such as topography, including the continental shelf. The Beaufort Gyre, located to the east of the NC region, is known for having the lowest salinity in the Arctic Ocean (Proshutinsky *et al.*, 2009). The freshwater from the Beaufort Gyre flows from the east of the Beaufort Sea to the NC region along the coast. It is suggested that this freshwater influence from the Beaufort Gyre contributes to the higher small phytoplankton contribution observed in the NC region. Yun *et al.* (2016) reported that wind pressure can also influence FWC. Therefore, in subsequent studies, wind, along with currents and the structure of water masses, should be considered as factors associated with FWC.

Based on the obtained results, within the model that can explain 68.9% of the variance in small phytoplankton contribution, FWC holds a significant position. Therefore, in the NC region, FWC is considered as an influential index for estimating small phytoplankton contribution. While early studies extensively analyzed various environmental factors, research focusing on quantifying the extent of their influence was lacking. This study addresses this gap and, specifically for the NC region, concludes that FWC holds a paramount influence, filling the gap in our understanding.

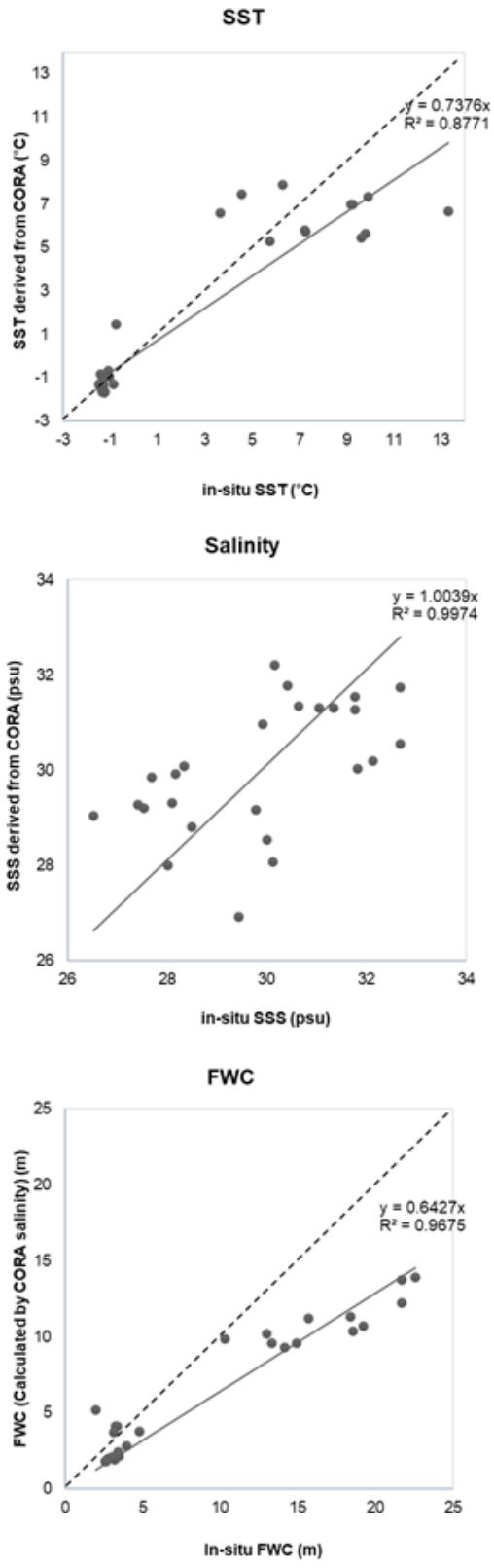

Figure 17. Validation of each environmental factors. All environmental factors of modeled data were well matched with *in-situ* data (R^2=0.8771 for SST; R^2=0.9974 for Salinity ; R^2=0.9675 for FWC).

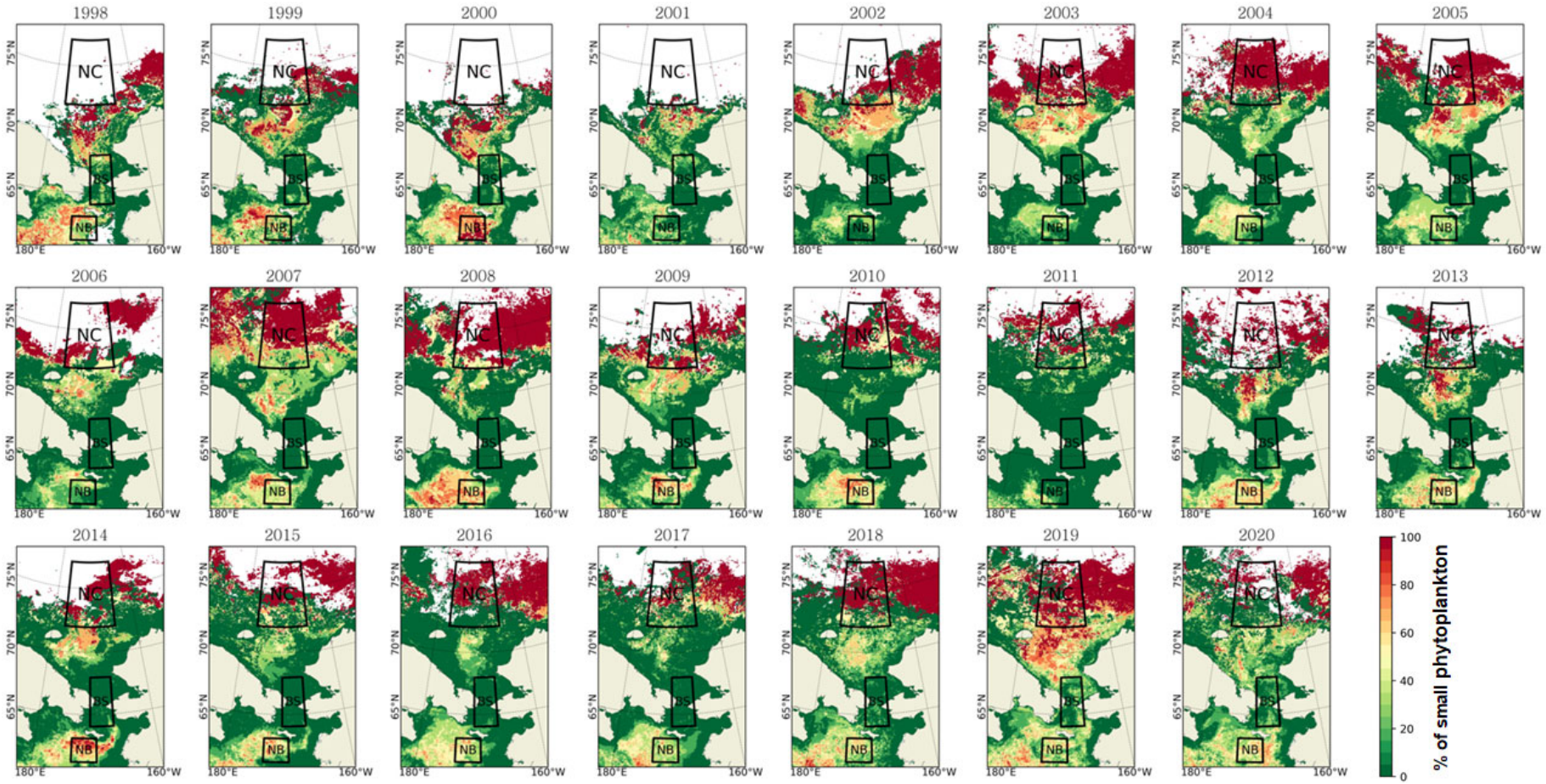

Figure 18. Annual small-dominant region in the Chukchi Sea and Bering Sea from 1998 to 2020. This is the result of calculating the dominance of small phytoplankton throughout the year

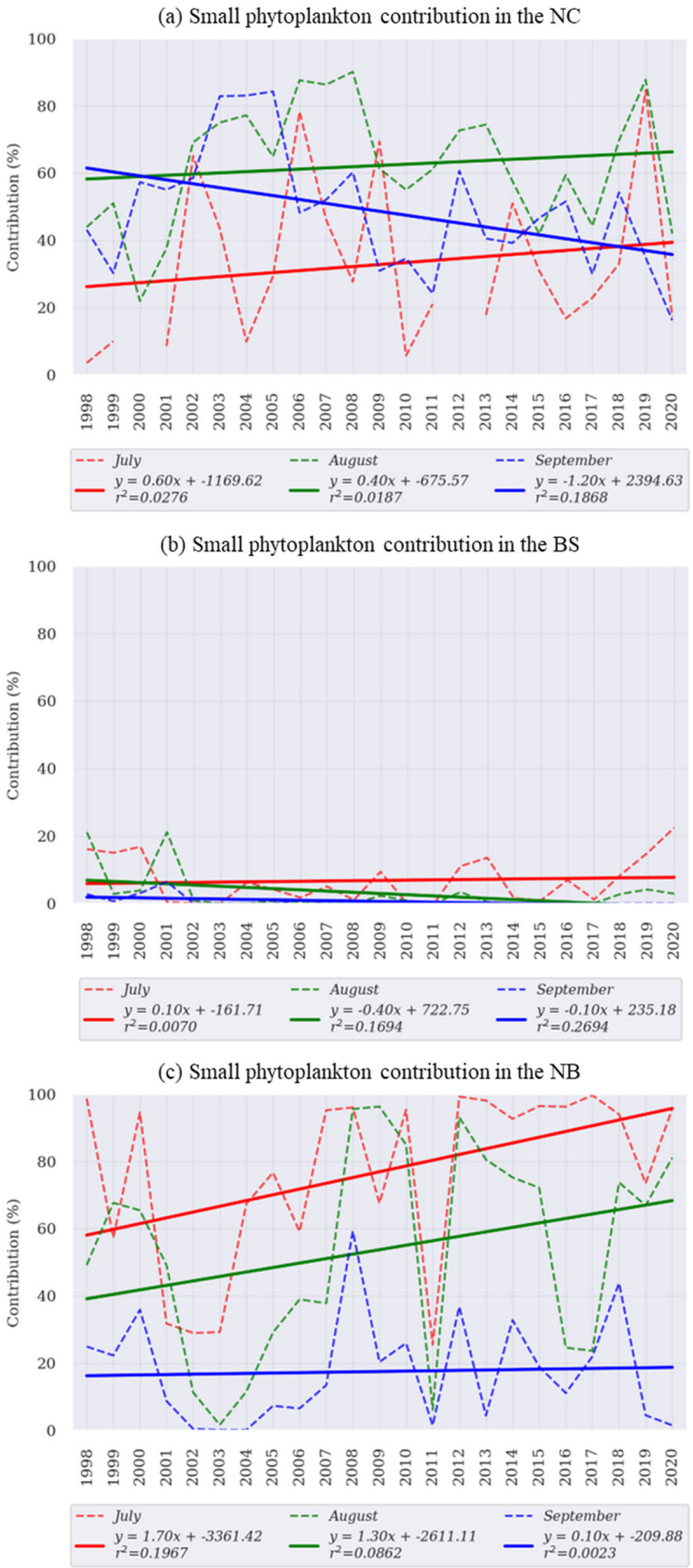

Figure 19. Monthly variation of small phytoplankton dominant regions depending on regions. a) is for the NC (b) and (c) are the BS and NB, respectively. The strait lines are trend lines of each month.

	May	June	July	August	September	October
1998			4%	44%	43%	
1999			10%	51%	30%	
2000				22%	57%	
2001			9%	38%	55%	
2002			65%	69%	58%	
2003		0%	43%	75%	83%	
2004			10%	77%	83%	
2005		0%	29%	65%	84%	
2006			78%	88%	48%	
2007		0%	46%	86%	52%	
2008		93%	28%	90%	60%	
2009		40%	69%	61%	31%	
2010		0%	6%	55%	35%	
2011		7%	21%	61%	24%	
2012				73%	61%	
2013			18%	74%	40%	
2014			51%	57%	39%	
2015			31%	42%	47%	
2016			17%	59%	51%	
2017		1%	23%	44%	30%	
2018		43%	33%	70%	54%	
2019		38%	85%	88%	35%	
2020		81%	17%	42%	16%	

0%
10%
20%
30%
40%
50%
60%
70%
80%
90%
100%

Figure 20. Annual time series of small phytoplankton contribution in the NC from 1998 to 2020.

Table 8. Small phytoplankton contribution of each PDO phase depending on regions. NC and NB exhibit inverse responses to changes in PDO.

Period	NC	BS	NB	Phase of PDO
1998-2001	32.9%	5.8%	32.2%	**Negative**
2002-2006	56.2%	1.0%	20.8%	**Positive**
2007-2013	45.2%	1.4%	40.4%	**Negative**
2014-2017	35.2%	0.8%	43.3%	**Positive**
2018-2020	50.1%	8.7%	39.8%	**Positive to Negative**

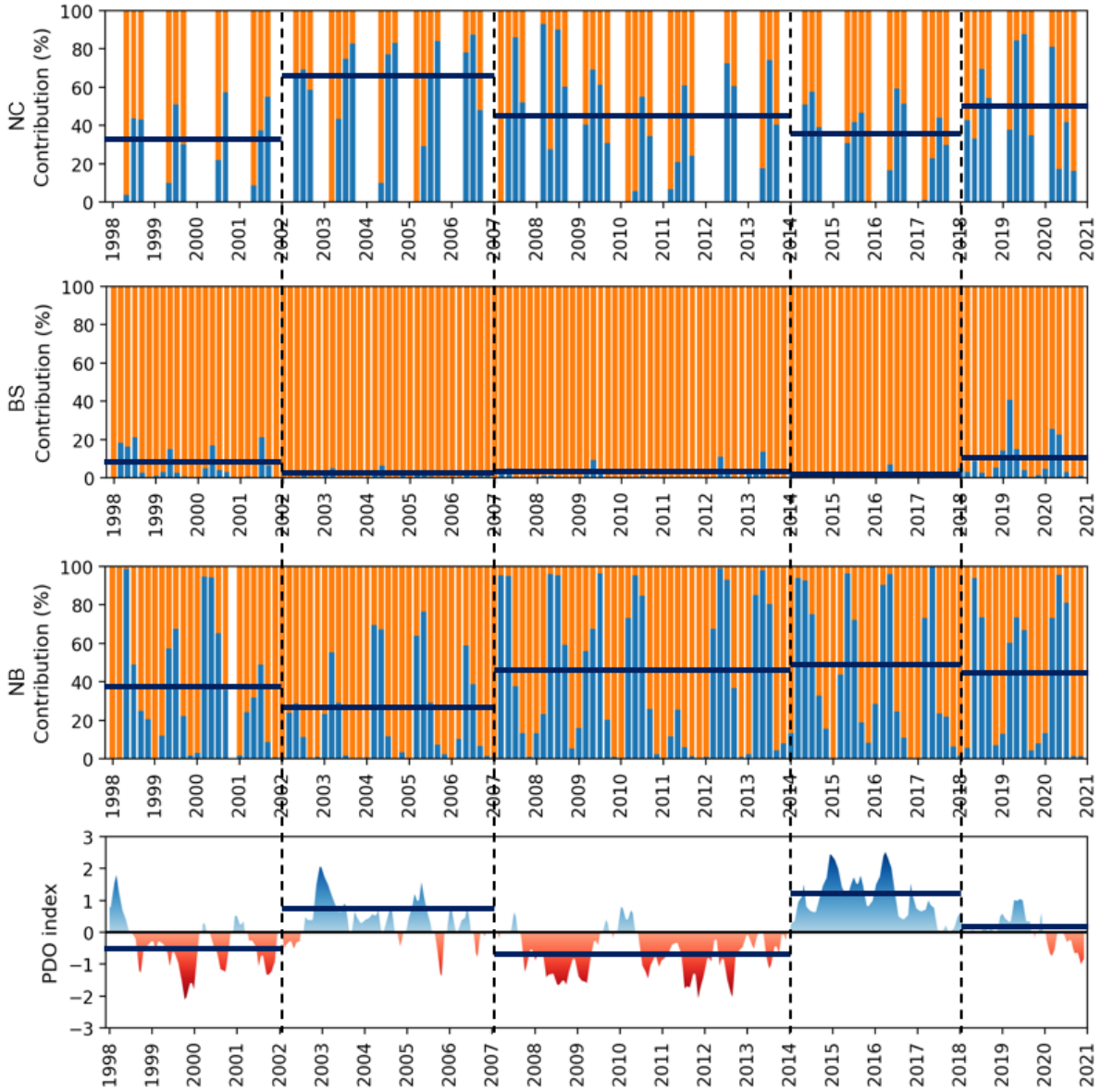

Figure 21. Monthly time series of small phytoplankton contribution with PDO index. Each region exhibits variations in response to changes in PDO.

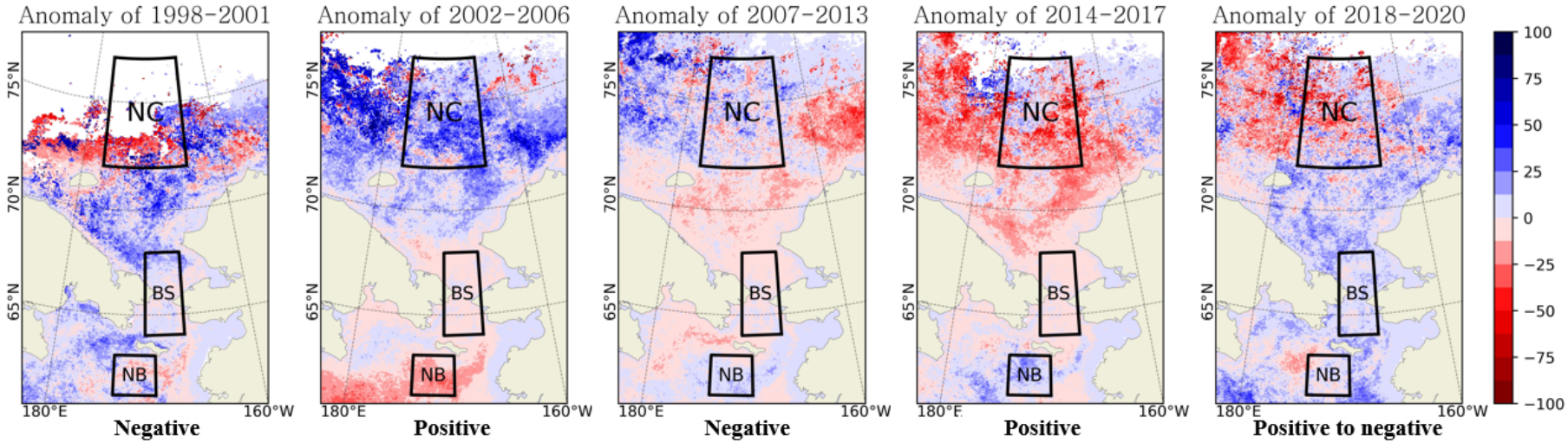

Figure 22. Anomaly map of small phytoplankton contribution of each PDO phase. Anomalies were calculated from the overall mean baseline, and variations can be observed based on each PDO phase.

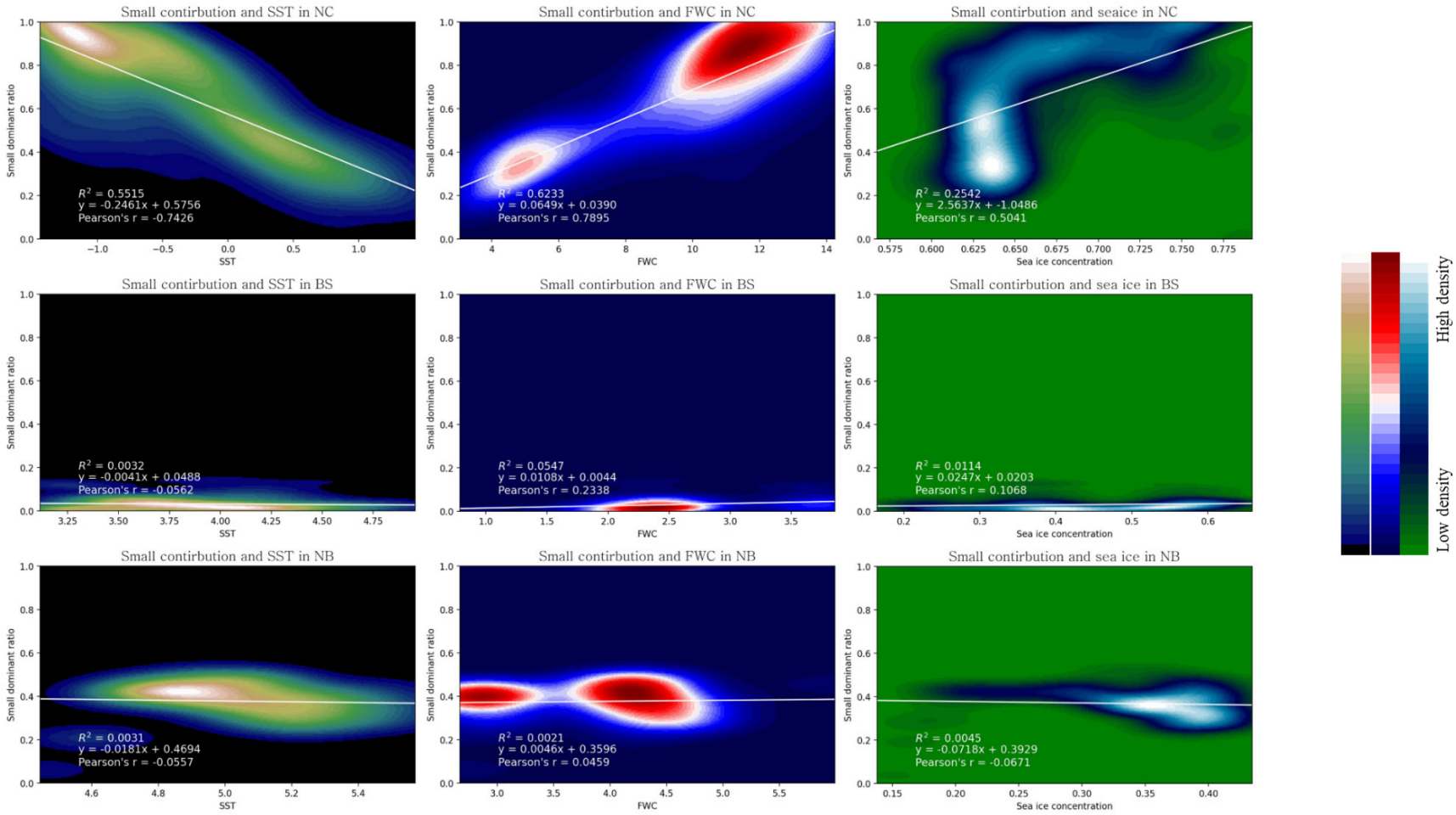

Figure 23. The relationship among SST, FWC, sea ice and small phytoplankton contribution. NC: n=577, BS: n=151, NB: n=69; P-values of sea ice and small phytoplankton contribution were p<0.5 (NC), p<0.01 (NB), p<0.01 (BS), SST and small phytoplankton contribution : p<0.01 for NC, NB, BS, FWC and small phytoplankton : p<0.01 for NC, NB, BS

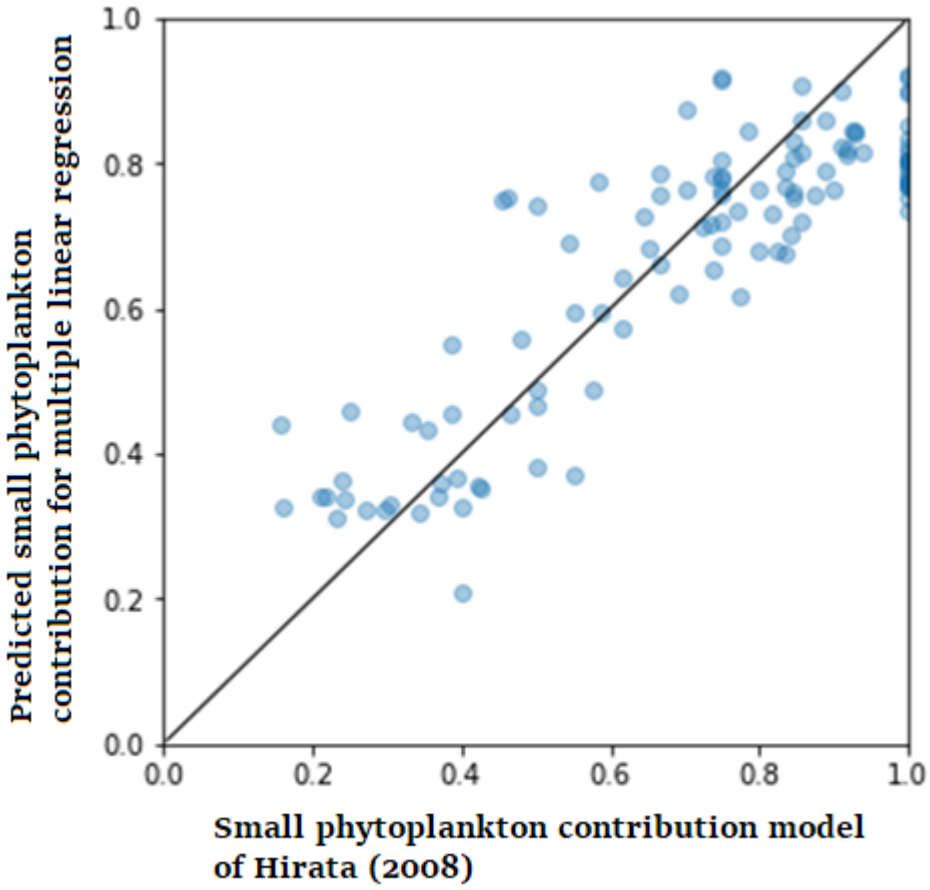

Figure 24. Multiple regression result of small phytoplankton contribution (n=581, p< 0.1 for SST, SSS, FWC, p< 0.5 for Sea ice concentration).

Table 9. Regression coefficient of each environmental factors. FWC is the most explainable factor for small phytoplankton contribution in the NC.

	Regression coefficient	Std error	t (t-test)	P>|t|
constant	0.6561	0.006	114.908	0
SST	-0.1054	0.018	-5.806	0
SSS	0.0473	0.011	4.496	0
FWC	0.1632	0.013	**12.439**	0
Sea ice	-0.0229	0.009	-2.471	0.014

Chapter 5

Summary and Conclusion

5.1 Summary and connection of chapters

This concluding chapter synthesizes the preceding sections to achieve the outlined objectives of my research. As introduced earlier, this dissertation aims to provide novel insights into small phytoplankton dynamics and factors in the Arctic Ocean through a comprehensive and systematic analysis. Utilizing robust data based on satellite-derived small phytoplankton contributions and environmental factors from various models, the paper concludes that small phytoplankton contributions were mainly controlled by Freshwater Content (FWC) in the North Chukchi (NC) region. The characteristics of small phytoplankton observed in this study in the NC were independent and distinctive compared to the Southern Chukchi Sea. This chapter consolidates these outcomes, emphasizing the significance of small phytoplankton contributions to the Arctic Ocean and exploring avenues for potential expansion within further research on the small phytoplankton dynamics in the Pacific-Arctic Ocean. Within this final chapter, we aim to discuss the broader implications of our findings, delving into a deeper understanding of small phytoplankton in the Arctic Ocean and its practical value within the Arctic Ocean ecosystem.

In chapter 2, this chapter researched dominant phytoplankton communities and biochemical characteristics in the Arctic Ocean. Two Arctic research cruises were conducted in the Chukchi Sea aboard the icebreaker R/N Araon in 2016 (ARA07B) and mainly in the northern Bering Sea aboard T/S Oshoro-Maru in 2017 (OS040) to determine dominant phytoplankton communities and the relative contribution of small phytoplankton (<2 μm) to total primary production. The dominant phytoplankton communities were diatoms and *Phaeocystis* during ARA07B, whereas diatoms and Prasinophyte (Type 2) were observed during OS040. Based on AHC analysis, the primary productions of total and small phytoplankton communities varied depending on the sea area. Overall, high primary productions and low contributions of small phytoplankton during both study periods were distributed in the Bering Strait region, affected by nutrient-enriched BSW. Different biochemical compositions between small and large phytoplankton were observed. The small phytoplankton group had a higher POC:chlorophyll-*a* (t-test, $p < 0.01$) and PON:chlorophyll-*a* ratio than large phytoplankton, suggesting that small phytoplankton have higher carbon and nitrogen contents per unit of chlorophyll-*a* concentration (Lee *et al.*, 2013). This chapter also found that small phytoplankton contribution has strong positive correlation with FWC in the northern Chukchi Sea (NC). Additionally, small phytoplankton had lower C:N ratios than large phytoplankton, indicating that small phytoplankton incorporate more nitrogen in relation to carbon into their bodies and thus produce nitrogen-rich organic matters (Bhavya *et al.*, 2018), which could be relatively faster regenerated than carbon-rich organic matters such as carbohydrates (Kim *et al.*, 2018; Hodal and Kristiansen, 2008). Therefore, further studies on small phytoplankton, which could be an essential basic food source in the Arctic ecosystem, should be conducted under the current warming ocean scenario. Chapter 3 were conducted for optical method validation and Climatological Analysis. This chapter successfully validated an optical method for predicting PSCs,

achieving an accuracy of 84% in identifying dominant size groups. Climatological analysis revealed distinct regional patterns in small phytoplankton dominance, with the North Chukchi consistently showing substantial contributions throughout the year. The Bering Strait exhibited low and consistent small phytoplankton contributions, while the North Bering displayed a peak in July, likely following the phytoplankton bloom. These findings emphasize the ecological significance of small phytoplankton, especially in the North Chukchi, and suggest a link between their dominance and sea ice conditions. Further research, especially with more extensive *in-situ* data, is needed to understand the dynamics of small phytoplankton in critical regions such as the Chukchi Shelf. This study contributes valuable insights into phytoplankton community structures and their seasonal variations in the Arctic Ocean, essential for understanding the impacts of changing environmental conditions on marine ecosystems. Chapter 4 focused on annual and decadal variations and environmental factors for small phytoplankton contribution on the Arctic Ocean. A rise in satellite data since 2002 on the NC revealed expanded areas dominated by small phytoplankton, likely linked to sea ice retreat. Monthly trends indicated a decline in September but a slight increase in July and August. Sea ice concentration correlated with small phytoplankton dominance. The BS region maintained a consistently low small phytoplankton contribution (<22%), possibly influenced by nutrient-rich conditions. A decline in PP was noted in the western Bering Strait. NB region experienced the lowest small phytoplankton contribution in 2011 but showed increasing trends in July and August. Decadal variation with PDO index changes in small phytoplankton contribution correlated with PDO fluctuations. The NC saw contributions ranging from 32.9% to 56.2%, the BS remained relatively stable (0.8% to 8.7%), and the NB showed an increasing trend from 27.0% to 43.3%. Opposing tendencies in the NC and NB suggested the influence of PDO-like SST anomalies, impacting sea ice conditions. A significant negative correlation between SST and small phytoplankton contribution was observed in the NC. FWC exhibited a positive influence in the NC but showed modest correlations in the BS and NB. Sea ice concentration notably impacted the NC. Multiple regression analysis identified FWC as the most significant variable in the NC, explaining 69.8% of the variance. Beaufort gyre in eastern area of NC has the lowest salinity in arctic ocean (Proshutinsky *et al.*, 2009). The freshwater of Beaufort gyre flows from the east of Beaufort Sea to NC region along the coast. This FWC of Beaufort gyre is presumed to have affected to high small phytoplankton contribution in NC with freshwater supplement (Manucharyan and Isachsen, 2019; Zhuang *et al.*, 2021). The difference in small phytoplankton contribution between the NC and BS is likely attributed to the inflow of FWC from the Beaufort Gyre in the Canada Basin. Therefore, in subsequent research, further investigation into the physical connection between the Beaufort Gyre and the NC would likely enhance our understanding of the characteristics of small phytoplankton in the NC. In *in-situ* measurement (Chapter2), FWC in NC were averaged 15m (2-22m) and euphotic zone were averaged 49.7m (22-92m). This imply halocline which was shallower than FWC depth led to oligotrophic in NC. For this reason, high contribution of small phytoplankton in NC is supposed to be high and is expected to change due to fresh water flowing into the Beaufort gyre such as live run off and ice melting. In this study, FWC in NC is on increasing steadily. Therefore, we can predict that the contribution of small phytoplankton contribution will continue to increase with increasing trend of FWC (Figure 25).

5.2. Conclusion

In conclusion, these chapters paint a nuanced picture of small phytoplankton in the Arctic Ocean. Small phytoplankton, with their unique biochemical characteristics, play a vital role in the ecosystem. Their dynamics are intricately tied to regional factors, including sea ice conditions and PDO. The NC region, characterized by its sensitivity to FWC, emerged as a focal point for understanding small phytoplankton variations. In previous studies, research on the relationship between small phytoplankton and the environment was limited to the southern part of the Chukchi Sea, focused on short-term analyses. These studies provided only fragmented knowledge about the effects of various environmental factors. However, this research illuminated how the contribution of small phytoplankton fluctuates over a period of more than 20 years and clarified the extent to which various environmental factors influence small phytoplankton. Based on this, predictions were made about potential future changes in small phytoplankton in the NC. This research advances our understanding of small phytoplankton in the Arctic Ocean, shedding light on their ecological role and the complex interactions shaping their dynamics. These insights hold significance for predicting and managing the impacts of ongoing environmental changes in the Arctic. The study not only contributes to the scientific understanding of phytoplankton dynamics but also underscores the importance of region-specific considerations in ecological research.

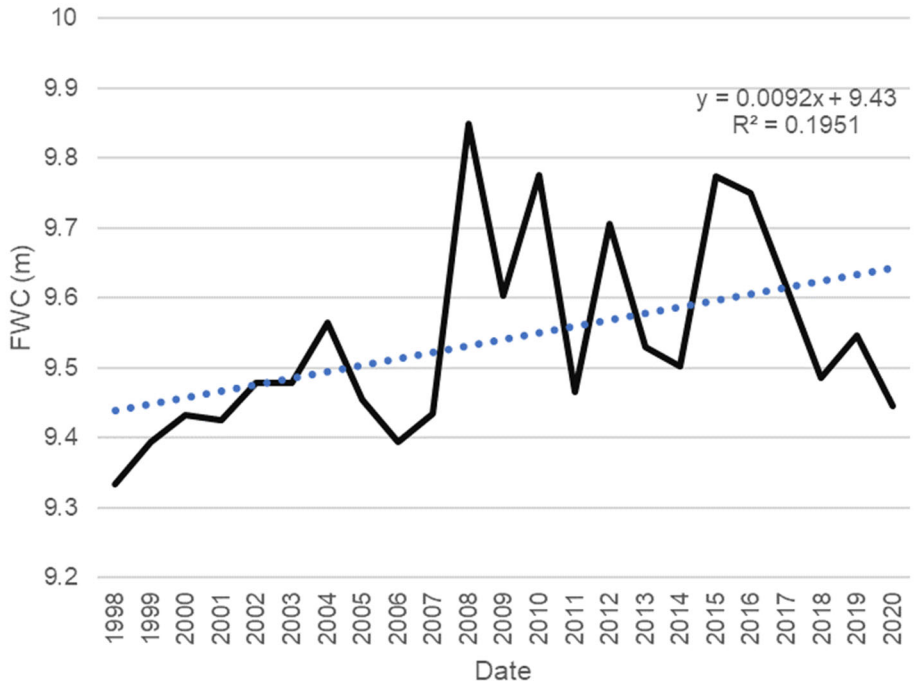

Figure 25. Increasing trend of FWC during 1998 to 2020. FWC was calculated following Carmack *et al.* (2008) using modeled salinity (Global Ocean-Delayed Mode gridded CORA *in-situ* Observations objective analysis in Delayed Mode)

Acknowledgements

I would like to express my gratitude to all those who contributed to this research. First and foremost, I would like to express my deepest gratitude to Prof. Toru Hirawake (National Institute of Polar Research) for his invaluable guidance and expertise throughout this research journey. Seeing his unwavering guidance and support, even in challenging times, has enriched my personal growth and character. My gratitude is also extended to Prof. Sang Heon Lee (Pusan National University). I am deeply grateful for his patience and support as a collaborator, always believing in me and ensuring I never gave up, with his profound understanding and care. I learned from both of them that the doctoral journey not only encompasses academic growth but also fosters personal development. would also like to express my gratitude to Associate Prof, Hiroto Abe (Hokkaido University). I also extend my gratitude to my colleagues and juniors in the research lab. I thanks to Amane Fujiwara (Japan Agency for Marine-Earth Science and Technology : JAMSTEC) for teaching and supporting me in a laboratory experiment, Waga Hisatomo (International Arctic Research Center, University of Alaska Fairbanks) for advice of research, and thanks to other members of our laboratory, Shun Zhang, Makoto Smapei, Tomomi Yagi, Seira Suzuki, Yukiko Kudo and juniors who had good relationship with me. I hope to thank to Shoko Tatamisashi for supporting lab experiments of Mass-spectrometer. I am thankful to the members of the review committee, Prof. Mukai Tohru (Hokkaido University), Assistant Prof. Matsuno Kohei (Hokkaido University), Prof. Ooki Atsushi (Hokkaido University) for their insight of ocean science and gentle advice. Also, I thanks to members of Marine Ecological Lab (PML, Pusan National University), Huitae Joo, Kwan-Woo Kim, Yejin Kim, and Jae Joong Kang for research advice. I wish to thank the captains and crews of the T/S Osoro-maru and R/V Araon. Their efforts were instrumental in the successful completion of this study. Also, I thanks to Yewon Kim help for sampling. Special thanks to Myong Joon Kim, a member of PML, and Seok Jin Yoon (National Institute of Fisheries Science) for their moral support as friendship. Moreover, I am grateful to Yoonji, Jaehong, and Mingoo, Yu Sato, Mio and LNT members, Prof. Setsuko Kobayashi and Akiko Ito, Dr. Dong Hwan Shin, Kaori Hiramatsu, Takemura Eigo with whom I shared many enjoyable moments. Last but not least, our sincere thanks go to my family to support and trust me.

This research was supported by Arctic Challenge for Sustainability (ArCS) and Arctic Challenge for Sustainability II (ArCS-II) Projects of the Ministry of Education, Culture, Sports, Science and Technology of Japan (MEXT) and by the Global Changes Observation Mission-Climate (GCOM-C) project of the Japan Aerospace Exploration Agency (JAXA). This study also was part of the projected titled “Korea-Arctic Ocean Warming and Responses of Ecosystem (K-AWARE, KOPRI)”, funded by the Ministry of Ocean and Fisheries, Korea.

References

Aagaard, K., Carmack, E.C., 1989. The role of sea ice and other fresh water in the Arctic circulation. J Geophys Res Oceans 94. https://doi.org/10.1029/jc094ic10p14485

Aagaard, K., Roach, A.T., Schumacher, J.D., 1985. On the wind-driven variability of the flow through Bering Strait. J Geophys Res 90. https://doi.org/10.1029/JC090iC04p07213

Agawin, N.S.R., Duarte, C.M., Agustí, S., 2000. Nutrient and temperature control of the contribution of picoplankton to phytoplankton biomass and production. Limnol Oceanogr 45. https://doi.org/10.4319/lo.2000.45.3.0591

Aiken, J., Hardman-Mountford, N.J., Barlow, R., Fishwick, J., Hirata, T., Smyth, T., 2008. Functional links between bioenergetics and bio-optical traits of phytoplankton taxonomic groups: An overarching hypothesis with applications for ocean colour remote sensing. J Plankton Res. https://doi.org/10.1093/plankt/fbm098

Ardyna, M., Arrigo, K.R., 2020. Phytoplankton dynamics in a changing Arctic Ocean. Nat Clim Chang. https://doi.org/10.1038/s41558-020-0905-y

Ardyna, M., Mundy, C.J., Mills, M.M., Oziel, L., Grondin, P.L., Lacour, L., Verin, G., Van Dijken, G., Ras, J., Alou-Font, E., Babin, M., Gosselin, M., Tremblay, J.É., Raimbault, P., Assmy, P., Nicolaus, M., Claustre, H., Arrigo, K.R., 2020. Environmental drivers of under-ice phytoplankton bloom dynamics in the Arctic Ocean. Elementa 8. https://doi.org/10.1525/elementa.430

Arin, L., Morán, X.A.G., Estrada, M., 2002. Phytoplankton size distribution and growth rates in the Alboran Sea (SW Mediterranean): Short term variability related to mesoscale hydrodynamics. J Plankton Res 24. https://doi.org/10.1093/plankt/24.10.1019

Arrigo, K.R., van Dijken, G.L., 2015. Continued increases in Arctic Ocean primary production. Prog Oceanogr 136. https://doi.org/10.1016/j.pocean.2015.05.002

Basu, S., Mackey, K.R.M., 2018. Phytoplankton as key mediators of the biological carbon pump: Their responses to a changing climate. Sustainability (Switzerland). https://doi.org/10.3390/su10030869

Berelson, W.M., 2001. The flux of particulate organic carbon into the ocean interior: A comparison of four U.S. JGOFS regional studies. Oceanography 14. https://doi.org/10.5670/oceanog.2001.07

Bhavya, P.S., Kang, J.J., Jang, H.K., Joo, H., Lee, J.H., Lee, J.H., Park, J.W., Kim, K., Kim, H.C., Lee, S.H., 2020. The contribution of small phytoplankton communities to the total dissolved inorganic nitrogen assimilation rates in the East/Japan Sea: An experimental evaluation. J Mar Sci Eng 8. https://doi.org/10.3390/jmse8110854

Bouman, H., Platt, T., Sathyendranath, S., Stuart, V., 2005. Dependence of light-saturated photosynthesis on temperature and community structure. Deep Sea Res 1 Oceanogr Res Pap 52. https://doi.org/10.1016/j.dsr.2005.01.008

Brewin, R.J.W., Sathyendranath, S., Hirata, T., Lavender, S.J., Barciela, R.M., Hardman-Mountford, N.J., 2010. A three-component model of phytoplankton size class for the Atlantic Ocean. Ecol Modell 221.

https://doi.org/10.1016/j.ecolmodel.2010.02.014

Brewin, R.J.W., Sathyendranath, S., Müller, D., Brockmann, C., Deschamps, P.Y., Devred, E., Doerffer, R., Fomferra, N., Franz, B., Grant, M., Groom, S., Horseman, A., Hu, C., Krasemann, H., Lee, Z.P., Maritorena, S., Mélin, F., Peters, M., Platt, T., Regner, P., Smyth, T., Steinmetz, F., Swinton, J., Werdell, J., White, G.N., 2015. The Ocean Colour Climate Change Initiative: III. A round-robin comparison on in-water bio-optical algorithms. Remote Sens Environ 162. https://doi.org/10.1016/j.rse.2013.09.016

Bricaud, A., Ciotti, A.M., Gentili, B., 2012. Spatial-temporal variations in phytoplankton size and colored detrital matter absorption at global and regional scales, as derived from twelve years of SeaWiFS data (1998-2009). Global Biogeochem Cycles 26. https://doi.org/10.1029/2010GB003952

Cabanes, C., Grouazel, A., Von Schuckmann, K., Hamon, M., Turpin, V., Coatanoan, C., Paris, F., Guinehut, S., Boone, C., Ferry, N., De Boyer Montégut, C., Carval, T., Reverdin, G., Pouliquen, S., Le Traon, P.Y., 2013. The CORA dataset: Validation and diagnostics of *in-situ* ocean temperature and salinity measurements. Ocean Science 9. https://doi.org/10.5194/os-9-1-2013

Carmack, E., McLaughlin, F., Yamamoto-Kawai, M., Itoh, M., Shimada, K., Krishfield, R., Proshutinsky, A., 2008. Freshwater storage in the northern ocean and the special role of the beaufort gyre, in: Arctic-Subarctic Ocean Fluxes: Defining the Role of the Northern Seas in Climate. https://doi.org/10.1007/978-1-4020-6774-7_8

Chisholm, S.W., 1992. Phytoplankton size. In: Falkowski, P.G.,Woodhead, A.D. (Eds.), Primary Productivity and Biogeochemical Cycles in the Sea. Plenum, New York.

Ciotti, A.M., Bricaud, A., 2006. Retrievals of a size parameter for phytoplankton and spectral light absorption by colored detrital matter from water-leaving radiances at SeaWiFS channels in a continental shelf region off Brazil. Limnol Oceanogr Methods 4. https://doi.org/10.4319/lom.2006.4.237

Coachman, L.K., Aagaard, K., 1974. Physical Oceanography of Arctic and Subarctic Seas, in: Marine Geology and Oceanography of the Arctic Seas. https://doi.org/10.1007/978-3-642-87411-6_1

Codispoti, L.A., Flagg, C.N., Swift, J.H., 2009. Hydrographic conditions during the 2004 SBI process experiments. Deep Sea Res 2 Top Stud Oceanogr 56. https://doi.org/10.1016/j.dsr2.2008.10.013

Cooper, L.W., Whitledge, T.E., Grebmeier, J.M., Weingartner, T., 1997. The nutrient, salinity, and stable oxygen isotope composition of Bering and Chukchi Seas waters in and near the Bering Strait. J Geophys Res Oceans 102. https://doi.org/10.1029/97JC00015

Cottrell, M.T., Kirchman, D.L., 2009. Photoheterotrophic microbes in the arctic ocean in summer and winter. Appl Environ Microbiol 75. https://doi.org/10.1128/AEM.00117-09

Coupel, P., Jin, H.Y., Joo, M., Horner, R., Bouvet, H.A., Sicre, M.A., Gascard, J.C., Chen, J.F., Garcon, V., Ruiz-Pino, D., 2012. Phytoplankton distribution in unusually low sea ice cover over the Pacific Arctic. Biogeosciences 9. https://doi.org/10.5194/bg-9-4835-2012

Coupel, P., Matsuoka, A., Ruiz-Pino, D., Gosselin, M., Marie, D., Tremblay, J.E., Babin, M., 2015. Pigment signatures of phytoplankton communities in the Beaufort Sea. Biogeosciences 12. https://doi.org/10.5194/bg-12-991-2015

Crawford, A., Stroeve, J., Smith, A., Jahn, A., 2021. Arctic open-water periods are projected to lengthen dramatically by 2100. Commun Earth Environ 2. https://doi.org/10.1038/s43247-021-00183-x

Danielson, S.L., Ahkinga, O., Ashjian, C., Basyuk, E., Cooper, L.W., Eisner, L., Farley, E., Iken, K.B., Grebmeier, J.M., Juranek, L., Khen, G., Jayne, S.R., Kikuchi, T., Ladd, C., Lu, K., McCabe, R.M., Moore, G.W.K., Nishino, S., Ozenna, F., Pickart, R.S., Polyakov, I., Stabeno, P.J., Thoman, R., Williams, W.J., Wood, K., Weingartner, T.J., 2020. Manifestation and consequences of warming and altered heat fluxes over the Bering and Chukchi Sea continental shelves. Deep Sea Res 2 Top Stud Oceanogr 177. https://doi.org/10.1016/j.dsr2.2020.104781

Devred, E., Sathyendranath, S., Stuart, V., Platt, T., 2011. A three component classification of phytoplankton absorption spectra: Application to ocean-color data. Remote Sens Environ 115. https://doi.org/10.1016/j.rse.2011.04.025

Dunbar, M.J., 1976. Bering Strait: The Regional Physical Oceanography, by L.K. Coachman, K.A. Aagaard, R.B. Tripp. Arctic 29. https://doi.org/10.14430/arctic3020

Fahrbach, E., Meincke, J., Østerhus, S., Rohardt, G., Schauer, U., Tverberg, V., Verduin, J., 2001. Direct measurements of volume transports through Fram Strait. Polar Res 20. https://doi.org/10.1111/j.1751-8369.2001.tb00059.x

Falkowski, P.G., Barber, R.T., Smetacek, V., 1998. Biogeochemical controls and feedbacks on ocean primary production. Science (1979). https://doi.org/10.1126/science.281.5374.200

Finkel, Z. V., Vaillancourt, C.J., Irwin, A.J., Reavie, E.D., Smol, J.P., 2009. Environmental control of diatom community size structure varies across aquatic ecosystems. Proceedings of the Royal Society B: Biological Sciences 276. https://doi.org/10.1098/rspb.2008.1610

Frey, K.E., Comiso, J.C., Cooper, L.W., Grebmeier, J.M., Stock, L. V, 2021. Arctic Ocean Primary Productivity: The Response of Marine Algae to Climate Warming and Sea Ice Decline. Arctic Report Card 2021.

Frey, K.E., Kinney, J.C., Stock, L. V., Osinski, R., 2022. SIDEBAR OBSERVATIONS OF DECLINING PRIMARY PRODUCTIVITY IN THE WESTERN BERING STRAIT. Oceanography. https://doi.org/10.5670/oceanog.2022.123

Frey, K.E., Moore, G.W.K., Cooper, L.W., Grebmeier, J.M., 2015. Divergent patterns of recent sea ice cover across the Bering, Chukchi, and Beaufort seas of the Pacific Arctic Region. Prog Oceanogr 136. https://doi.org/10.1016/j.pocean.2015.05.009

Frigstad, H., Andersen, T., Ballerby, R.G.J., Silyakova, A., Hessen, D.O. 2014 Variation in the seston C:N ratio of the Arctic Ocean and pan-Arctic shelves. J. Marine Syst, 129, 214-223, https://doi.org/10.1016/j.jmarsys.2013.06.004.

Fu, W., Moore, K., Primeau, F.W., Lindsay, K., Randerson J.T., 2020. A Growing Freshwater Lens in the Arctic Ocean With Sustained Climate Warming Disrupts Marine Ecosystem Function. J. Geophys. Res. Biogeosci. 125, 12. https://doi.org/10.1029/2020JG005693

Fujiwara, A., Hirawake, T., Suzuki, K., Eisner, L., Imai, I., Nishino, S., Kikuchi, T., Saitoh, S.I., 2016. Influence of timing of sea ice retreat on phytoplankton size during marginal ice zone bloom period on the Chukchi and Bering shelves. Biogeosciences 13. https://doi.org/10.5194/bg-13-115-2016

Fujiwara, A., Hirawake, T., Suzuki, K., Saitoh, S.I., 2011. Remote sensing of size structure of phytoplankton communities using optical properties of the Chukchi and Bering Sea shelf region. Biogeosciences 8. https://doi.org/10.5194/bg-8-3567-2011

Fujiwara, A., Nishino, S., Matsuno, K., Onodera, J., Kawaguchi, Y., Hirawake, T., Suzuki, K., Inoue, J., Kikuchi, T., 2018. Changes in phytoplankton community structure during wind-induced fall bloom on the central Chukchi shelf. Polar Biol 41. https://doi.org/10.1007/s00300-018-2284-7

Gradinger, R., Lenz, J., 1995. Seasonal occurrence of picocyanobacteria in the Greenland Sea and central Arctic Ocean. Polar Biol 15. https://doi.org/10.1007/BF00239722

Grebmeier, J., McRoy, C., Feder, H., 1988. Pelagic-benthic coupling on the shelf of the northern Bering and Chukchi Seas. I. Food supply source and benthic bio-mass. Mar Ecol Prog Ser 48. https://doi.org/10.3354/meps048057

Grebmeier, J.M., 2012. Shifting patterns of life in the pacific Arctic and sub-Arctic Seas. Ann Rev Mar Sci 4. https://doi.org/10.1146/annurev-marine-120710-100926

Grebmeier, J.M., Bluhm, B.A., Cooper, L.W., Denisenko, S.G., Iken, K., Kędra, M., Serratos, C., 2015. Time-series benthic community composition and biomass and associated environmental characteristics in the Chukchi Sea during the RUSALCA 2004–2012 program. Oceanography 28. https://doi.org/10.5670/oceanog.2015.61

Grebmeier, J.M., Cooper, L.W., Feder, H.M., Sirenko, B.I., 2006. Ecosystem dynamics of the Pacific-influenced Northern Bering and Chukchi Seas in the Amerasian Arctic. Prog Oceanogr 71. https://doi.org/10.1016/j.pocean.2006.10.001

Haine, T.W.N., Curry, B., Gerdes, R., Hansen, E., Karcher, M., Lee, C., Rudels, B., Spreen, G., de Steur, L.,

Stewart, K.D., Woodgate, R., 2015. Arctic freshwater export: Status, mechanisms, and prospects. Glob Planet Change. https://doi.org/10.1016/j.gloplacha.2014.11.013

Harada, N., 2016. Review: Potential catastrophic reduction of sea ice in the western Arctic Ocean: Its impact on biogeochemical cycles and marine ecosystems. Glob Planet Change. https://doi.org/10.1016/j.gloplacha.2015.11.005

He, R., Wooller, M.J., Pohlman, J.W., Quensen, J., Tiedje, J.M., Leigh, M.B., 2012. Diversity of active aerobic methanotrophs along depth profiles of arctic and subarctic lake water column and sediments. ISME Journal 6. https://doi.org/10.1038/ismej.2012.34

Hirata, T., Aiken, J., Hardman-Mountford, N., Smyth, T.J., Barlow, R.G., 2008. An absorption model to determine phytoplankton size classes from satellite ocean colour. Remote Sens Environ 112. https://doi.org/10.1016/j.rse.2008.03.011

Hirata, T., Hardman-Mountford, N.J., Brewin, R.J.W., Aiken, J., Barlow, R., Suzuki, K., Isada, T., Howell, E., Hashioka, T., Noguchi-Aita, M., Yamanaka, Y., 2011. Synoptic relationships between surface Chlorophyll-a and diagnostic pigments specific to phytoplankton functional types. Biogeosciences 8. https://doi.org/10.5194/bg-8-311-2011

Hodal, H., Kristiansen, S., 2008. The importance of small-celled phytoplankton in spring blooms at the marginal ice zone in the northern Barents Sea. Deep Sea Res 2 Top Stud Oceanogr 55. https://doi.org/10.1016/j.dsr2.2008.05.012

Holland, M.M., Finnis, J., Barrett, A.P., Serreze, M.C., 2007. Projected changes in Arctic Ocean freshwater budgets. J Geophys Res Biogeosci 112. https://doi.org/10.1029/2006JG000354

Huntington, H.P., Danielson, S.L., Wiese, F.K., Baker, M., Boveng, P., Citta, J.J., Robertis, A.D., Dickson, D.M.S, Farley, E., George, J.C., Iken, K., Kimmel, D.G., Kuletz, K., Ladd, C., Levine, R., Quakenbush, L., Stabeno, P., Stafford, K.M., Stockwell, D., Wilson, C., 2020. Evidence suggests potential transformation of the Pacific Arctic ecosystem is underway. Nat Clim Chang. 10, 342–348 (2020). https://doi.org/10.1038/s41558-020-0695-2

IOCCG, 2014. Phytoplankton functional types from Space. Reports and Monographs of the International OceanColour Coordinating Group.

Jones, E.P., Anderson, L.G., Jutterström, S., Swift, J.H., 2008. Sources and distribution of fresh water in the East Greenland Current. Prog Oceanogr 78. https://doi.org/10.1016/j.pocean.2007.06.003

Joo, H.T., Lee, J.H., Kang, C.K., An, S., Kang, S.H., Lim, J.H., Joo, H.M., Lee, S.H., 2013. Macromolecular production of phytoplankton in the northern bering sea, 2007. Polar Biol 37. https://doi.org/10.1007/s00300-013-1439-9

Kahru, M., Brotas, V., Manzano-Sarabia, M., Mitchell, B.G., 2011. Are phytoplankton blooms occurring

earlier in the Arctic? Glob Chang Biol 17. https://doi.org/10.1111/j.1365-2486.2010.02312.x

Key, T., McCarthy, A., Campbell, D.A., Six, C., Roy, S., Finkel, Z. V., 2010. Cell size trade-offs govern light exploitation strategies in marine phytoplankton. Environ Microbiol 12. https://doi.org/10.1111/j.1462-2920.2009.02046.x

Kim, H.K., Seo, K.H., Yeh, S.W., Kang, N.Y., Moon, B.K., 2020. Asymmetric impact of Central Pacific ENSO on the reduction of tropical cyclone genesis frequency over the western North Pacific since the late 1990s. Clim Dyn 54. https://doi.org/10.1007/s00382-019-05020-8

Kodaira, T., Waseda, T., Nose, T., Inoue, J., 2020. Record high Pacific Arctic seawater temperatures and delayed sea ice advance in response to episodic atmospheric blocking. Sci Rep 10. https://doi.org/10.1038/s41598-020-77488-y

Kostadinov, T.S., Siegel, D.A., Maritorena, S., 2009. Retrieval of the particle size distribution from satellite ocean color observations. J Geophys Res Oceans 114. https://doi.org/10.1029/2009JC005303

Lee, S.H., Joo, H.M., Yun, M.S., Whitledge, T.E., 2012. Recent phytoplankton productivity of the northern Bering Sea during early summer in 2007. Polar Biol 35. https://doi.org/10.1007/s00300-011-1035-9

Lee, S.H., Ryu, J., Lee, D., Park, J.-W., Kwon, J.-I., Zhao, J., Son, S., 2019. Spatial variations of small phytoplankton contributions in the Northern Bering Sea and the Southern Chukchi Sea. GIsci Remote Sens 56. https://doi.org/10.1080/15481603.2019.1571265

Lee, S.H., Ryu, J., Park, J.-W., Lee, D., Kwon, J.-I., Zhao, J., Son, S.H., 2018. Improved Chlorophyll-a Algorithm for the Satellite Ocean Color Data in the Northern Bering Sea and Southern Chukchi Sea. Ocean Science Journal 53. https://doi.org/10.1007/s12601-018-0011-5

Lee, S.H., Sun Yun, M., Kyung Kim, B., Joo, H.T., Kang, S.H., Keun Kang, C., Whitledge, T.E., 2013. Contribution of small phytoplankton to total primary production in the Chukchi Sea. Cont Shelf Res 68. https://doi.org/10.1016/j.csr.2013.08.008

Lee, S.H., Whitledge, T.E., Kang, S.H., 2007. Recent carbon and nitrogen uptake rates of phytoplankton in Bering Strait and the Chukchi Sea. Cont Shelf Res 27. https://doi.org/10.1016/j.csr.2007.05.009

Lee, S.H., Yun, M.S., Jang, H.K., Kang, J.J., Kim, K., Lee, D., Jo, N., Park, S.H., Lee, J.H., Ahn, S.H., Stockwell, D.A., Whitledge, T.E., 2023. Size-differential photosynthetic traits of phytoplankton in the Chukchi Sea. Cont Shelf Res 255. https://doi.org/10.1016/j.csr.2023.104933

Legendre, L., Le Fèvre, J., 1991. From Individual Plankton Cells To Pelagic Marine Ecosystems And To Global Biogeochemical Cycles, in: Particle Analysis in Oceanography. https://doi.org/10.1007/978-3-642-75121-9_11

Li, W.K.W., 1998. Annual average abundance of heterotrophic bacteria and Synechococcus in surface ocean

waters. Limnol Oceanogr 43. https://doi.org/10.4319/lo.1998.43.7.1746

Li, W.K.W., McLaughlin, F.A., Lovejoy, C., Carmack, E.C., 2009. Smallest algae thrive as the arctic ocean freshens. Science (1979). https://doi.org/10.1126/science.1179798

Li, Z., Li, L., Song, K., Cassar, N., 2013. Estimation of phytoplankton size fractions based on spectral features of remote sensing ocean color data. J Geophys Res Oceans 118. https://doi.org/10.1002/jgrc.20137

Liu, X., Devred, E., Johnson, C., 2018. Remote sensing of phytoplankton size class in northwest Atlantic from 1998 to 2016: Bio-optical algorithms comparison and application. Remote Sens (Basel) 10. https://doi.org/10.3390/rs10071028

Liu, Z., Risi, C., Codron, F., He, X., Poulsen, C.J., Wei, Z., Chen, D., Li, S., Bowen, G.J., 2021. Acceleration of western Arctic sea ice loss linked to the Pacific North American pattern. Nat Commun 12. https://doi.org/10.1038/s41467-021-21830-z

Lovejoy, C., Massana, R., Pedrós-Alió, C., 2006. Diversity and distribution of marine microbial eukaryotes in the arctic ocean and adjacent seas. Appl Environ Microbiol 72. https://doi.org/10.1128/AEM.72.5.3085-3095.2006

Lowry, K.E., Pickart, R.S., Mills, M.M., Brown, Z.W., van Dijken, G.L., Bates, N.R., Arrigo, K.R., 2015. The influence of winter water on phytoplankton blooms in the Chukchi Sea. Deep Sea Res 2 Top Stud Oceanogr 118. https://doi.org/10.1016/j.dsr2.2015.06.006

Lucas, S., Johannessen, J.A., Cancet, M., Pettersson, L.H., Esau, I., Rheinlænder, J.W., Ardhuin, F., Chapron, B., Korosov, A., Collard, F., Herlédan, S., Olason, E., Ferrari, R., Fouchet, E., Donlon, C., 2023. Knowledge Gaps and Impact of Future Satellite Missions to Facilitate Monitoring of Changes in the Arctic Ocean. Remote Sens (Basel). https://doi.org/10.3390/rs15112852

Manucharyan, G.E., Isachsen, P.E., 2019. Critical Role of Continental Slopes in Halocline and Eddy Dynamics of the Ekman-Driven Beaufort Gyre. J Geophys Res Oceans 124. https://doi.org/10.1029/2018JC014624

Marañón, E., 2015. Cell Size as a key determinant of phytoplankton metabolism and community structure. Ann Rev Mar Sci 7. https://doi.org/10.1146/annurev-marine-010814-015955

Mélin, F., Vantrepotte, V., Chuprin, A., Grant, M., Jackson, T., Sathyendranath, S., 2017. Assessing the fitness-for-purpose of satellite multi-mission ocean color climate data records: A protocol applied to OC-CCI chlorophyll-a data. Remote Sens Environ 203. https://doi.org/10.1016/j.rse.2017.03.039

Morán, X.A.G., López-Urrutia, Á., Calvo-Díaz, A., LI, W.K.W., 2010. Increasing importance of small phytoplankton in a warmer ocean. Glob Chang Biol 16. https://doi.org/10.1111/j.1365-2486.2009.01960.x

Morel, A., Bricaud, A., 1981. Theoretical results concerning light absorption in a discrete medium, and application to specific absorption of phytoplankton. Deep Sea Research Part A, Oceanographic Research Papers 28. https://doi.org/10.1016/0198-0149(81)90039-X

Mosharov, S.A., Druzhkova, E.I., Sazhin, A.F., Khlebopashev, P. V., Drozdova, A.N., Belyaev, N.A., Azovsky, A.I., 2023. Structure and Productivity of the Phytoplankton Community in the Southwestern Kara Sea in Early Summer. J Mar Sci Eng 11. https://doi.org/10.3390/jmse11040832

Mouw, C.B., Yoder, J.A., 2010. Optical determination of phytoplankton size composition from global SeaWiFS imagery. J Geophys Res Oceans 115. https://doi.org/10.1029/2010JC006337

Nair, A., Sathyendranath, S., Platt, T., Morales, J., Stuart, V., Forget, M.H., Devred, E., Bouman, H., 2008. Remote sensing of phytoplankton functional types. Remote Sens Environ 112. https://doi.org/10.1016/j.rse.2008.01.021

Neeley, A.R., Harris, L.A., Frey, K.E., 2018. Unraveling Phytoplankton Community Dynamics in the Northern Chukchi Sea Under Sea-Ice-Covered and Sea-Ice-Free Conditions. Geophys Res Lett 45. https://doi.org/10.1029/2018GL077684

Nishino, S., Kikuchi, T., Fujiwara, A., Hirawake, T., Aoyama, M., 2016. Water mass characteristics and their temporal changes in a biological hotspot in the southern Chukchi Sea. Biogeosciences 13. https://doi.org/10.5194/bg-13-2563-2016

Overland, J.E., Stabeno, P.J., 2004. Is the climate of the bering sea warming and affecting the ecosystem? Eos (Washington DC) 85. https://doi.org/10.1029/2004EO330001

Park, J.-W., Kim, Y., Kim, K.-W., Fujiwara, A., Waga, H., Kang, J.J., Lee, S.-H., Yang, E.-J., Hirawake, T., 2022. Contribution of Small Phytoplankton to Primary Production in the Northern Bering and Chukchi Seas. Water (Switzerland) 14. https://doi.org/10.3390/w14020235

Platt, T., Bouman, H., Devred, E., Fuentes-Yaco, C., Sathyendranath, S., 2005. Physical forcing and phytoplankton distributions. Sci Mar 69. https://doi.org/10.3989/scimar.2005.69s155

Proshutinsky, A., Krishfield, R., Timmermans, M.-L., Toole, J., Carmack, E., McLaughlin, F., Williams, W.J., Zimmermann, S., Itoh, M., Shimada, K., 2009. Beaufort Gyre freshwater reservoir: State and variability from observations. J Geophys Res 114. https://doi.org/10.1029/2008jc005104

Rantanen, M., Karpechko, A.Y., Lipponen, A., Nordling, K., Hyvärinen, O., Ruosteenoja, K., Vihma, T., Laaksonen, A., 2022. The Arctic has warmed nearly four times faster than the globe since 1979. Commun Earth Environ 3. https://doi.org/10.1038/s43247-022-00498-3

Roy, S., Sathyendranath, S., Bouman, H., Platt, T., 2013. The global distribution of phytoplankton size spectrum and size classes from their light-absorption spectra derived from satellite data. Remote Sens Environ 139. https://doi.org/10.1016/j.rse.2013.08.004

Sadanandan Bhavya, P., Han Lee, J., Won Lee, H., Joong Kang, J., Hyung Lee, J., Lee, D., Hyun An, S., Stockwell, D.A., Whitledge, T.E., Heon Lee, S., 2018. First in situ estimations of small phytoplankton carbon and nitrogen uptake rates in the Kara, Laptev, and East Siberian seas. Biogeosciences 15. https://doi.org/10.5194/bg-15-5503-2018

Sambrotto, R.N., Goering, J.J., Mcroy, C.P., 1984. Large yearly production of phytoplankton in the western Bering Strait. Science (1979) 225. https://doi.org/10.1126/science.225.4667.1147

Screen, J.A., Deser, C., Smith, D.M., Zhang, X., Blackport, R., Kushner, P.J., Oudar, T., McCusker, K.E., Sun, L., 2018. Consistency and discrepancy in the atmospheric response to Arctic sea-ice loss across climate models. Nat Geosci 11. https://doi.org/10.1038/s41561-018-0059-y

Screen, J.A., Francis, J.A., 2016. Contribution of sea-ice loss to Arctic amplification is regulated by Pacific Ocean decadal variability. Nat Clim Chang 6. https://doi.org/10.1038/nclimate3011

Serreze, M.C., Barrett, A.P., Slater, A.G., Woodgate, R.A., Aagaard, K., Lammers, R.B., Steele, M., Moritz, R., Meredith, M., Lee, C.M., 2006. The large-scale freshwater cycle of the Arctic. J Geophys Res Oceans 111. https://doi.org/10.1029/2005JC003424

Sherr, E.B., Sherr, B.F., Wheeler, P.A., Thompson, K., 2003. Temporal and spatial variation in stocks of autotrophic and heterotrophic microbes in the upper water column of the central Arctic Ocean. Deep Sea Res 1 Oceanogr Res Pap 50. https://doi.org/10.1016/S0967-0637(03)00031-1

Sieburth, J.M.N., Smetacek, V., Lenz, J., 1978. Pelagic ecosystem structure: Heterotrophic compartments of the plankton and their relationship to plankton size fractions. Limnol Oceanogr. https://doi.org/10.4319/lo.1978.23.6.1256

Siegel, D.A., Buesseler, K.O., Doney, S.C., Sailley, S.F., Behrenfeld, M.J., Boyd, P.W., 2014. Global assessment of ocean carbon export by combining satellite observations and food-web models. Global Biogeochem Cycles 28. https://doi.org/10.1002/2013GB004743

Simon, A., Gastineau, G., Frankignoul, C., Lapin, V., Ortega, P., 2022. Pacific Decadal Oscillation modulates the Arctic sea-ice loss influence on the midlatitude atmospheric circulation in winter. Weather and Climate Dynamics 3. https://doi.org/10.5194/wcd-3-845-2022

Son, S.H., Campbell, J., Dowell, M., Yoo, S., Noh, J., 2005. Primary production in the Yellow Sea determined by ocean color remote sensing. Mar Ecol Prog Ser 303. https://doi.org/10.3354/meps303091

Son, S.H., Kim, Y.H., Kwon, J. Il, Kim, H.C., Park, K.S., 2014. Characterization of spatial and temporal variation of suspended sediments in the Yellow and East China Seas using satellite ocean color data. GIsci Remote Sens 51. https://doi.org/10.1080/15481603.2014.895580

Spall, M.A., Pickart, R.S., Li, M., Itoh, M., Lin, P., Kikuchi, T., Qi, Y., 2018. Transport of Pacific Water Into

the Canada Basin and the Formation of the Chukchi Slope Current. J Geophys Res Oceans 123. https://doi.org/10.1029/2018JC013825

Springer, A.M., McRoy, C.P., 1993. The paradox of pelagic food webs in the northern Bering Sea-III. Patterns of primary production. Cont Shelf Res 13. https://doi.org/10.1016/0278-4343(93)90095-F

Steele, M., Morison, J., Ermold, W., Rigor, I., Ortmeyer, M., Shimada, K., 2004. Circulation of summer Pacific halocline water in the Arctic Ocean. J. Geophys. Res. Oceans. 109. https://doi.org/10.1029/2003JC002009

Stroeve, J., Notz, D., 2018. Changing state of Arctic sea ice across all seasons. Environmental Research Letters. https://doi.org/10.1088/1748-9326/aade56

Svendsen, L., Keenlyside, N., Bethke, I., Gao, Y., Omrani, N.E., 2018. Pacific contribution to the early twentieth-century warming in the Arctic. Nat Clim Chang. https://doi.org/10.1038/s41558-018-0247-1

Svendsen, L., Keenlyside, N., Muilwijk, M., Bethke, I., Omrani, N.E., Gao, Y., 2021. Pacific contribution to decadal surface temperature trends in the Arctic during the twentieth century. Clim Dyn 57. https://doi.org/10.1007/s00382-021-05868-9

Szekely, T., Gourrion, J., Pouliquen, S., Reverdin, G., 2019. The CORA 5.2 dataset for global in situ temperature and salinity measurements: Data description and validation. Ocean Science 15. https://doi.org/10.5194/os-15-1601-2019

Terrado, R., Lovejoy, C., Massana, R., Vincent, W.F., 2008. Microbial food web responses to light and nutrients beneath the coastal Arctic Ocean sea ice during the winter-spring transition. Journal of Marine Systems 74. https://doi.org/10.1016/j.jmarsys.2007.11.001

Terrado, R., Scarcella, K., Thaler, M., Vincent, W.F., Lovejoy, C., 2013. Small phytoplankton in Arctic seas: vulnerability to climate change. Biodiversity 14. https://doi.org/10.1080/14888386.2012.704839

Turner, J.T., 2015. Zooplankton fecal pellets, marine snow, phytodetritus and the ocean's biological pump. Prog Oceanogr. https://doi.org/10.1016/j.pocean.2014.08.005

Uitz, J., Claustre, H., Gentili, B., Stramski, D., 2010. Phytoplankton class-specific primary production in the world's oceans: Seasonal and interannual variability from satellite observations. Global Biogeochem Cycles 24. https://doi.org/10.1029/2009GB003680

Uitz, J., Claustre, H., Morel, A., Hooker, S.B., 2006. Vertical distribution of phytoplankton communities in open ocean: An assessment based on surface chlorophyll. J Geophys Res Oceans 111. https://doi.org/10.1029/2005JC003207

Waga, H., Hirawake, T., Fujiwara, A., Grebmeier, J.M., Saitoh, S.I., 2019. Impact of spatiotemporal

variability in phytoplankton size structure on benthic macrofaunal distribution in the Pacific Arctic. Deep Sea Res 2 Top Stud Oceanogr 162. https://doi.org/10.1016/j.dsr2.2018.10.008

Waga, H., Hirawake, T., Fujiwara, A., Kikuchi, T., Nishino, S., Suzuki, K., Takao, S., Saitoh, S.I., 2017. Differences in rate and direction of shifts between phytoplankton size structure and sea surface temperature. Remote Sens (Basel) 9. https://doi.org/10.3390/rs9030222

Walsh, J.J., Dieterle, D.A., Chen, F.R., Lenes, J.M., Maslowski, W., Cassano, J.J., Whitledge, T.E., Stockwell, D., Flint, M., Sukhanova, I.N., Christensen, J., 2011. Trophic cascades and future harmful algal blooms within ice-free Arctic Seas north of Bering Strait: A simulation analysis. Prog Oceanogr 91. https://doi.org/10.1016/j.pocean.2011.02.001

Wassmann, P., & D. Slagstad, M. Vernet, G. Mitchell & F. Rey, 1990: Mass sedimentation of Phaeocystis pouchetii in the Barents Sea. Mar. Ecol. Prog. Ser., 66: 183–195. https://doi.org/10.1007/BF00394048

Wang, M., Overland, J.E., 2015. Projected future duration of the sea-ice-free season in the Alaskan Arctic. Prog Oceanogr 136. https://doi.org/10.1016/j.pocean.2015.01.001

Woodgate, R.A., 2018. Increases in the Pacific inflow to the Arctic from 1990 to 2015, and insights into seasonal trends and driving mechanisms from year-round Bering Strait mooring data. Prog Oceanogr 160. https://doi.org/10.1016/j.pocean.2017.12.007

Woodgate, R.A., Aagaard, K., 2005. Revising the Bering Strait freshwater flux into the Arctic Ocean. Geophys Res Lett 32. https://doi.org/10.1029/2004GL021747

Woodgate, R.A., Aagaard, K., Weingartner, T.J., 2005. Monthly temperature, salinity, and transport variability of the Bering Strait through flow. Geophys Res Lett 32. https://doi.org/10.1029/2004GL021880

Woodgate, R.A., Weingartner, T., Lindsay, R., 2010. The 2007 Bering Strait oceanic heat flux and anomalous Arctic sea-ice retreat. Geophys Res Lett 37. https://doi.org/10.1029/2009GL041621

Yun, M.S., Joo, H.M., Kang, J.J., Park, J.W., Lee, J.H., Kang, S.-H., Sun, J., Lee, S.H., 2019. Potential Implications of Changing Photosynthetic End-Products of Phytoplankton Caused by Sea Ice Conditions in the Northern Chukchi Sea. Front Microbiol 10. https://doi.org/10.3389/fmicb.2019.02274

Yun, M.S., Joo, H.T., Park, J.W., Kang, J.J., Kang, S.-H., Lee, S.H., 2018. Lipid-rich and protein-poor carbon allocation patterns of phytoplankton in the northern Chukchi Sea, 2011. Cont Shelf Res 158. https://doi.org/10.1016/j.csr.2018.03.002

Yun, M.S., Whitledge, T.E., Kong, M., Lee, S.H., 2014. Low primary production in the Chukchi Sea shelf, 2009. Cont Shelf Res 76. https://doi.org/10.1016/j.csr.2014.01.001

Yun, M.S., Whitledge, T.E., Stockwell, D., Son, S.H., Lee, J.H., Park, J.W., Lee, D.B., Park, J., Lee, S.H., 2016. Primary production in the Chukchi Sea with potential effects of freshwater content. Biogeosciences 13. https://doi.org/10.5194/bg-13-737-2016

Zhuang, Y., Jin, H., Cai, W.J., Li, H., Jin, M., Qi, D., Chen, J., 2021. Freshening leads to a three-decade trend of declining nutrients in the western Arctic Ocean. Environmental Research Letters 16. https://doi.org/10.1088/1748-9326/abf58b

Appendix

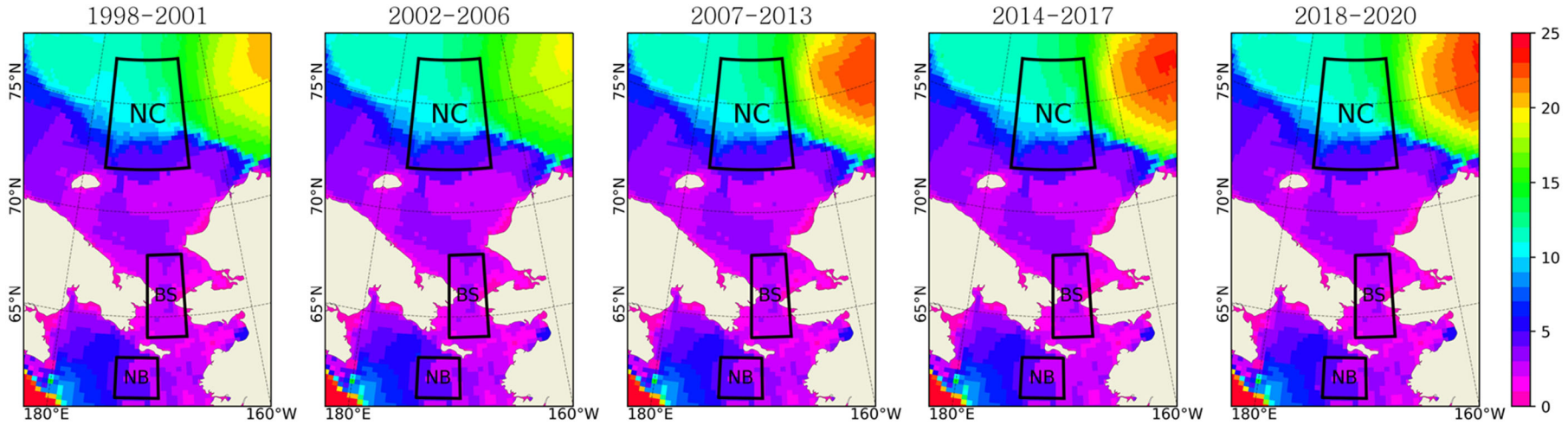

Appendix 1. FWC (m) with PDO period. Each of period. The characteristic feature of the Beaufort Gyre is the increase and decrease of FWC, with no significant variations observed in BS and NB.

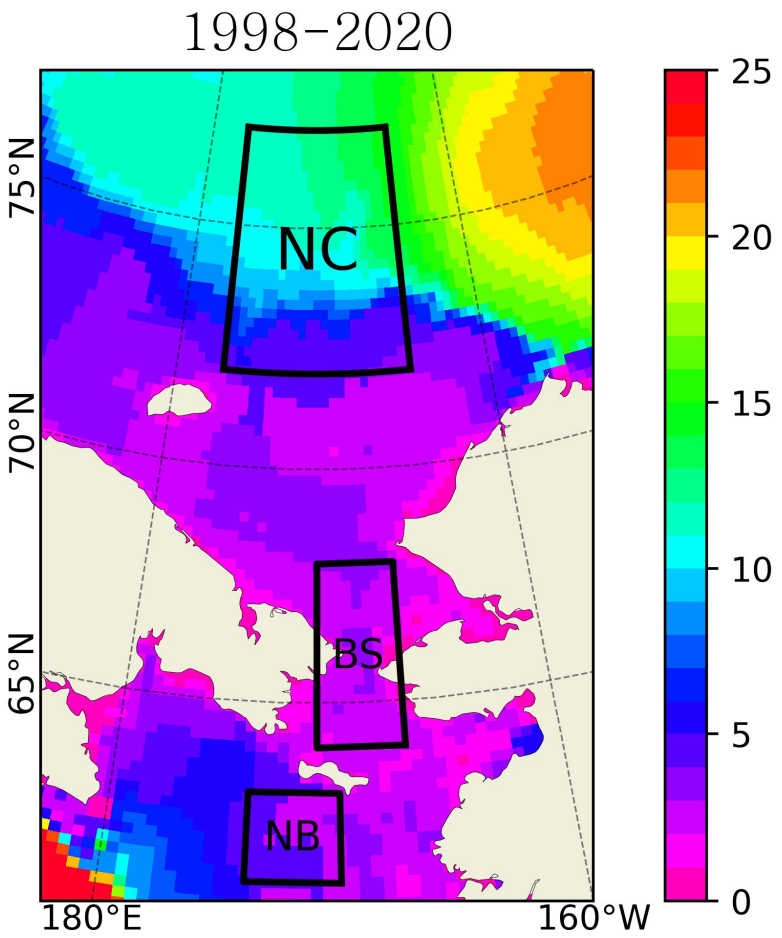

Appendix 2. FWC (m) climatology from 1998 to 2020. The FWC trend in NC appears to resemble the topography and seems to be influenced by the Beaufort Gyre.

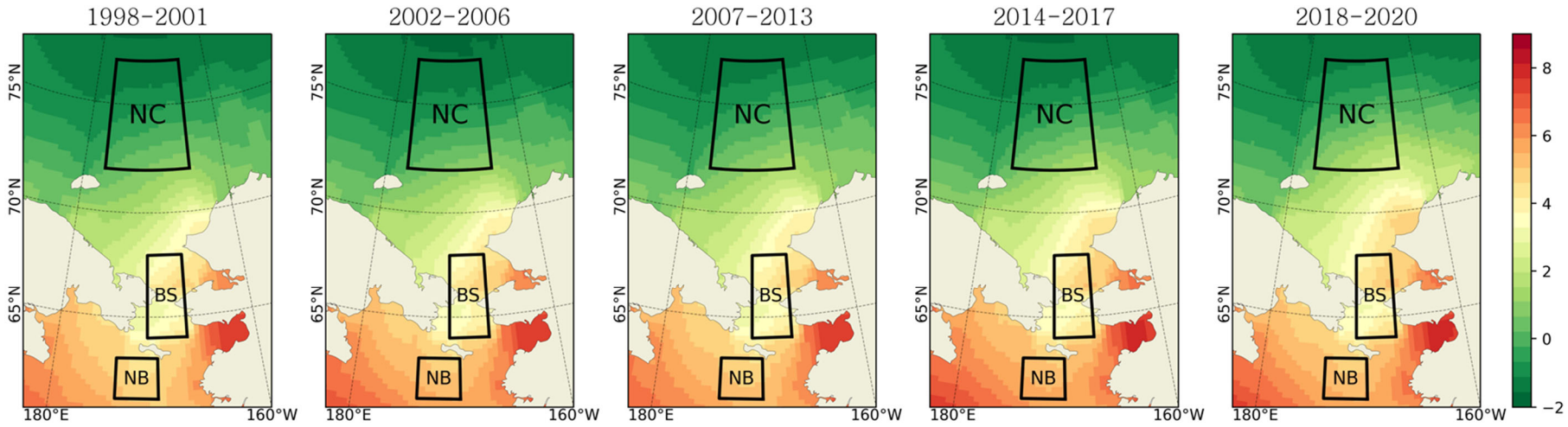

Appendix 3. SST (°C) with PDO period**.** SST was derived from Global Ocean-Delayed Mode gridded CORA *In-situ* Observations objective analysis in Delayed Mode (Cabanes *et al.*, 2013; Szekely *et al.*, 2019)

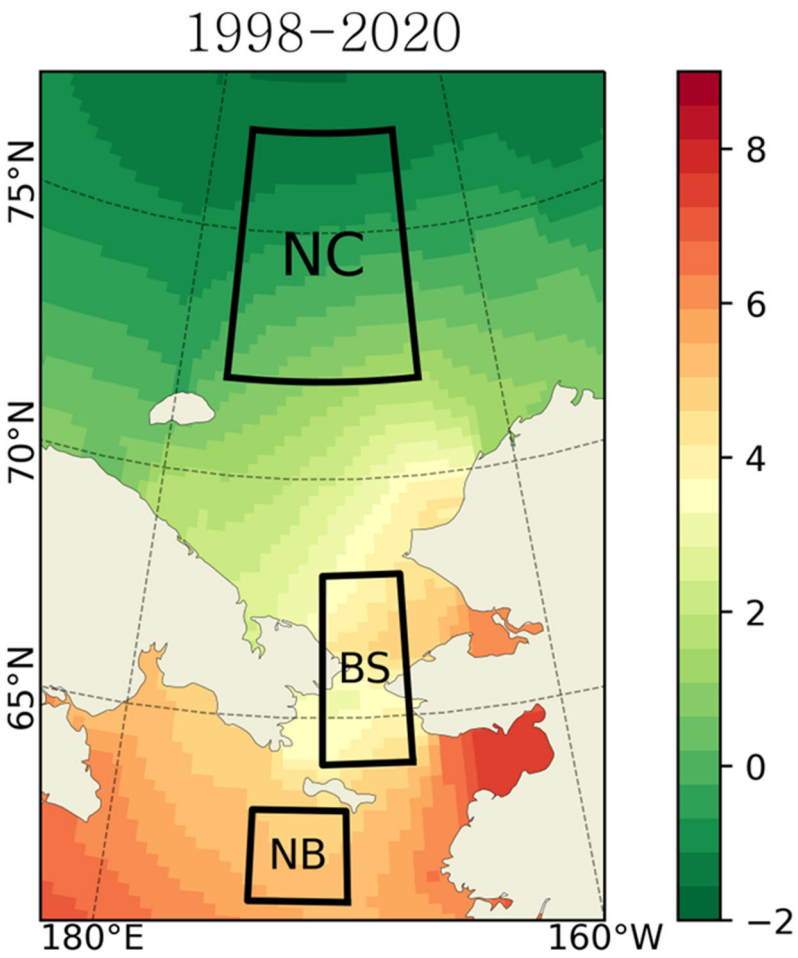

Appendix 4. SST (°C) climatology from 1998 to 2020 (Global Ocean-Delayed Mode gridded CORA *In-situ* Observations objective analysis in Delayed Mode; Cabanes *et al.*, 2013; Szekely *et al.*, 2019)